

**Runoff generation in a steep snow-dominated watershed in
Alberta's southern Rocky Mountains**

by

Sheena Ann Spencer

A thesis submitted in partial fulfillment of the requirements for the degree of

Doctor of Philosophy

in

Water and Land Resources

Department of Renewable Resources

University of Alberta

© Sheena Ann Spencer, 2019

Abstract

Star Creek is a snowmelt-dominated, steep mountain watershed with shallow soils, deep glacial till, and fractured sedimentary bedrock in the eastern slopes of Alberta's Rocky Mountains.

Measurements of streamflow quantity and chemistry at variable scales, water table dynamics, and precipitation were used to describe the first order controls on runoff generation in Star Creek watershed and its sub-watersheds. Specifically, 1) precipitation-runoff relationships and watershed storage were quantified; 2) timing and drivers of hydrologic connectivity were identified; and 3) source water contributions to streamflow were estimated. Multi-year precipitation patterns changed from dry (2008-2012) to wet (2013-2014) conditions and caused an increase in unit area discharge for all but one sub-watershed. Despite a change in annual flow contribution and total discharge, event-scale rainfall-runoff responses did not change. The annual snowmelt pulse saturated the landscape, created the main period of hydrologic connectivity in the watershed, and controlled the magnitude of event-scale rainfall-runoff responses. Streamflow contributions did not correlate with upslope accumulated area. Rather, the overall watershed structure, groundwater upwelling, and the distribution of snowmelt processes influenced the quantity of streamflow contributions. Two locations of subsurface storage were identified: shallow subsurface storage and bedrock storage. Shallow subsurface storage includes the soil and glacial till layers and influences event runoff, hillslope connectedness, and the carry-over of precipitation effects from fall to the next water year. Bedrock storage influences annual discharge because of the dominance of vertical percolation and groundwater recharge and high annual groundwater contribution to streamflow.

An initial displacement of old water stored in the hillslope over winter occurred at the onset of snowmelt before the stream responded significantly. This was followed by a dilution effect as the main snowmelt freshet streamflow pulse was generated by large volumes of snowmelt in the

upper elevations and alpine zone. Late summer streamflow was dominated by either soil drainage or groundwater that was recharged in the alpine zone. In Star East, fall baseflows were dissimilar from all measured sources, but groundwater seep temperatures suggest that it was likely from a deeper groundwater source. This conceptualization of runoff generation can be used to anticipate how watersheds in the front-range Rocky Mountains may respond to disturbance (wildfire and logging) and climate change. These results can also be used to understand other watershed processes such as the potential sources of dissolved organic carbon and the flow pathways to the stream.

Preface

This thesis is original work by Sheena Spencer. Chapters 2 to 4 of this dissertation were written as manuscripts for publication. Historical stream discharge, water quality, and meteorological data were collected and quality controlled by Uldis Silins and the Southern Rockies Watershed Project crew. All other experiments were designed and implemented by me with help in the field by the SRWP crew. I analyzed and interpreted all data presented in this thesis and am lead author on all chapters. Additional contributions by others are noted below.

Chapter 2 was submitted to Water Resources Research and is currently being revised for publication. The manuscript was co-authored by Uldis Silins and Axel Anderson.

Chapter 3 was co-authored by Uldis Silins, Axel Anderson, and Adrian Collins. Kevin Bladon quantified the upslope accumulated area and provided guidance for using those data. Permits to conduct salt dilution gauging experiments were obtained from the Alberta Government under the Water Act (Code of Practice for Hydrologic Tracing Analysis Studies) and Fisheries and Oceans Canada due to the presence of Westslope Cutthroat Trout (*Oncorhynchus clarkii lewisi*) in the lower reaches of Star Creek. The public was notified 30 days prior to each experiment according to the Code of Practice regulations.

Chapter 4 was co-authored by Adrian Collins, Axel Anderson, and Uldis Silins. Adrian Collins also provided R code and guidance for linear discriminant analyses and principal component analyses.

Acknowledgements

I would like to thank my supervisors, Dr. Uldis Silins and Dr. Axel Anderson, for allowing me to take this project and run with it and for providing feedback when I needed it. I am grateful for everything you taught me throughout this process. Thank you to Dr. Adrian Collins for providing technical support and advice along the way as a member of my committee. To my examination committee, Dr. Masaki Hayashi and Dr. David Olefeldt, thank you for your insightful questions and helpful comments that improved my thesis.

Thank you to Dr. Kevin Devito for our many discussions throughout my PhD and for teaching me a different way to think about watershed hydrology. I would also like to thank Dr. Jim Buttle and Dr. Kevin Bladon for lending me your time and expertise in data analysis.

This work would not have been possible without the help from the many Southern Rockies Watershed Project crew members that have collected and analyzed data since 2004. Chris Williams, Amanda Martens, Melaina Weiss, Evan Esch, Kalli Herlein, Eric Lastiwka, Veronica Martens, Kirk Hawthorn, Shauna Stack, Chrystyn Skinner, and Aryn Sherritt, thank you for all your hard work in the field. You are rockstars! To my fellow graduate students, Amy Goodbrand, Milly Corrigan, Mike Stewart, Melissa Howard, Kira Puntteney, Samantha Karpyschin, Dan Greenacre, Bec Baldock and Derek Mueller, who helped in the field or were there to listen or give me feedback as I tried to interpret my results and write my thesis, thank you. To Dr. Mike Stone and Dr. Monica Emelko, thank you for your support and advice in life and academia.

I would like to acknowledge the following agencies for financial support: Alberta Innovates, Alberta Environment and Parks, Forest Resource Improvement Association of Alberta, and the Department of Renewable Resources.

Thank you to my family for standing by me through yet another degree! And to my friends, thank you for the laughter. You all kept me sane and reminded me that there is always fun to be had.

Finally, I'd like to thank Chris Williams for your unwavering love and support. You were with me from the onset of this research to the last word on the page, in the field and at home, through the fun and the stress. I am so lucky to have you as my partner in life. I could not have done this without you. You and Olive mean the world to me.

Table of Contents

Abstract.....	ii
Preface.....	iv
Acknowledgements.....	v
Table of Contents.....	vii
List of Tables.....	x
List of Figures	xi
Chapter 1. Introduction.....	1
Chapter 2. Temporal and spatial variation in precipitation-streamflow dynamics and implications for resistance in the eastern slopes of Alberta’s Rocky Mountains	8
2.1. Introduction	8
2.2. Study site	12
2.3. Methods	13
2.3.1. Long-term temporal variation in precipitation-runoff relationships	13
2.3.1.1. Precipitation.....	13
2.3.1.2. Streamflow.....	14
2.3.2. Short-term temporal variation in precipitation-runoff relationships.....	14
2.3.2.1. Event-based rainfall-runoff responses	14
2.3.2.2. Seasonal antecedent conditions.....	15
2.3.3. Spatial variation in storage characteristics.....	15
2.3.3.1. Water balance approach.....	15
2.3.3.2. Baseflow recession	18
2.4. Results	20
2.4.1. Temporal variation in precipitation-runoff relationships	20
2.4.1.1. Long-term coupling	20
2.4.1.2. Short-term coupling	21
2.4.2. Watershed storage.....	22
2.4.2.1. Temporal trends.....	22
2.4.2.2. Spatial trends.....	23
2.5. Discussion.....	24
2.5.1. Temporal patterns in precipitation-runoff relationships	24
2.5.1.1. Long-term coupling	24
2.5.1.2. Short-term coupling	25
2.5.2. Spatial patterns in precipitation-runoff relationships	26
2.5.2.1. Sub-watershed comparison	26
2.5.2.2. Shallow subsurface storage.....	28
2.5.2.3. Deeper bedrock storage	30
2.5.3. Runoff mechanisms and the implications for resistance to change	31
2.6. Conclusions.....	33

2.7. Tables	34
2.8. Figures	35

Chapter 3. The influence of watershed structure and climatic regimes on subsurface streamflow contributions in a steep watershed in Alberta’s southern Rocky Mountains 43

3.1. Introduction	43
3.2. Study site	46
3.3. Methods	47
3.3.1. Differential gauging	47
3.3.2. Longitudinal stream water chemistry	48
3.3.3. Landscape controls on flow contributions	49
3.3.3.1. Upslope Accumulated Area	49
3.3.3.2. Downslope Index	49
3.3.3.3. Potential solar radiation	50
3.3.4. Watershed-scale precipitation and streamflow	50
3.3.4.1. Precipitation	50
3.3.4.2. Streamflow	51
3.3.5. Hillslope groundwater wells	51
3.4. Results	51
3.4.1. Differential gauging	51
3.4.1.1. High flow	51
3.4.1.2. Recession flow	52
3.4.1.3. Baseflow	53
3.4.1.4. Baseflow comparison (2014 -2015)	53
3.4.2. Longitudinal water chemistry	54
3.4.3. Topographic indices	55
3.4.3.1. Upslope Accumulated Area	55
3.4.3.2. Downslope Index	55
3.4.3.3. Solar radiation index	56
3.4.4. Snow and stream response	56
3.5. Discussion	57
3.5.1. Topography	58
3.5.2. Watershed structure	60
3.5.3. Snowpack and snowmelt distribution	63
3.5.4. Sensitivity to change	64
3.6. Conclusion	66
3.7. Tables	68
3.8. Figures	70

Chapter 4. Source water contributions in a glacial till and fractured sedimentary bedrock dominated Rocky Mountain watershed 82

4.1. Introduction	82
4.2. Study Site	84

4.3. Methods	85
4.3.1. Stream water chemistry	85
4.3.2. Source water chemistry	85
4.3.2.1. Rainfall and snowmelt.....	86
4.3.2.2. Soil water	86
4.3.2.3. Hillslope groundwater	87
4.3.2.4. Groundwater seeps	87
4.3.2.5. Bedrock and till groundwater	87
4.4. Data Processing.....	88
4.5. Results	90
4.5.1. Tracer and source water group selection.....	90
4.5.2. Source water characterization	91
4.5.2.1. Star West Lower	91
4.5.2.2. Star West Upper	92
4.5.2.3. Star East Lower	93
4.5.2.4. Star East Upper	93
4.5.3. Stream water characterization	94
4.5.3.1. Star West Lower	94
4.5.3.2. Star West Upper	95
4.5.3.3. Star East Lower	95
4.5.3.4. Star East Upper	96
4.6. Discussion.....	96
4.6.1. Temporal and spatial variation in source water	96
4.6.2. Temporal variation in stream water contributions	99
4.6.3. Conceptualization of streamflow generation	101
4.7. Conclusion	101
4.8. Figures	103
Chapter 5. Synthesis	115
5.1. Conceptualization of runoff generation in Star Creek	118
5.2. Watershed resistance	121
5.3. Future Research	123
References	125
Appendix A: Supplementary figures	138

List of Tables

Table 2.1: Annual unit (sub-watershed) contribution of streamflow depth (mm yr^{-1}).....	34
Table 2.2: Range in dynamic storage (dV_{WB} ; mm) for water years in dry and wet periods.	34
Table 3.1: Stream discharge at differential gauging point locations within Star Creek sub-watersheds. Discharges were estimated by differential calculations. Blank values for McLaren (14, 15, 16) and Star East Upper (13) indicate no flow at those stations.	68
Table 3.2: UAA and L for all differential gauging reaches. Ordered in decreasing UAA...	69
Table 3.3: Maximum snow depth (m) and the snow-free date for Star Alpine and Star Main stations in 2014 and 2015.	69

List of Figures

Figure 2.1: Map of Star Creek watershed in southwest Alberta, Canada.	35
Figure 2.2: The difference between area-weighted annual precipitation and the 10-year mean annual precipitation across the water years of record for Star Creek watershed.	36
Figure 2.3: Event-based comparison between dry and wet periods for SW and SE forks. Rise in discharge (hydrograph response; mm) as a function of event precipitation (mm).	37
Figure 2.4: Hillslope well responses from 3 locations in Star Creek (Star Lower, SEL, SWU). a) 2014 water year. Hillslope responds during snowmelt and during large storm (70 mm) in early summer. Large storm in late summer only resulted in small groundwater well response (50 mm). b) 2015 water year. Similar patterns were observed but drier conditions resulted in lower groundwater levels.	38
Figure 2.5: The relationship between annual runoff ratios and winter precipitation for SW (blue) and SE (red) watersheds. Closed circles represent years with wet conditions the previous fall. Open circles represent years with dry conditions the previous fall.	39
Figure 2.6: Relationship between watershed storage and stream discharge for 2006 to 2014 water years. SW in blue and SE in red. Water year starts at zero cumulative dV_{WB} (mm, grey dashed line) and hysteresis loop goes counterclockwise (green arrow).	40
Figure 2.7: Recession analysis plots for Star West Lower (SWL), Star West Upper (SWU), Star East Lower (SEL), and Star East Upper (SEU).	41
Figure 2.8: Conceptual block diagram of storage zones for alpine and sub-alpine regions in Star Creek watershed and the eastern slopes of the Rocky Mountains. Hydrograph was compiled from mean daily discharge at SM station at the outlet of Star Creek. Numbers on block diagrams and hydrograph refer to the portion of the landscape that is driving the corresponding portion of the hydrograph.	42
Figure 3.1: Star Creek watershed. Inset 1 shows watershed location within Alberta, Canada. Inset 2 shows watershed location within the Rocky Mountains, on the east side of the Continental Divide.	70
Figure 3.2: Stream reaches (Q1-16) and delineated watersheds for differential streamflow gauging in Star Creek.	71
Figure 3.3: Stream hydrographs for 2014 (left plots) and 2015 (right plots). Yellow circles on the hydrographs indicate dates of differential gauging. Precipitation is shown with a reverse secondary axis. Top sub-plot shows snow depth at alpine and lower elevation sites. Bottom sub-plots show groundwater responses in riparian and hillslope wells for Star Main and Star West Upper as representative wells for the lower and upper watershed.	72
Figure 3.4: Streamflow contributions as a percent of flow at the outlet at the reach scale (average 600 m sections) for three flow conditions in 2015: High flow (June 5/6), recession flow (July 21), and baseflow (Aug 25).	73

Figure 3.5: Streamflow contributions as a percent of flow at the outlet for baseflow in 2015 (Aug 25) and 2014 (Aug 25).....	74
Figure 3.6: Specific conductivity of stream water from outlet at Star Main (0 m) to upper reaches of all forks for 2014 season: High flow (June 6), recession (July 17), and baseflow (Sept 19). Q1-16 correspond to the differential gauging reach numbers in Table 3.1.....	75
Figure 3.7: Specific conductivity of stream water from outlet at Star Main (0 m) to upper reaches of all forks for 2015 season: High flow (May 21), recession (July 7/8), and baseflow (Sept 8). Q1-16 correspond to the differential gauging reach numbers in Table 3.1.....	76
Figure 3.8: Flow contribution (as a percent of flow at the outlet) as a function of UAA. Flow contributions were calculated from differential gauging experiments at three flow conditions in 2015 and for baseflow in 2014. UAA for 1 m stream lengths were upscaled to total sub-reach contribution for each differential gauging sub-reach. All sites, including large alpine reaches, were included in the plots.....	77
Figure 3.9: Flow contribution (as a percent of flow at the outlet) as a function of UAA. Alpine reaches were excluded from the plots. Colours indicate the contribution of hillslope sizes (>10,000 m ²) within each differential gauging reach and transition from red to dark green represent only small hillslopes to many large hillslopes, respectively: Red - few sections were 10,000 - 20,000 m ² and one > 30,000 m ² , Yellow - eight sections were 10,000 - 30,000 m ² and one large draw > 100,000 m ² , Dark Green – few sections were 10,000 - 20,000 m ² , two sections 30,000 - 60,000 m ² and two large draws > 100,000 m ²	78
Figure 3.10: DI (solved for L) map with scaled colours. Red represents small L and shorter distances water must travel to decrease 10 m. Blue represents large L and longer distances water must travel to decrease 10 m. Insets were focused areas with identified seeps or tributaries and have a separate scale.....	79
Figure 3.11: Correspondence of regions with L >80 with surficial geology and bedrock geology.....	80
Figure 3.12: Potential solar radiation for the 2014 melt season (April 1 - June 20). Processed using Area Solar Radiation in ArcGIS.....	81
Figure 4.1: Map of Star Creek watershed. Suction lysimeter and hillslope groundwater well locations are magnified in green boxes. Map inset shows location of Star Creek in relation to North York Creek and the town of Coleman, Alberta.....	103
Figure 4.2: Bivariate plots of stream water chemistry at Star East Lower (left) and Star East Upper (right). Ions are measured in mg/l. Top half of plots represents the Pearson's correlation coefficient (r) for the linear relation between each solute.....	104
Figure 4.3: Bivariate plots of stream water chemistry at Star West Lower (left) and Star West Upper (right). Ions are measured in mg/l. Top half of plots represents the Pearson's correlation coefficient (r) for the linear relation between each solute.....	105

Figure 4.4: Box plots for Star East Lower showing the ranges in chemistry for potential sources..... 106

Figure 4.5: Box plots for Star East Upper showing the ranges in chemistry for potential sources..... 107

Figure 4.6: Box plots for Star West Lower showing the ranges in chemistry for potential sources..... 108

Figure 4.7: Box plots for Star West Upper showing the ranges in chemistry for potential sources..... 109

Figure 4.8: Star West Lower stream water chemistry from April to October in 2-D mixing space, which was derived from principal components analysis. Source water (precipitation, hillslope groundwater, till groundwater, and bedrock groundwater) was projected into the stream water mixing space. PC1 and PC2 represent the first and second principal components. 110

Figure 4.9: Star West Upper stream water chemistry from April to October in 2-D mixing space, which was derived from principal components analysis. Source water (precipitation, riparian water, and hillslope groundwater) was projected into the stream water mixing space. PC1 and PC2 represent the first and second principal components. 111

Figure 4.10: Star East Lower stream water chemistry from April to October in 2-D mixing space, which was derived from principal components analysis. Source water (precipitation, hillslope groundwater, till groundwater, bedrock groundwater, and seep 27) was projected into the stream water mixing space. PC1 and PC2 represent the first and second principal components. 112

Figure 4.11: Star East Upper stream water chemistry from April to October in 2-D mixing space, which was derived from principal components analysis. Source water (precipitation, hillslope groundwater, and seep 35) was projected into the stream water mixing space. PC1 and PC2 represent the first and second principal components. 113

Figure 4.12: Hillslope groundwater from all sub-watershed sites in 2-D mixing space, which was derived from principal components analysis of Star Main stream water. PC1 and PC2 represent the first and second principal components. 114

Figure 5.1: Conceptualization of runoff generation in Star Creek. Numbers on hydrograph correspond to numbers in subsurface block diagram and are described in Section 5.1. 121

Chapter 1. Introduction

The eastern slopes of the Canadian Rocky Mountains are a major source of Alberta's drinking water (Emelko et al., 2011) and a key habitat zone for threatened species such as Westslope Cutthroat Trout (*Oncorhynchus clarkii lewisi*) (Fisheries and Oceans Canada, 2014). However, extensive forest disturbance from forestry, wildfires, mining, and insect outbreaks occurs in this region. While hydrologists have been studying the effects of forest disturbance on streamflow quantity for over a century (Wagon Wheel Gap; Bates and Henry, 1928), responses are highly varied due to differences in disturbance type, vegetation type, and study location (which influences factors such as precipitation inputs and soil moisture storage) (Stednick, 1996; Brown et al., 2005). Several long-term research sites were established in Alberta in the 1960s and in more recent decades to determine the hydrological effects of forest harvesting in the eastern slopes and foothills of the Rocky Mountains (Spencer et al., 2016). A lack of significant change in streamflow was observed in Marmot Creek (Harder et al., 2015), Tri-Creeks (Andres et al., 1987; Goodbrand and Anderson, 2016), and the Crowsnest Pass (Southern Rockies Watershed Project) (Silins et al., 2016; Williams et al., 2015). Although Harder et al. (2015) suggested that this was due to complex subsurface flow pathways and large subsurface storage capacity, there is little known about runoff generation in these critical source water areas.

The eastern slopes have fractured and faulted, permeable sedimentary bedrock overlain by deep, unconsolidated glacial till and shallow soils (AGS, 2004). Thus, it is difficult to apply conceptualizations of runoff generation from steep mountain watersheds with shallow soils and/or relatively impermeable bedrock (e.g., Maimai in New Zealand (McGlynn et al., 2002), Fudoji in Japan (Uchida et al., 2003), HJ Andrews in USA (McGuire et al., 2005), and the Canadian Shield (Creed and Band, 1998; Buttle et al., 2004)) because flow pathways and runoff mechanisms could be substantially different. Further, much of this research is conducted in rain-

dominated areas so the climatological drivers (rainfall amount and intensity) would differ as well. Of the existing research in the eastern slopes, studies have been either conducted in the high alpine regions (e.g., McClymont et al., 2010; Hood and Hayashi, 2015; Paznekas and Hayashi, 2016), on the other side of the continental divide in British Columbia (e.g., Smith et al., 2014; Kuras et al., 2008), or using modelling work (DeBeer and Pomeroy, 2010; Fang et al., 2013). While we can learn from these studies and others in regions with permeable bedrock and/or deep glacial till (e.g., the Catskill Mountains in New York and Sleepers River Watershed in Vermont), there remains a clear need to develop a robust conceptualization of hydrological response for the eastern slopes to inform forest managers and determine how watersheds in this region may respond to forest disturbance.

Precipitation-runoff relationships

Runoff generation in steep forested watersheds is often dominated by subsurface flow (Weiler et al., 2005). While surface topography can control where saturation occurs (Anderson and Burt, 1978; Rinderer et al., 2016), subsurface topography can also be the dominant control on which areas of the landscape become saturated and ultimately contribute to runoff (Tromp-van Meerveld and McDonnell, 2006b). In these watersheds, depression storage needs to be filled before significant runoff can occur and has been shown to create threshold responses (Tromp-van Meerveld and McDonnell, 2006a, 2006b; Detty and McGuire, 2010a; Spence and Woo, 2003). For example, for 147 rainstorms in the Panola Mountain Research Watershed, Tromp-van Meerveld and McDonnell (2006a) found that below 55 mm of rainfall, little subsurface stormflow occurred, whereas above 55 mm of rainfall, subsurface stormflow was approximately two orders of magnitude greater.

Differences in rainfall-runoff responses can also be partly attributed to antecedent moisture and storage capacity in soil (Buttle et al., 2004) and glacial till (Burns et al., 1998; Shanley et al.,

2015). Buttle et al. (2004), for example, showed that thin soils resulted in a near linear rainfall-runoff relationship in the Experimental Lakes Region in Ontario; whereas, for thicker soils, antecedent wetness needed to be accounted for as well as rainfall depth. The importance of storage thresholds was also highlighted in the Gårdsjön Covered Catchment Experiment in Sweden, where runoff increased rapidly above a storage threshold of 230 mm (10% increase for every 1 mm of additional storage) (Seibert et al., 2011).

In regions with deep surficial deposits, precipitation and antecedent moisture patterns over longer time scales (e.g., inter-seasonal or multi-year) can drive runoff (Devito et al., 2005; Istanbuluoglu et al., 2012). Storage-runoff patterns are important to consider in steep mountain watersheds with high storage capacity as the variable or delayed release of water stored in the subsurface can be important for low streamflow discharge (Shanley et al., 2015; Floriancic et al., 2018). For instance, differences in low flow between years was mainly a function of storage potential in the Poschiavino watershed in Switzerland, where smaller storage potential prior to snow accumulation resulted in greater flows during the low flow season (Floriancic et al., 2018). Similarly, the age of groundwater contributing to summer low flows in the Catskill Mountains in New York was 6-22 months (Burns et al., 1998); again, showing that regions with high storage capacity can be influenced by longer time scales. Thus, storage capacity should be accounted for when modelling or conceptualizing runoff generation in these steep mountain regions with deep surficial deposits.

Hydrologic connectivity

Hydrologic connectivity between the hillslope and the stream (via subsurface saturated flow) was suggested as a way of understanding the structural controls on runoff generation (Hopp and McDonnell, 2009) and scaling runoff generation up to the watershed (Jencso et al., 2009). This is important because there can be areas within a watershed where storage has been filled

and saturation occurred, but if they are not connected to the stream they will not contribute to runoff (Gannon et al., 2014). Hydrologic connectivity is often driven by topography (Jencso et al., 2009; Detty and McGuire, 2010b; Covino and McGlynn, 2007). Jencso et al. (2009) concluded that hydrologic connectivity occurred for longer periods of time on hillslopes with larger rather than smaller upslope accumulated areas. However, the timing of hydrologic connectivity is not consistent between regions. Hydrologic connectivity occurred most frequently during the snowmelt period in the Tenderfoot Creek Experimental Forest in Montana due to increased watershed moisture (Jencso et al., 2009). In contrast, hydrologic connectivity was most prevalent during the dormant season in Hubbard Brook Experimental Forest in New Hampshire due to climate conditions and minimal evapotranspiration losses (Detty and McGuire, 2010a).

Watersheds with a history of glacial erosion and deposition can create complex subsurface flow pathways that are not necessarily visible in surface topography. Langston et al. (2011), for example, showed how a proglacial landscape (glacial alpine moraine) might contain features capable of blocking flow (e.g., ground ice and buried ice) and creating complex connections and disconnections between surface water features. Although this research examined surface water features rather than streamflow generation, it is relevant as subsurface glacial features occur throughout a watershed and have the potential to interrupt or complicate subsurface flow and hydrologic connectivity between the hillslope and the stream.

In snow-dominated watersheds, snowmelt can be the main time period when hydrologic connectivity occurs (McNamara et al., 2005; Kuras et al., 2008). However, snow accumulation and snowmelt may not be homogenous or continuous across a watershed (DeBeer and Pomeroy, 2010; Smith et al., 2014). Factors such as elevation, aspect, vegetation, wind, and energy inputs create a highly variable snowpack (Jost et al., 2007; DeBeer and Pomeroy, 2010). In steep watersheds, elevational gradients can result in rain or snowmelt occurring at lower

elevations, while snow was accumulating at higher elevations (Jost et al., 2007). Differences in snowpack depth and energy inputs may create some snow-free areas, while the snowpack is still melting in other areas (DeBeer and Pomeroy, 2010). This heterogenous distribution of snow accumulation and snowmelt can complicate where and when saturation and hydrologic connectivity occurs due to the subsequent variability in landscape wetness and antecedent conditions (Smith, 2011). While some research has begun to describe various aspects of runoff generation in watersheds with glacial deposits and/or sedimentary bedrock, such as runoff thresholds (Buttle et al., 2004), subsurface flow systems (Burns et al., 1998), and hydrologic connectivity (Detty and McGuire, 2010b), there is still a clear need to develop a conceptual model of runoff generation in steep snow-dominated mountain regions with both deep heterogeneous surficial deposits and permeable bedrock.

Southern Rockies Watershed Project

The Southern Rockies Watershed Project (SRWP) has been monitoring the hydrological impacts of the Lost Creek wildfire since 2004 and has found a significant impact on water quality parameters, such as nitrogen, phosphorus, dissolved organic carbon, and sediment (Silins et al., 2016). However, there were no significant differences in rainfall-generated quickflow in the 10 years after the fire (Williams et al., 2015). The SRWP was entering Phase II of the research in 2014, in which three harvest types (clear cut, strip cut, and variable retention) would occur in the three sub-watersheds (Star West, Star East, and McLaren, respectively) of Star Creek, a reference watershed from Phase I. Stream discharge has been monitored at three sites (Star Main, Star East Lower and Star West Lower) within the watershed since 2005 and two additional sites (Star East Upper and Star West Upper) since late 2008. Prior to the initiation of the research presented here, streamflow contributions for each of the sub-watersheds were calculated for four water years (2009-2012) and were highly variable between sub-watersheds. Star West Upper and Star East Upper sub-watersheds contributed more than the lower sub-

watersheds. Star East Lower contributed a small volume of flow to the overall watershed and was fairly consistent between years. In contrast, Star West Lower was highly variable between years, gaining or losing annual streamflow in various years. Star Lower (the mainstem below the confluence of Star East, Star West, and McLaren) gained more streamflow than all other sites, and more than the watershed area or annual precipitation would suggest. These differences in streamflow contributions suggested that runoff generation among sub-watersheds was complex and led to questions surrounding the storage and release of water in the subsurface of these sub-watersheds. This also suggested that before we could interpret the results from the forest harvest types in the three sub-watersheds used in Phase II of SRWP, we needed to develop a bespoke conceptual understanding of runoff generation in this snow-dominated region.

Thus, the main objective of this research was to develop a robust conceptual understanding of runoff generation in Star Creek by 1) quantifying precipitation-runoff relationships and watershed storage; 2) characterizing how and when hydrologic connectivity between hillslopes and streams occur, and; 3) characterizing differential source water contributions to streamflow across the dominant hydrologic season. The following chapters detail the research undertaken to address this main objective. Chapter 2 characterizes annual and seasonal precipitation-runoff relationships in the Star East and Star West sub-watersheds. Temporal and spatial variation in these dynamics were linked to quantifications of dynamic storage in the two sub-watersheds. Chapter 3 uses instantaneous stream discharge measurements and stream water chemistry to quantify streamflow contributions at a smaller scale than the sub-watershed. Structural and climatological controls were used to explain streamflow contributions at variable flow conditions to represent changes in hydrologic connectivity. Chapter 4 describes the temporal and spatial variability in source water and stream water using principal component analysis and end-member mixing theory. This chapter outlines when various potential stream water sources were contributing to stream water.

Collectively, results from these studies were used to develop a conceptual model of runoff generation (Chapter 5) to better understand how the combination of glacial till and fractured sedimentary bedrock may influence precipitation-runoff relationships, hydrologic connectivity, and runoff generation in steep watersheds in Alberta's southern Rocky Mountains. The conceptual model was used to infer why streamflow in these watersheds may not change following forest disturbance. Conceptualization of runoff generation in the eastern slopes are important for understanding the controls on flood events and climate change or disturbance effects on peak flows. Results from this research can be used by landscape managers to plan which regions might be best to harvest to limit the hydrologic effects of disturbance. The conceptual model will also help determine potential source zones and timing of dissolved organic carbon reaching the stream, an important parameter for drinking water treatability.

Chapter 2. Temporal and spatial variation in precipitation-streamflow dynamics and implications for resistance in the eastern slopes of Alberta's Rocky Mountains¹

2.1. Introduction

Increases in global surface temperatures due to climate change can increase the proportion of rain to snow, advance the timing of snowmelt, and reduce snow water equivalent in high elevation mountainous regions (Pomeroy et al., 2015). These changes in precipitation storage and input will directly affect the timing and quantity of runoff in responsive watersheds.

However, it is unknown how this may affect runoff dynamics in more hydrologically resistant or resilient watersheds due to the complex mechanisms driving runoff responses in these systems.

Standard conceptual models of runoff generation in mountainous watersheds have generally been developed in rainfall dominated landscapes with topographically driven runoff, local flow processes and relatively defined impermeable boundaries (Hewlett & Hibbert, 1967; Mosely, 1979; Uchida et al., 2003). Shallow soils and decreasing soil hydraulic conductivity with depth lead to low subsurface storage capacity, responsive watersheds, and visible changes in stream contributing area over time (variable source area concept; Hewlett & Hibbert, 1967).

Conversely, in mountainous regions with heterogeneous surficial deposits, permeable or fractured bedrock, or large subsurface storage capacity (in soils or glacial till), runoff generation is more complex (Gabrielli et al., 2012; Hale et al., 2016). In fact, some researchers suggested that these complexities increase mean transit times (Hale & McDonnell, 2016) and attenuate the runoff response to increased precipitation inputs thereby muting the impacts associated with forest disturbance and climate change (Harder et al., 2015).

¹ This chapter is currently being revised for publication in Water Resources Research

Differences in bedrock permeability and its control over storage and release of water has been the focus of recent multi-watershed comparison studies. Uchida et al. (2006) compared two physically similar steep watersheds with shallow soils in humid/wet climatic zones but differing bedrock permeability and water retention characteristics (Maimai, New Zealand and Fudoji, Japan). Greater bedrock permeability and soil drainable porosity in Fudoji resulted in longer mean residence time and larger potential storage, which in turn lead to more stable baseflows. Hale and McDonnell (2016) compared transit times for weathered fractured sedimentary bedrock in the Oregon Coast Range with less permeable volcanic bedrock in the Western Cascades Range where both shallow lateral flow and shorter mean transit times was more prevalent in watersheds with less permeable bedrock. Similarly, Pfister et al. (2017) also showed that mean transit times increased with greater bedrock permeability for 16 watersheds in Luxembourg. Watersheds with less permeable bedrock were more likely to fill watershed storage quickly and exhibit precipitation-runoff threshold behavior during wetter periods. Conversely, dampened peak flows and greater winter baseflows were observed in watersheds with highly permeable bedrock (Pfister et al., 2017).

The presence of glacial till deposits has been shown to add further complexity to subsurface flow pathways, storage and precipitation-runoff dynamics, but most studies have been conducted in lower relief (Amvrosiadi et al., 2017; Comer & Zimmerman, 1969; Shanley et al., 2015) or flatter boreal or peat dominated watersheds (Devito et al., 2005, 2012; Redding & Devito, 2008, 2010; Tetzlaff et al., 2015). In these studies, climatic controls and antecedent conditions (such as inter-annual variation in total precipitation or seasonal precipitation patterns) were critical in explaining groundwater table responses, landscape connectivity, and how or when streams responded to precipitation inputs (Devito et al., 2012; Nippgen et al., 2016; Tomasella et al., 2008). For instance, Devito et al. (2012) showed that antecedent precipitation from the previous years or seasons can play an important role in watershed storage and

precipitation-runoff patterns in subsequent years. Furthermore, the complexity and heterogeneity of subsurface deposits can lead to highly differing patterns of water release (e.g., hydrograph recession characteristics) between neighboring watersheds (Shanley et al., 2015). Few studies on precipitation-runoff dynamics in watersheds with significant till deposits have been conducted in steep mountainous watersheds (Kuras et al., 2008; Smith et al., 2014). For instance, Cotton Creek Experimental Watershed is a snow-dominated montane watershed with deep permeable glacial tills in southeast British Columbia (Smith et al., 2014). Variable saturated hydraulic conductivity at depth resulted in percolation-excess runoff pathways that largely controlled where runoff occurred (Smith et al., 2014).

The forgoing illustrates current gaps in conceptual understanding of watershed behavior for watersheds with complex multi-layered subsurface structures. In particular, the coupling of storage dynamics and precipitation-runoff responses is poorly understood for these systems. In the eastern slopes of the Canadian Rocky Mountains, fractured sedimentary bedrock is common in these folded and faulted regions and does not form an impermeable boundary for percolation of water. Deep glacial till, composed of a mixture of fine sediments to cobbles and other glacial features (e.g., moraines, and clay lenses), add complexity to the subsurface storage and flow pathways that are not evident from surface topography alone (Langston et al., 2011). While Harder et al. (2015) suggested that streamflow in this headwater region may be more resilient to climatic change and disturbance due to the large storage capacity and complex flow pathways, the mechanisms controlling the damping of disturbance effects on streamflow remain poorly understood. Snowpack storage is also an important factor in this region. The eastern slopes of the Canadian Rocky Mountains are snow dominated which governs how and when runoff occurs due to the above-ground storage of snowfall and the timing of snowmelt. Peak flow is often driven by the quantity of snow water equivalent in the higher elevation alpine zones because it contributes the most water to the stream (Harder et al., 2015). Snowmelt can

also recharge groundwater (Smith & Redding, 2012) or overwhelm percolation rates and result in a perched water table and lateral flow to the stream (Kuras et al., 2008; Smith et al., 2014). Due to this enhanced recharge, summer low flows can be sensitive to snow accumulation in alpine watersheds (Jenicek et al., 2016).

Complex precipitation-runoff relationships in mountainous regions with both thick surficial deposits and highly permeable bedrock are poorly understood. When considered together, the combination of watershed controls produced by multi-layered subsurface structures and seasonal snowpack storage create multiple possible flow pathways, large storage capacity and resistant or resilient watersheds. Star Creek watershed is a long-term instrumented watershed as part of the Southern Rockies Watershed Project (SRWP) in the eastern slopes of the Rocky Mountains (Figure 2.1). Phase II of the SRWP investigated, among other objectives, the hydrological implications of three harvest treatments in Star Creek's sub-watersheds. Runoff is generally thought to be topographically driven, but deep, heterogeneous surficial deposits from the Wisconsin glaciation may create complex subsurface flow that may not follow surface or bedrock topography. The main objective of this study was to characterize precipitation-runoff relationships in two adjacent Rocky Mountain watersheds with potentially complex subsurface structures consisting of thick surficial glacial deposits overlaying highly fractured permeable bedrock. The research approach included characterizing 1) both long- and short-term temporal variation in precipitation-runoff relationships and 2) spatial variation in precipitation-runoff relationships and dynamic storage among two adjacent sub-watersheds. These in turn were used to 3) develop a conceptual model to better understand how variation in the subsurface controls may govern precipitation-runoff relationships in historically glaciated Rocky Mountain regions. This is important to interpret differences in watershed responses to disturbance or climate change in mountainous regions.

2.2. Study site

Star Creek (10.4 km²; 49° 36' 37" N 114° 33' 22" W) is a snowmelt-dominated watershed, with peak streamflow occurring on average in late May. Average annual precipitation is 990 mm in the sub-alpine (1732 m a.s.l.) and 720 mm lower in the watershed at Star Main (SM; 1482 m a.s.l.). Precipitation falls as snow from October to April/May (50-60% of annual precipitation); summer convective storms and autumn rains dominate precipitation in the warmer seasons (June to September). Mean monthly temperatures range from 15 °C in July to -6 °C in December. The stream is comprised of two main forks (Star East (SE) and Star West (SW)) and a smaller ephemeral stream (McLaren). This study focuses on the East (1540-2516 m a.s.l.) and West (1537-2628 m a.s.l.) sub-watersheds, which are separated into upper and lower sections (Figure 2.1).

Forest cover is predominantly lodgepole pine (*Pinus contorta*) and subalpine fir (*Abies lasiocarpa*), with small proportions of Engelmann spruce (*Picea engelmannii*), white spruce (*Picea glauca*), trembling aspen (*Populus tremuloides*), and Douglas fir (*Pseudotsuga menziesii* var. *glauca*). In the alpine area (>1900 m), small shrubs and grasses grow on bedrock and talus slopes (Dixon et al., 2014; Silins et al., 2009). Soils are Brunisols (Silins et al., 2009); however, local variations in aspect, elevation, and soil moisture result in slight variations in soil horizons and soil depth throughout the watershed. The regional geology is composed of sedimentary bedrock from three geologic formations: Upper Paleozoic formation, Belly River-St. Mary Succession, and Alberta Group formation. In general, all formations are composed of shale and sandstone, with sporadic carbonaceous layers (AGS, 2004). The landscape has undergone glacial erosion and deposition as recent as the Wisconsin glaciation (Gov. AB., 1996). Surficial geology is composed primarily of colluvium, talus slopes, and slightly leached till.

SW sub-watershed has two natural reservoirs, a marshy wetland in the alpine and a small pond below Star West Upper streamflow gauging station; both maintain water year-round. The pond

was caused by a landslide that impounded the stream. Much of the stream above the Star West Upper gauging station flows over bedrock, whereas cobbles and pool-riffle sequences dominate the lower reaches. Permanent surface reservoirs are not present in SE sub-watershed. In the upper alpine area, ephemeral stream channels are dendritic and channels are composed of colluvium rather than bedrock outcrops. Tall vertical cliffs are present in most of the upper ridges of the alpine regions in both sub-watersheds, although Mt. McLaren is less vertical than Mt. Parish and Mt. Chinook so SE sub-watershed has slightly less vertical relief than SW sub-watershed.

2.3. Methods

2.3.1. Long-term temporal variation in precipitation-runoff relationships

2.3.1.1. Precipitation

Precipitation was measured at low elevation (SM, Star Confluence, Star Bench, McLaren, and North York Main) and high elevation (Star West High, Star East High, Star Alpine, North York High) sites from 2005 to 2014 with a Jarek tipping bucket gauge (Geoscientific, Vancouver, Canada) with an alter shield to reduce the effects of wind-driven undercatch. Gauges were fitted with anti-freeze overflow systems for measuring snow (water equivalent) during winter months. Mean area weighted annual precipitation was calculated for the watershed for each water year (WY) using the Thiessen polygon method. The start and end dates of each WY were variable and were determined by the date that snow started accumulating in the alpine area. This was based on continuous snow depth measurements (SR50 ultrasonic snow depth sensor; Campbell Scientific, Logan, UT, USA) at Star Alpine and precipitation phase (rain-snow) separation after Kienzle (2008). Total annual precipitation (WY) was compared to the 10-year mean annual precipitation to identify which years were above and below the 10-year mean.

2.3.1.2. Streamflow

Five hydrometric gauging stations were distributed throughout Star Creek. Star Main (SM), Star East Lower (SEL), and Star West Lower (SWL) stations were installed in January 2005. Star West Upper (SWU) and Star East Upper (SEU) stations were installed in October 2008. All stations have complete records from 2009 to 2014 WY. Although stream channels were relatively stable, stage-discharge relationships were developed for each of the stations for each year because channel cross-sections can change over multiple years. Stream discharge was measured with a SonTek velocity meter (SonTek/Xylem In., San Diego, CA, USA) 12-18 times from April to October each year based on the US Geological Survey streamflow gauging protocol. 10-minute continuous stage data from HOBO pressure transducers (Onset Computer Corp., Bourne, MA, USA) were converted into 10-minute discharge data, average daily discharge, and annual discharge. Discharge was converted into annual unit area discharge differential ($[\text{station discharge} - \text{upstream station discharge}]/\text{sub-watershed area}$; in mm d^{-1}) for each sub-watershed as an indicator of the contribution of each sub-watershed to streamflow.

2.3.2. Short-term temporal variation in precipitation-runoff relationships

2.3.2.1. Event-based rainfall-runoff responses

Daily precipitation data between July and September were separated into events, with a minimum event size of 5 mm and time between events of six hours. Stream unit area discharge was quantified at the start of the rainfall event and at the peak. The difference between stream discharge at the start of the event and at peak discharge was calculated for all events and referred to here as “event rise”. Rainfall-runoff responses were grouped and compared across dry (2009 or 2010) and wet (2013 or 2014) years.

Four hillslope groundwater wells were installed to depth of refusal (0.8-1.5 m) in summer 2013. Wells were located 30-50 m upstream from the streamflow gauging stations at SEL, SWL, and SWU and approximately 100 m downstream from the confluence on the mainstem. Water table

depth was monitored with Odyssey capacitance loggers (Dataflow Systems Ltd., New Zealand) at 10-minute intervals and a water level beeper (Heron Instruments Inc., Ont., Canada) every other week from April to October.

2.3.2.2. Seasonal antecedent conditions

Total precipitation was separated into winter precipitation (mainly snowfall), summer rainfall, and fall rainfall and were calculated for each sub-watershed (SE and SW) based on the Thiessen area weighted average of all precipitation gauges in and surrounding the watershed. The period covered by each category varied each year depending on when snow started accumulating in the winter (on average in late October) and when rainfall began in the spring (on average early May). Fall rainfall began September 1 each year as an estimate of when transpiration slowed significantly and groundwater levels rose. A lack of groundwater wells prior to 2013 did not allow for a dynamic classification for the start of fall rainfall. Annual runoff ratios were calculated for each WY and categorized based on total fall precipitation from the previous WY (dry fall or wet fall).

2.3.3. Spatial variation in storage characteristics

2.3.3.1. Water balance approach

Watershed storage is calculated most often in rain-dominated watersheds following a pronounced dry period to identify storage thresholds that explain the delay in streamflow response (Hale et al., 2016; Sayama et al., 2011). In this study site, snowmelt dominated the hydrograph; streamflow responses were initiated when snowmelt saturated the landscape and produced runoff. This was followed by summer conditions, where the landscape drained and subsurface flow pathways likely became disconnected. Rather than identifying thresholds associated with streamflow initiation as in other studies, we were interested in identifying the drying thresholds as flow pathways became disconnected following spring snowmelt and the differences in these dynamics between adjacent sub-watersheds.

Dynamic storage (dV), as defined in Staudinger et al. (2017), is the hydrologically active storage, which considers streamflow and evapotranspiration fluxes. dV (mm) was estimated using the water balance approach as described in Sayama et al. (2011):

$$dV = P - Q - ET \quad (1-1)$$

where P = precipitation (mm); Q = discharge (mm); ET = evapotranspiration (mm), as calculated with the Penman equation from climate station data (below). dV was calculated independently for each WY and represents how storage changed over the course of the WY starting at zero on October 15 of each year. We did not include the carry-over of storage from one year to the next. dV as calculated by the water balance approach will be referred to as dV_{WB} .

Meteorological parameters (e.g., net radiation ($W\ m^{-2}$) (NR-LITE, Campbell Scientific, Inc., Utah, USA), temperature ($^{\circ}C$)/relative humidity (%) (HMP50, Vaisala, Helsinki, Finland), and wind speed ($m\ s^{-1}$) (Model 05103, R.M. Young Company, Michigan, USA)) were measured at SM. Small periods of missing data were gap filled with data from surrounding stations (Star Alpine, North York Main, North York High, and South York) by linear regressions or direct replacement where linear regressions were not possible. These data were used to calculate potential evapotranspiration (PET) using the Penman Equation (E_o) (Dunne & Leopold, 1978):

$$E_o = \frac{\frac{\Delta}{\gamma}H + E_a}{\frac{\Delta}{\gamma} + 1} \quad (1-2)$$

where, H is net radiation ($cm\ day^{-1}$) and $\frac{\Delta}{\gamma}$ is Penman's dimensionless parameter (equation 1-4).

E_a describes "the contribution of mass-transfer to evaporation" ($cm\ day^{-1}$), which was calculated using the empirical relationship (Dunne & Leopold, 1978):

$$E_a = (0.013 + 0.00016\mu_2)(e_{sa} - e_a) \quad (1-3)$$

where, μ_2 = windspeed (km/day), e_{sa} = saturation vapour pressure (mb), e_a = atmospheric vapour pressure (mb). Penman's dimensionless parameter ($\frac{\Delta}{\gamma}$) was calculated by the following equation (Dingman, 2002):

$$\Delta = \frac{2508.3}{(T+237.3)^2} \times \exp\left(\frac{17.3T}{T+237.3}\right) \quad (1-4)$$

where, T = temperature (°C). Δ (kPa K⁻¹) is then divided by the psychrometric constant (γ , commonly estimated as 0.066 kPa K⁻¹).

Estimates of PET were reduced by a factor of 0.85 for an estimate of actual evapotranspiration (AET) after Pike (1964).

Errors in dV_{WB} can arise from each water balance component. Errors in streamflow measurement are assumed at approximately +/- 10% based on US Geological Survey and Water Survey of Canada approximations for the velocity-area method. Streamflow was measured weekly during high flows and every other week for the rest of the snow-free period to capture the large variation in streamflow. Streams are well armored and channels were generally stable throughout the year. Area weighted average precipitation was estimated using the Thiessen polygon method from distributed climate stations. While this method does not account for orographic effects, nine (seven in Star Creek and two in an adjacent watershed) well distributed precipitation gauges across a range of elevations enables robust estimation of watershed precipitation. The standard deviation of precipitation measured for the 2005-2014 WYs across precipitation gauge was approximately 10-14% of total precipitation at a particular gauge. Despite use of alter shields, under-catch associated with wind can still be a source of measurement error particularly in winter and would likely underestimate dV_{WB} . However, Cherlet et al. (2018) compared precipitation events in the winter and summer measured with the Jarek tipping bucket gauge with alter shield and a double fenced intercomparison reference gauge

with a weighing gauge (T-200B, Geonor, New Jersey, USA) and showed that most events matched closely between gauges (~4% difference in total precipitation). Undercatch was observed only for a few large snow events (Cherlet et al., 2018). Evapotranspiration is the largest source of error in dV_{WB} because it was not measured directly. The Penman equation estimates free-water evaporation based on meteorological parameters (atmospheric demand for moisture) measured at the bottom of the watershed. Thus, while not a direct measurement of evapotranspiration, this is likely a better estimate of water availability than a simple temperature-based estimate of PET. PET likely overestimates AET resulting in an overestimate of the range in dV_{WB} as more water would be removed from the water balance over the WY than was available to evaporate. A correction was applied to reduce PET to better approximate AET for a more conservative estimate of dV_{WB} . The corrected values were also compared to annual estimates AET as the sum of interception plus average transpiration from another study in a nearby watershed (Williams et al., 2019) and in Star Creek in 2016-2017, respectively. These estimates were within 5% of the corrected PET estimate on an annual timestep.

2.3.3.2. Baseflow recession

Baseflow recession dynamics can provide insights into the consistency of baseflow sources. Baseflow recessions were calculated for 2009-2014 WYs during times when evapotranspiration, rainfall and snowmelt were negligible (Kirchner, 2009; Sayama et al., 2011). Nighttime data were used to reduce the influence of evapotranspiration. Late summer baseflow data (July and August) were used to eliminate the snowmelt pulse that dominated the hydrograph during spring and early summer. Days with more than 1 mm of rainfall 6 hours prior to nighttime were removed to eliminate the effects of rainfall. Recession slopes ($-dQ/dt$) and average discharge were calculated for 4-hr periods (Q_1 : 19:00-22:59, Q_2 : 23:00-2:59, Q_3 : 3:00-6:59) to reduce small fluctuations in discharge that can be caused by instrument error (Sayama et al., 2011). For each

period $-dQ/dt$ and Q were calculated as $(Q_1 - Q_2)/4$, $(Q_1 + Q_2)/2$ and $(Q_2 - Q_3)/4$, $(Q_2 + Q_3)/2$, respectively (Sayama et al., 2011).

Assuming discharge is a function of watershed storage, the recession slopes were used to estimate dV_{Bf} for each sub-watershed as the difference in storage between average maximum and minimum discharge for the same late summer baseflow period (July and August) outlined above (Buttle, 2016; Kirchner, 2009). Here dV_{Bf} is used to signify the differences between these estimates and dV estimates from the water balance approach (dV_{WB}). We used multiple methods to estimate watershed storage to compare the similarities in results as parallel lines of evidence (Staudinger et al., 2017). To estimate dV_{Bf} from recession slopes, the discharge sensitivity function, $g(Q)$, was calculated for the same times as above ($ET \approx 0$, $P=0$; Kirchner, 2009):

$$g(Q) = \frac{dQ}{dS} \approx \frac{-\frac{dQ}{dt}}{Q} \mid P=0, ET \approx 0 \quad (1-5)$$

This discharge sensitivity function can be rearranged to estimate dS as:

$$\int dS = \int \frac{dQ}{g(Q)} \quad (1-6)$$

Baseflow recession plots were then reduced to a single-value function of discharge. Q and $-dQ/dt$ were binned for ranges in Q that represented at least 1% of the range in Q and for which the standard error was smaller than half the mean flow (Kirchner, 2009). An average of Q and $-dQ/dt$ values were calculated within each bin as a single value for each bin. Binned means were transformed and plotted as $\ln(-dQ/dt)$ and $\ln(Q)$ and a quadratic equation was fit to the data (Appendix A – Figure A1). The quadratic equation was used to determine the coefficients for:

$$\ln(g(Q)) = \ln\left(\frac{-dQ/dt}{Q}\right) \approx c_1 + c_2 \ln(Q) + c_3 (\ln(Q))^2 \quad (1-7)$$

Coefficients c_1 and c_3 come directly from the quadratic equation ($y=c_3x^2 + kx + c_1$), but c_2 was the recession slope (k) – 1 (Kirchner, 2009). Equation 1-7 was solved for $\ln(g(Q))$, which was subsequently transformed into $g(Q)$ and used in equation 1-5 to solve for dS . The relationship between dS and Q (Appendix A – Figure A2) was used to calculate dV_{Bf} . dV_{Bf} is the difference in calculated dS for the average maximum and minimum discharge from the recession slopes.

2.4. Results

2.4.1. Temporal variation in precipitation-runoff relationships

2.4.1.1. Long-term coupling

2.4.1.1.1. Precipitation patterns

When the total annual precipitation for each WY was compared to the 10-year average annual precipitation, clear wet and dry periods were evident (Figure 2.2). Total precipitation between 2008-2011 WY was less than the 10-year average annual precipitation (74-179 mm) while precipitation between 2013-2014 WY was greater than average (125-245 mm). Precipitation in 2012 was approximately average. The same analysis was performed for a longer-term precipitation record (1955-2016) from nearby Blairmore, AB (Alberta Climate Information Service; elevation of 1310 m) to determine if the dry and wet patterns associated with the 10-year record were visible in the longer 62-year record. The wet period showed much greater precipitation than the 62-year average (235-291 mm), but the dry years were not consistent across the period. Precipitation during the 2007-2008 WYs was 16-96 mm below the long-term average, while precipitation during 2009-2011 was 77-274 mm greater. Despite this difference, we still referred to the multi-year trends identified from the 10-year data record as the dry period (2008-2011) and the wet period (2013-2014) because these data were based on a much denser network of precipitation gauges at various elevations throughout the our specific study watersheds and it is not likely that storage patterns persist over multiple decades.

2.4.1.1.2. Annual unit area discharge

The transition from the multi-year dry period to multi-year wet period corresponded with an increase in annual streamflow (unit area discharge) from 2009-2014 (Table 2.1). While considerable variation was observed between sub-watersheds, most had less than average unit area discharge for 2009 and 2010 and above average unit area discharge from 2012 to 2014. SWL changed from a losing sub-watershed during the multi-year dry period to a strongly gaining sub-watershed from 2012-2014. For SEL there was a weaker increase in unit area discharge during the wet period. In general, the two alpine sub-watersheds (SWU and SEU) contributed most of the unit area discharge as a percent of the overall discharge at the outlet at SM. The trend for Star Lower (SL), the sub-watershed associated with the mainstem only (SL=SM-SE-SW-McLaren; Figure 2.1), was opposite from the other sub-watersheds. In the dry period, more discharge was measured at the gauging site than total incoming precipitation in the watershed (mean P = 840 mm/yr; 2009-2011). In the wet period, SL no longer contributed large quantities of discharge, rather it lost water in 2014, with less discharge than the combination of the tributaries above it. Star Lower discharge contributions (2615 mm) in 2011 far exceeded all other years and may be due to errors in streamflow gauging at SM, SEL, SWL, and/or McLaren. However, the same quality control measures were taken in 2011 as all other years so it is not clear why the discharge contributions were so large. Despite this, these data were included in Table 2.1.

2.4.1.2. Short-term coupling

2.4.1.2.1. Rainfall-runoff patterns

Despite the strong increase in unit area discharge across multi-year dry to wet periods, there was no difference in the hydrograph response for event-based rainfall-runoff responses between the dry and wet period in SE or SW sub-watersheds (Figure 2.3). No obvious differences in runoff responses were observed between months (July-September) despite

differences in hillslope groundwater levels over those months (Figures 2.4a and b). Hillslope groundwater wells responded primarily to snowmelt pulses or large rainfall events during the spring at SEL, SM, and SWU; SWL hillslope groundwater well remained dry year-round. For instance, the 50+ mm event in early June 2015 produced a large response in all wells, whereas a similar event in early September 2015 only produced a small response in the SEL groundwater well (Figure 2.4b). The water table may have responded below the depth of the well at all other locations, but this could not be verified. However, this does indicate that water levels were closer to the ground surface (and the landscape was wetter) in early June compared to early September. Similar responses were also observed for hillslope wells in 2014 (Figure 2.4a).

2.4.1.2.2. Winter precipitation-runoff patterns

The general relationship between winter precipitation and annual runoff ratios were poor. Rather, when antecedent conditions from the previous fall were accounted for, two trends in winter precipitation-runoff relations became evident (Figure 2.5). For years with a preceding wet fall, runoff ratios were greater than for years with a preceding dry fall.

2.4.2. Watershed storage

2.4.2.1. Temporal trends

In contrast to the relationships between dV_{WB} and runoff typically observed in rainfall dominated systems, cumulative dV_{WB} thresholds were counter-clockwise in these snow-dominated systems (Figure 2.6). The hysteresis observed here is due to the initial storage of snow above ground in winter months, followed by a sharp increase in discharge coincident with snowmelt, then a drainage period where both discharge and storage decreased. The overall ranges of cumulative dV_{WB} were smaller for 2006 and 2008-2011 (Average: 440 mm and 334 mm for SW and SE, respectively) and larger for 2007 and 2012-2014 (Average: 645 mm and 510 mm for SW and SE, respectively; Table 2.2). This pattern corresponded with the wet and dry precipitation

periods (Figure 2.2) and the increased unit area discharges (Table 2.1) because more water moved through the watershed in wet years than in dry years. An exception to this pattern was 2012, which was a transitional year with average precipitation but had a large range in cumulative dV_{WB} . Deficits in dV_{WB} occurred over each water year and would not be possible to sustain over multiple years. Some uncertainty exists in each water balance component, as discussed in Section 2.3.3.1., and would influence dV_{WB} estimates. Undercatch of precipitation, particularly over winter, and overestimation of AET are the likely drivers of the deficit.

2.4.2.2. Spatial trends

The differences in unit area discharge between SE and SW sub-watersheds (Table 2.1) can be partially explained by the differences in storage. For a similar range in discharge, SW had a larger mean range in dV_{WB} (521 mm) than SE (404 mm; Figure 2.6); a paired t-test indicated the difference was statistically significant ($p < 0.001$, $\alpha = 0.05$). Estimates of dV_{Bf} (from recession analysis) for July and August 2009-2014 further corroborate this hypothesis. SEL and SEU had the smallest dV_{Bf} (33 mm and 35 mm, respectively). SWL had the largest dV_{Bf} (118 mm) followed by SWU (52 mm). Estimates of dV_{Bf} are smaller than dV_{WB} because dV_{Bf} were based on recession flow in July and August rather than across the entire WY. The differences between SW and SE sub-watersheds may be due to larger snowpack, more evapotranspiration and the larger storage capacity in SW than in SE.

Baseflow recession characteristics were similarly different between SE and SW. August low flows in SEL had less minimum discharge than in SWL (Figure 2.7). Low flows in SWL did not drop below 0.03 mm/hr, whereas low flows in SEL dropped below 0.02 mm/hr. This suggests that baseflow in SWL had a more consistent source that maintained streamflow in late summer than in SEL and larger storage capacity. The small pond (0.25 ha) above SWL gauging station was likely not large enough to considerably influence or maintain late summer baseflow.

Additionally, similar patterns were observed above the pond at SWU, in which baseflow in all

years, except for 2012, did not fall below 0.04 mm/hr (Figure 2.7). The snowpack and summer rains from 2012 were approximately average so it is unclear why August low flows were the lowest on record, although it may be due to multiple years of dry conditions reducing the available storage potential. The storage associated with cirque tills and the year-round marshy area in SWU alpine may be partly responsible for maintaining baseflows in SW compared to those in SE.

2.5. Discussion

The results presented here provided insights into runoff generation processes in Star Creek. Large storage capacities suggest generally lower responsiveness to changes in precipitation forcing from forest disturbance or climate change than may be expected from other mountainous regions with shallower soils or tills and less permeable bedrock. Precipitation-runoff and storage dynamics observed here were used to develop a conceptual model, the precursor to modelling runoff generation in this region.

2.5.1. Temporal patterns in precipitation-runoff relationships

2.5.1.1. Long-term coupling

Annual precipitation in Star Creek watershed progressed from a dry period (2008-2012) to a wet period (2013-2014) over the years of record (Figure 2.2). Sequential multi-year patterns of lesser or greater precipitation can draw down or fill watershed storage and influence lagged behavior of watershed discharge (Devito et al., 2012). The influence of precipitation on streamflow was evident in annual unit area discharge trends over the same period (Table 2.1). For most sub-watersheds, 2009-2010 WYs had less than average discharge, whereas 2011-2014 WYs produced above average discharge. While this transition did not precisely match dry and wet years, the discharge trend was consistent with the broader precipitation pattern. The patterns were consistent with the long-term 62-year precipitation pattern where much greater

precipitation (270 mm) than average was observed from 2011-2014. The lowest baseflow for the years of record was in 2012 (Section 2.4.2.2.), which is consistent with the idea that watershed storage (specifically bedrock storage) was drawn down over a multi-year dry period (Devito et al., 2012). Multi-year precipitation patterns have also been shown to influence watershed storage and runoff ratios in other regions (Nippgen et al., 2016; Tomasella et al., 2008). For instance, the influence of precipitation from the previous year influenced runoff ratios the following year in Coweeta (Nippgen et al., 2016).

2.5.1.2. Short-term coupling

Although it appears that there were increases in precipitation and annual unit area discharge over the years of record, this did not lead to differences in event-based rainfall-runoff relationships. Other studies showed that wet antecedent moisture conditions increased subsurface lateral flow and runoff to streams compared to dry antecedent conditions (Ali et al., 2015; Devito et al., 2012; Pfister et al., 2017) and similar patterns were expected for the multi-year wet and dry patterns. However, neither SE nor SW watersheds showed a difference in runoff response between wet and dry years (Figure 2.3). The lack of difference between periods may have been partly due to the strong control of snowmelt on water table development. Shallow subsurface water tables (hillslope groundwater wells) responded primarily during snowmelt conditions (Figure 2.4). Smith et al. (2014) showed that snowmelt could overwhelm other runoff predictors (e.g., upslope contributing area and slope) during the spring freshet, which led to lateral flow in a snow-dominated watershed with deep glacial tills in southeast British Columbia. Similarly, Redding and Devito (2008) observed that while snowmelt in the Boreal forest can fill soil storage or overwhelm hydraulic conductivity mediated percolation and cause lateral flow, most rainfall events in that region do not. This suggests that multi-year precipitation trends regulated the baseflow component of the Star Creek hydrograph through vertical drainage in the soil or into the till rather than flowing laterally and contributing to

quickflow. In contrast, snowmelt and soil and glacial till storage were the primary controls on short-term trends such as rainfall-runoff dynamics. This also suggests that storage in this shallow subsurface zone functions as different flow system than deeper bedrock storage. A similar two system storage was suggested for the Catskill Mountains in New York, another region with glacial till and permeable sedimentary bedrock (Burns et al., 1998).

Jenicek et al. (2016) and Nippgen et al. (2016) argued the importance of multi-temporal scale precipitation patterns (monthly, seasonal, annual, multi-year) in the regulation of longer-term streamflow dynamics. Precipitation from September to mid-October (fall rainfall), during the period after evaporative losses from transpiration have declined or stopped, can fill shallow subsurface storage and increase the subsequent year's annual runoff ratios. The carry-over of storage and the difference in runoff were evident for both SE and SW sub-watersheds (Figure 2.5). More specifically, years categorized as dry fall or wet fall did not correspond with the multi-year dry and wet periods (Figure 2.2). These results are consistent with other studies showing that past precipitation can influence discharge on multiple temporal scales. Similar "watershed memory" was observed in the Coweeta experimental watershed in North Carolina, USA despite the shallow soils (1.2-3.5 m soil depth) (Nippgen et al., 2016). Similarly, groundwater fluctuations and streamflow had a multi-year memory responding to precipitation from the previous years or seasons in a humid Amazonian watershed (Tomasella et al., 2008). While this watershed had less topographic relief, deeper soils, and slower hydrologic responses than in Coweeta and Star Creek, similar patterns were observed in all three watersheds.

2.5.2. Spatial patterns in precipitation-runoff relationships

2.5.2.1. Sub-watershed comparison

Despite the lack of obvious differences in bedrock and surficial geology, considerable variation between sub-watershed responses was observed (Table 2.1). The pattern of transition from strongly increasing unit area discharge (in excess of incoming precipitation) during dry years to

average or losing discharge in wet years observed in the SL sub-watershed was opposite to that in all other sub-watersheds. The reason for this opposing trend is unclear and may be in part due to uncertainty in stream discharge measurements. In particular, very larger discharge contributions in SL in 2010 and 2011 may be enhanced due to compound uncertainties in discharge at SM, SWL, SEL, and McLaren. However, data are thoroughly assessed and quality controlled to develop reliable stage-discharge relationships and stream discharge hydrographs.

Watersheds with a history of glacial erosion and deposition can create complex subsurface flow pathways that are not visible in surface topography. For example, Langston et al. (2011) showed how a proglacial landscape (glacial alpine moraine) might contain features capable of blocking flow (e.g., ground ice and buried ice) and creating complex connections and disconnections between surface water features. While this research examined surface water features rather than streamflow generation, subsurface glacial features occur throughout a watershed and have the potential to interrupt or produce complexity in subsurface flow.

Similarly, Oda et al. (2013) showed that inter-watershed transfer of groundwater in the Tanzawa Mountains, Japan was responsible for large streamflow contributions in one watershed, compared to the adjacent watershed, which had a net loss of groundwater. They related this to the effective drainage area, suggesting that the area contributing to streamflow was likely larger than the surface area due to differences in subsurface topography (Oda et al., 2013).

Variation in watershed structural components, such as slope, soil drainage, jointing and faulting, can impose important additional hydrologic controls (Shanley et al., 2015). Structurally, the SW alpine region is surrounded by tall, near vertical headwalls that represents a large vertical subsurface hydraulic gradient and a large area for snow accumulation. In contrast, the SE alpine region does not contain the same near vertical headwalls around the entire alpine region but is partly surrounded by a more moderate, rounded peak and talus slopes of Mt. McLaren. Consequently, the SE alpine region does not have the same vertical hydraulic gradient that is

present in SW and may not have the same folding or fracture patterns. Watershed elevation, and in turn, the increased influence of snow can also influence streamflow behavior such as summer low flows and drought sensitivity (Staudinger et al., 2015). Furthermore, the alpine area in SW contains water year-round in a marshy area due to the presence of cirque tills and the stream is composed primarily of exposed bedrock starting at the outlet of the marshy area, whereas the stream channel in the SE alpine area is composed of colluvium with little exposed bedrock and goes dry mid-summer. Others have shown that these kinds of structural components can lead to important differences in runoff generation processes (Gabrielli et al., 2012; Hale & McDonnell, 2016) and hydrograph recession even in topographically similar neighboring watersheds (Shanley et al., 2015).

Despite consistencies in multiple lines of evidence that SW likely has a larger storage capacity than SE, some anomalies exist in the data. For instance, SW has higher runoff ratios (Figure 2.5), larger response to storms (Figure 2.3), and higher overall yield (Table 2.1) than SE. Moreover, the runoff ratios in SW often approached 0.8 when a wet fall preceded the WY, which is higher than expected for a watershed with large storage capacity. Undercatch of precipitation and uncertainties in stream discharge measurements may cause some of these inconsistencies. The inter-basin transfer of water may also partly explain the differences in runoff between SW and SE. However, more research is needed to expand the ideas presented in this chapter and determine potential explanations for these seemingly inconsistent results.

2.5.2.2. Shallow subsurface storage

While storage processes represented by dV_{Bf} and dV_{WB} metrics have been associated with streamflow response (Hale et al., 2016; McNamara et al., 2011; Sayama et al., 2011), dV_{WB} calculated using the water balance approaches has been almost exclusively examined for rainfall dominated watersheds (Hale et al., 2016; Pfister et al., 2017; Sayama et al., 2011). To the authors knowledge, Staudinger et al. (2017) was the first to use this analysis in snow

dominated watersheds, however, they did not describe the hysteretic pattern shown here. The timing of the subsurface disconnection of the hillslope and the stream (Figure 2.6) as dV_{WB} becomes negative (also reflected in groundwater well response) is an important threshold associated with storage capacity in the shallow subsurface (soil and glacial till). Thus, the range in cumulative dV_{WB} is important to compare different watersheds to assess potential differences in subsurface storage. SW had a larger range in cumulative dV_{WB} (521 mm) than SE (404 mm) suggesting that SW has a larger storage capacity. dV_{Bf} estimates reflect a similar pattern but values were much smaller because they exclusively represent baseflow conditions when much less water moved through the system. dV_{WB} estimates were similar to those reported by Hale et al. (2016) for a headwater watershed (485 mm) and at the downstream outlet (501 mm) in the Central Coast Range in Oregon. The region has similar geology (highly fractured sedimentary bedrock) and shallow soils as Star Creek watershed but has a saprolite layer rather than glacial till. Hale et al. (2016) attributed their dV_{WB} values to shallow subsurface storage (saprolite and highly fractured upper layer of bedrock 2-10 m thick), noting that total storage was an order of magnitude greater when taking into account the deeper fractured bedrock. Sayama et al. (2011) also reported similar estimates (232 - 651 mm) with the larger dV_{WB} for the watersheds with steeper slopes which are comparable to Star Creek. Hillslope groundwater well responses further corroborates the difference between SE and SW watersheds because although all wells responded during snowmelt, only the SEL groundwater well responded in the late summer (Figure 2.4), again, suggesting a smaller storage capacity than in SW. More wells are needed to substantiate these findings because hillslope groundwater levels can be influenced by factors other than storage, such as upslope accumulated area, variability in soils, and local slope (Jencso et al., 2009; Rinderer et al., 2014; Detty and McGuire, 2010b).

2.5.2.3. Deeper bedrock storage

Deeper bedrock storage cannot be estimated without the use of hydrological models (Staudinger et al., 2017; Shaw et al., 2013; Kosugi et al., 2011) or isotopes (Hale et al., 2016; Ajami et al., 2011). However, recession analysis can provide insights on the consistency of baseflow or groundwater sources to estimate differences in deeper bedrock storage (Sayama et al., 2011). August baseflows (discharge) in SEU were less than in SWU (Figure 2.7) suggesting that SWU had more consistent groundwater sources that maintained baseflow above 0.04 mm/hr., whereas the source of baseflow in SEU became depleted through the summer. This was also reflected in temporal variability (coefficient of variation) of sub-watershed unit area discharge (Table 2.1) where SWU was less variable than SEU (CV=0.19 and 0.25, respectively; Figure A3). The maintenance of greater flow in SWU watershed may be in part due to the larger alpine region and a larger snowpack in SWU because differences in snowpack composition can directly influence groundwater and streamflow response as snow in the upper watershed recharges bedrock groundwater sources (Jenicek et al., 2016; Smith et al., 2014). Other studies have shown that larger bedrock storage can result in greater or more stable baseflow (Pfister et al., 2017; Shanley et al., 2015; Staudinger et al., 2015; Uchida et al., 2006; Burns et al., 1998). While Shanley et al. (2015) showed that high storage capacity and low permeability dense glacial till in Vermont, USA could sustain baseflow through slow release of groundwater, the persistence of snow and a larger storage capacity in high elevation watersheds in Switzerland were responsible for maintaining flows during drought years when compared to lower elevation watersheds (Staudinger et al., 2015). This suggests that SW watershed likely had both greater shallow subsurface storage and a larger deep bedrock storage compared to SE.

Many other studies stress geologic and subsurface characteristics (e.g., fractures and porosity) as key factors regulating variable storage capacity (Gabielli et al., 2012; Pfister et al., 2017; Uchida et al., 2006). Gabielli et al. (2012) hypothesized that fractured bedrock added an

additional flow pathway and resulted in seepage losses in the HJ Andrews watershed in western USA, compared to the relatively impermeable Maimai watershed in New Zealand. Uchida et al. (2006) compared two relatively similar watersheds, Fudoji watershed in Japan (permeable bedrock) to Maimai watershed in New Zealand (nearly impermeable bedrock) and showed that more permeable bedrock resulted in greater storage capacity. In general, I hypothesize that the fractured bedrock and the permeable glacial till in Star Creek promoted both deep percolation and high storage rather than lateral flow for much of the year (Figure 2.4). While no notable differences in subsurface characteristics were evident during well installations or were visually evident in bedrock outcrops, extensive subsurface characterization was not possible across the 10 km² watershed. Thus, it is unclear whether differences in bedrock permeability due to fracturing or glacial till depth or texture were key factors driving the differences in runoff dynamics we observed between the SE and SW sub-watersheds.

2.5.3. Runoff mechanisms and the implications for resistance to change

The results of this study provide important conceptual insights into higher-order controls on precipitation-runoff dynamics exerted by watershed storage in post-glacial mountain regions with permeable fractured bedrock. While recent studies have shown that fractured or permeable bedrock was a key subsurface storage zone (Chen et al., 2018; Hale & McDonnell, 2016; Uchida et al., 2006) and deep soils or glacial till create complex subsurface flow pathways and large subsurface storage (Kuras et al., 2008; Shanley et al., 2015; Dahlke et al., 2012), none have quantified storage in multi-layered permeable subsurface storage structures. The combination of deep glacial till and permeable fractured bedrock adds further complexity to runoff generation dynamics (Detty and McGuire, 2010a; Burns et al., 1998) that likely leads to hydrologic resistance in the eastern slopes of the Canadian Rocky Mountains. The results described here suggest there were likely two zones of storage within these watersheds: shallow subsurface storage (soil and glacial till; (2) in Figure 2.8) and deeper bedrock storage (fractured

bedrock; (3) in Figure 2.8). Shallow subsurface storage was likely important for the carry-over of precipitation effects and streamflow response during snowmelt or for large events in late summer. Hillslope groundwater wells responded only during snowmelt and during larger events (Figure 2.4) likely due to a large shallow subsurface storage capacity. Event-based analyses showed no difference between multi-year wet and dry periods (Figure 2.3) because event flows were mediated by snowmelt ((1) in Figure 2.8) and shallow subsurface storage rather than bedrock storage. Further separation of storage in soil and glacial till requires analysis of water chemistry data and installation of wells in the till to determine how responses between these layers differ. Quantifying soil characteristics, such as porosity, water retention, and saturated hydraulic conductivity, would further clarify the differences between these layers. Annual discharge patterns were affected by multi-year precipitation patterns, which were likely more strongly influenced by bedrock storage (Table 2.1). The influence of variation in multi-year precipitation was only observable from spatial patterns in sub-watershed annual unit area discharge and not the event-scale runoff because at the annual time-step baseflow was a major contributor to streamflow (60-70% of annual flow).

Watersheds with steep slopes, permeable bedrock, and deep soils or glacial till have the potential for larger storage capacity and, in turn, may retain the excess water and buffer the stream from change (Harder et al., 2015). Conversely, watersheds with steep slopes and shallow bedrock may be more responsive to disturbance because there is little storage for the excess water to be retained. Understanding these dynamics are essential in developing a conceptual model of runoff generation to ensure that process-based models are accurately representing watershed flow systems and uncertainty in model predictions are minimized. These results also aid in the interpretation of streamflow responses following disturbance in watershed scale studies. Rather than focusing on the specific heterogeneities of runoff generation in a watershed, we can focus on larger storage features (Buttle, 2016; McNamara et

al., 2011) and watershed responsiveness (Carey et al., 2010) to determine whether a watershed may be resistant to change.

2.6. Conclusions

Multi-year precipitation patterns changed from dry (2008-2011) to wet (2013-2014) conditions, which caused an increase in unit area discharge for all but one sub-watershed. Despite a change in annual flow contribution and total discharge, event-scale rainfall-runoff responses did not change. Annual runoff ratios were influenced by the carry-over of storage from the previous fall and were larger following a wetter fall than a drier fall. Two zones of subsurface storage were identified based on precipitation-runoff dynamics and storage estimates: shallow subsurface storage and deeper bedrock storage. Shallow subsurface storage includes the soil and glacial till layers and influences event runoff, hillslope connectedness that was controlled by snowmelt, and the carry-over of precipitation from fall to the next WY. Deeper bedrock storage influences annual discharge because of the dominance of vertical percolation and groundwater recharge and high annual groundwater contribution to streamflow. Isotopic analyses are needed to determine the approximate age of the stored water and confirm these interpretations.

Despite the differences observed between sub-watersheds in Star Creek, watersheds in the eastern slopes are likely resistant to change due to deep surficial deposits, fractured sedimentary bedrock, large groundwater contributions, and complex subsurface flow pathways. Understanding these runoff generation mechanisms and the variation in precipitation-runoff response is important for understanding how a watershed might respond to disturbance or climate change. Storage should be better incorporated into conceptual models applied to these mountainous watersheds to better understand how they may respond to change. Multi-year and inter-annual precipitation patterns need to be considered to reduce the uncertainty in post-disturbance impacts on streamflow.

2.7. Tables

Table 2.1: Annual unit (sub-watershed) contribution of streamflow depth (mm yr⁻¹)

Year	SWU	SEU	SWL	SEL	SL
2009	694	361	-48	119	934
2010	840	497	108	210	1183
2011	1228	633	-146	435	2615
2012	1025	743	356	405	600
2013	1031	702	524	335	602
2014	900	706	994	593	-402
Mean	953	607	298	350	922

Table 2.2: Range in dynamic storage (dV_{WB} ; mm) for water years in dry and wet periods.

Year	dV_{WB} range (mm)	
	SW	SE
2006	514	396
2008	412	326
2009	342	242
2010	312	222
2011	570	442
Dry period mean	430	326
2007	667	540
2012	697	535
2013	492	408
2014	684	528
Wet period mean	635	503

2.8. Figures

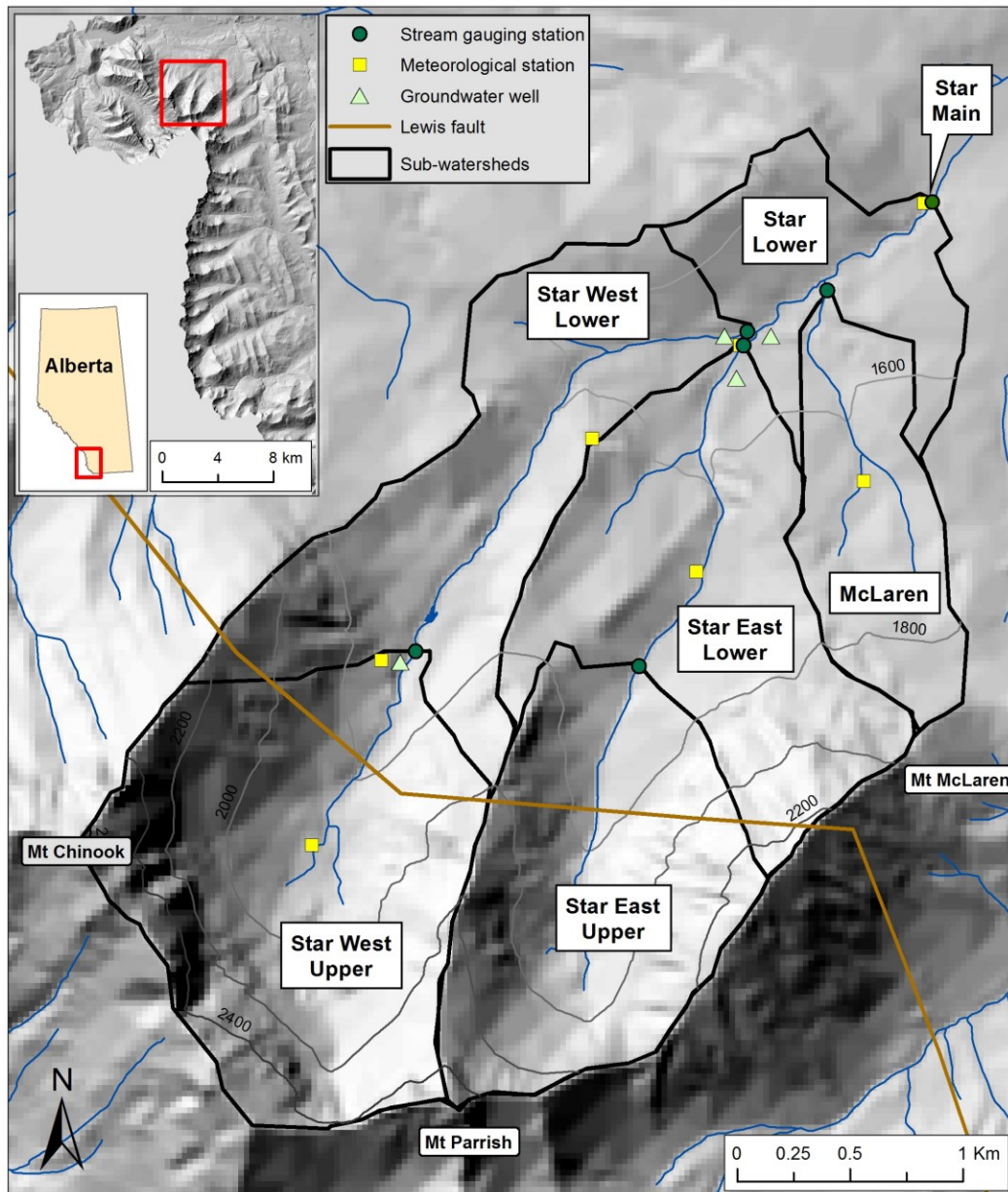


Figure 2.1: Map of Star Creek watershed in southwest Alberta, Canada.

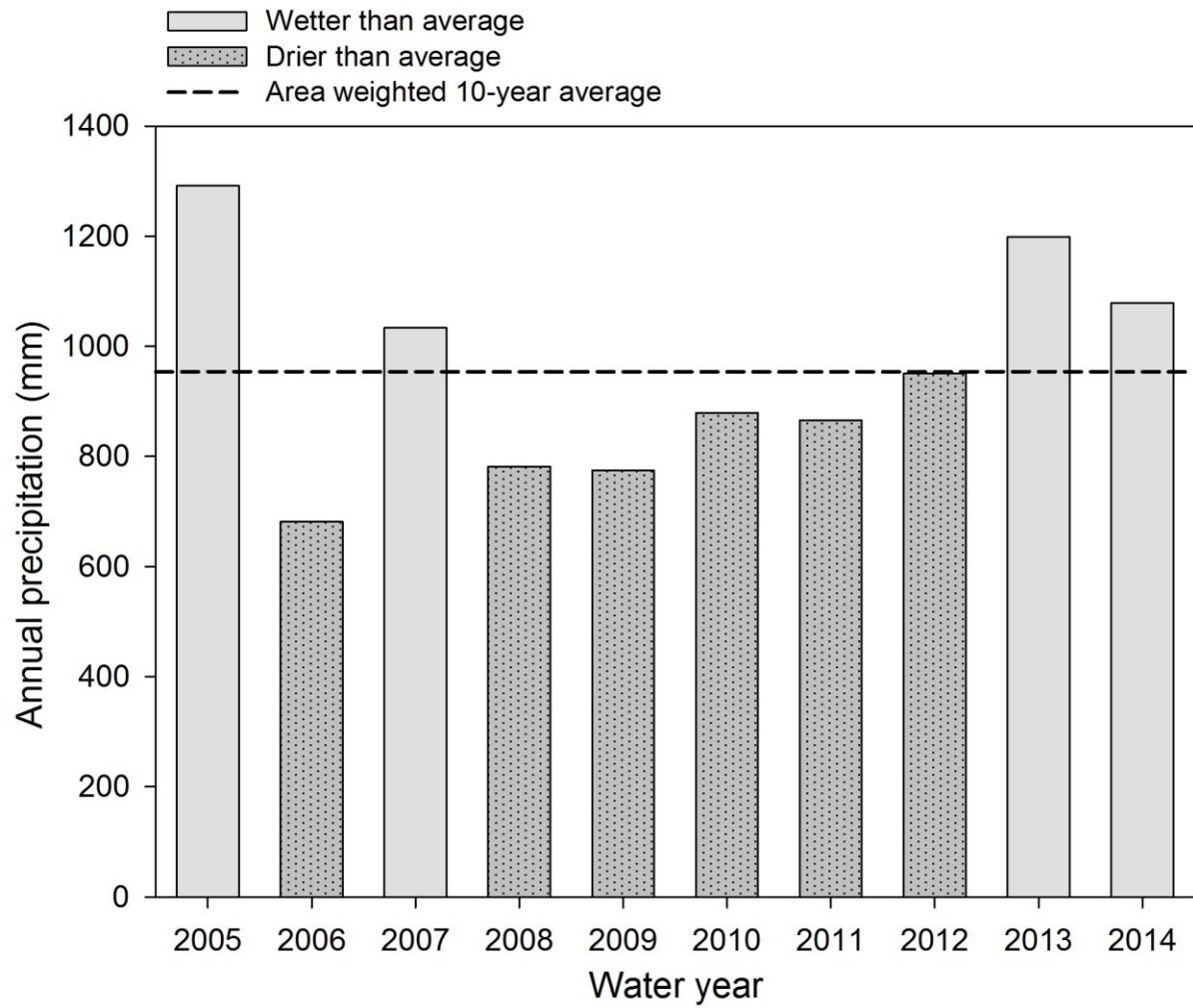


Figure 2.2: The difference between area-weighted annual precipitation and the 10-year mean annual precipitation across the water years of record for Star Creek watershed.

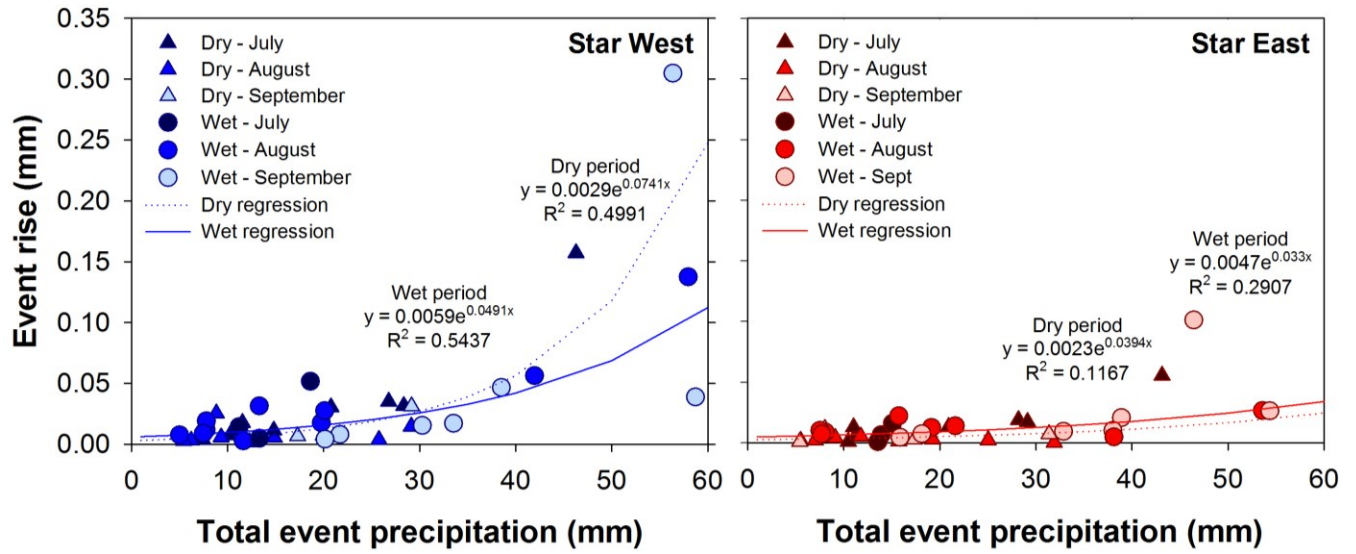


Figure 2.3: Event-based comparison between dry and wet periods for SW and SE forks. Rise in discharge (hydrograph response; mm) as a function of event precipitation (mm).

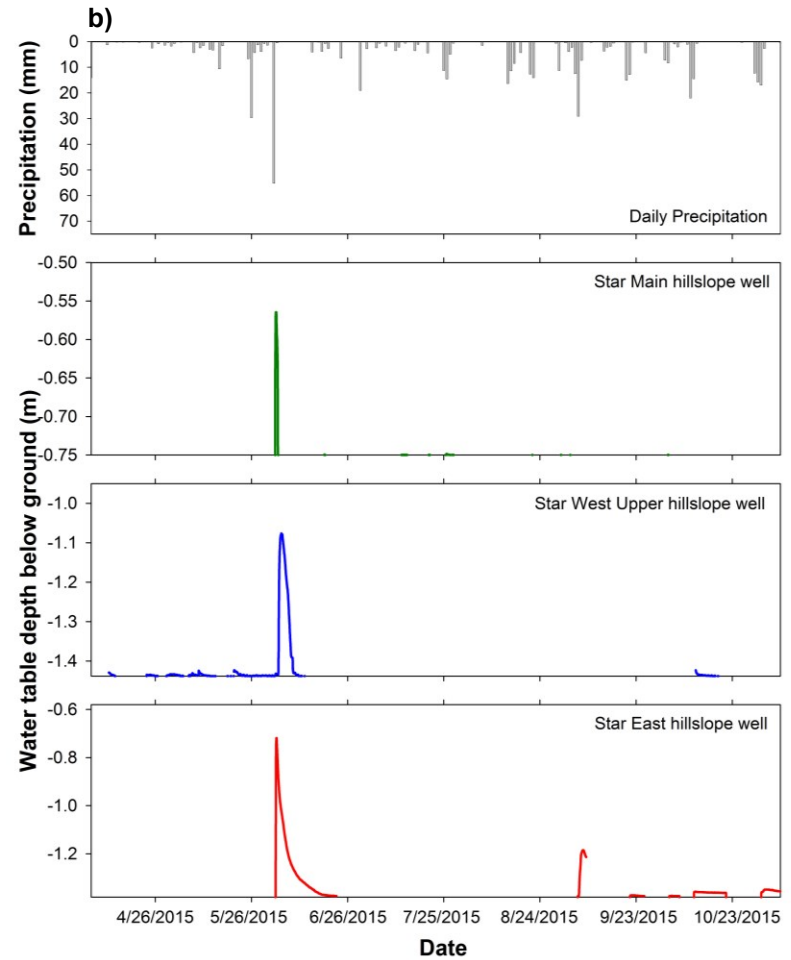
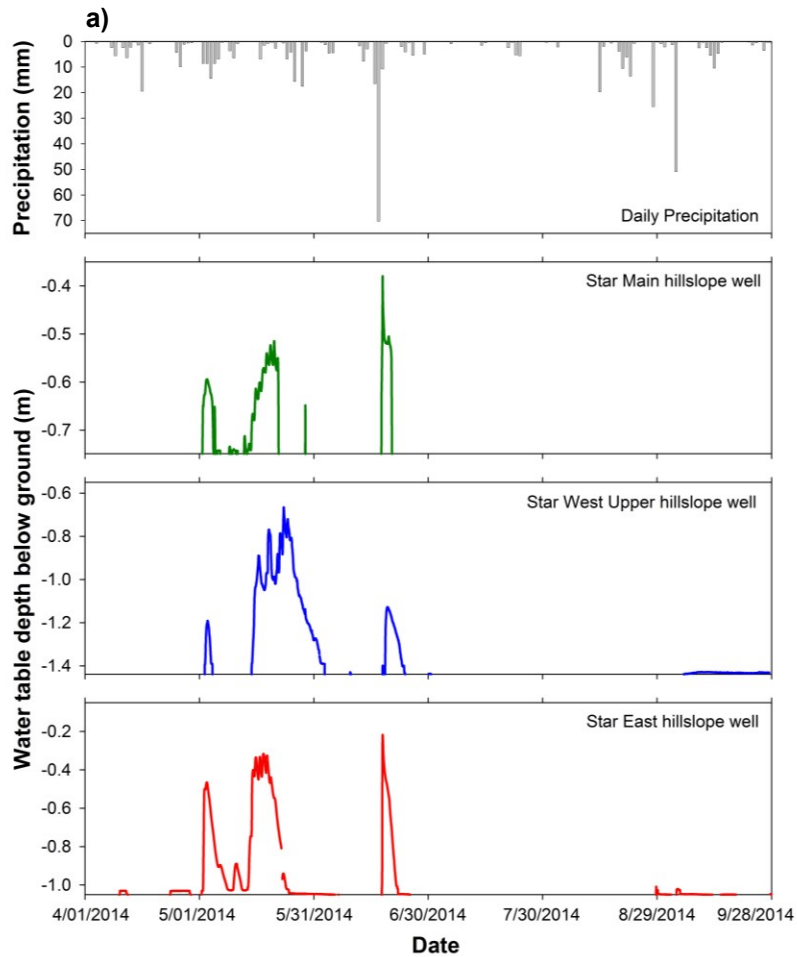


Figure 2.4: Hillslope well responses from 3 locations in Star Creek (Star Lower, SEL, SWU). a) 2014 water year. Hillslope responds during snowmelt and during large storm (70 mm) in early summer. Large storm in late summer only resulted in small groundwater well response (50 mm). b) 2015 water year. Similar patterns were observed but drier conditions resulted in lower groundwater levels.

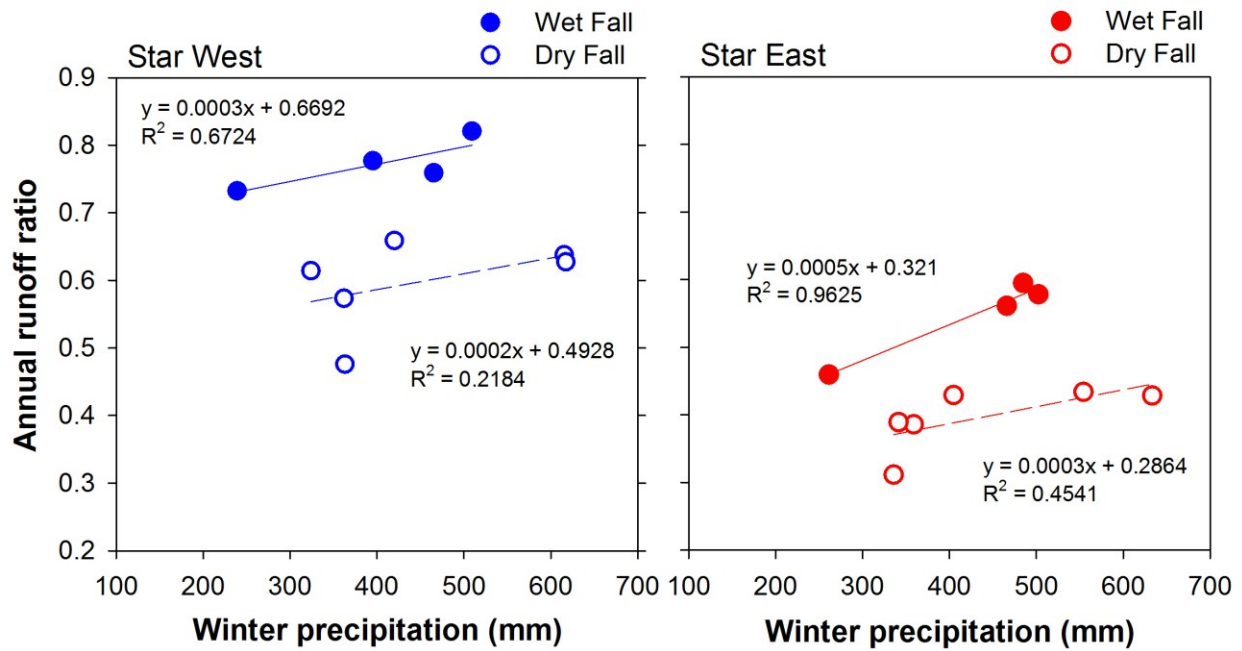


Figure 2.5: The relationship between annual runoff ratios and winter precipitation for SW (blue) and SE (red) watersheds. Closed circles represent years with wet conditions the previous fall. Open circles represent years with dry conditions the previous fall.

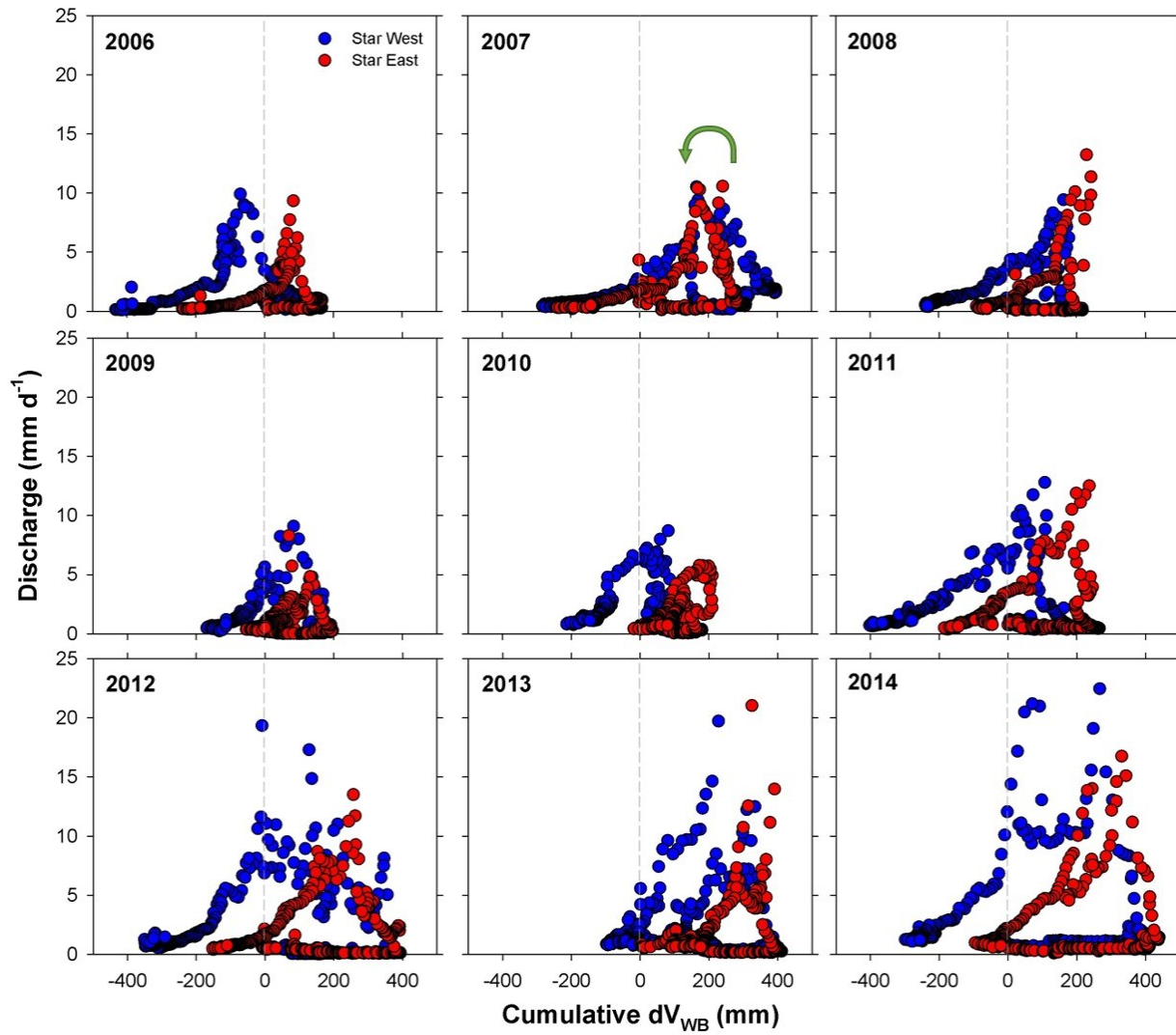


Figure 2.6: Relationship between watershed storage and stream discharge for 2006 to 2014 water years. SW in blue and SE in red. Water year starts at zero cumulative dV_{WB} (mm, grey dashed line) and hysteresis loop goes counterclockwise (green arrow).

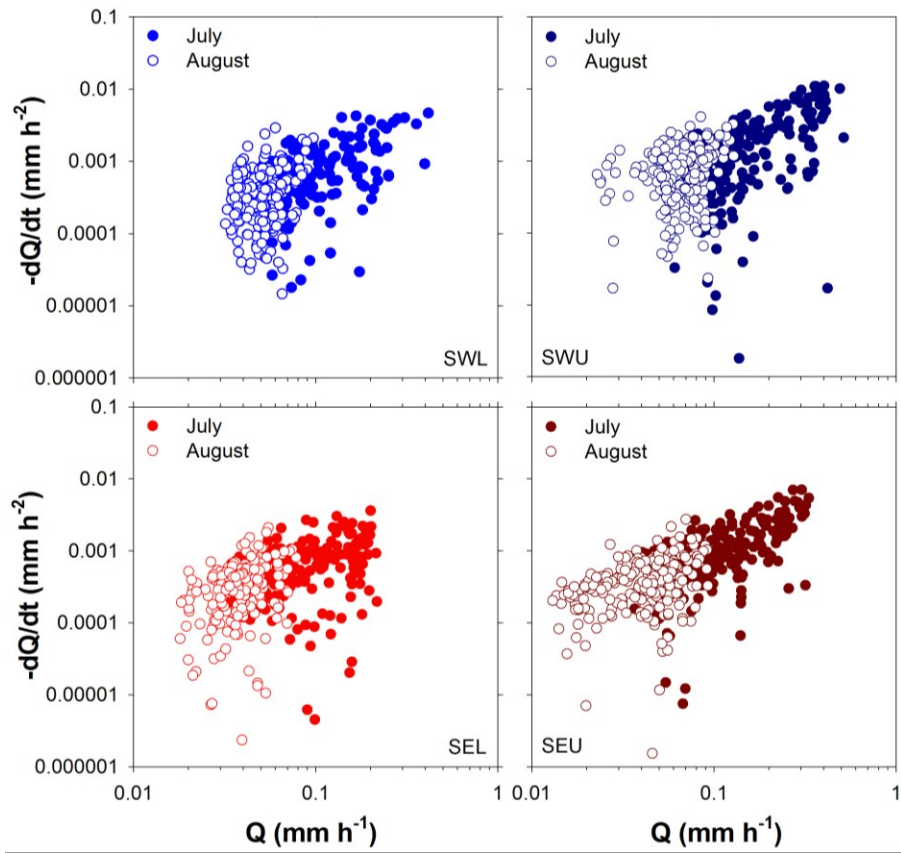


Figure 2.7: Recession analysis plots for Star West Lower (SWL), Star West Upper (SWU), Star East Lower (SEL), and Star East Upper (SEU).

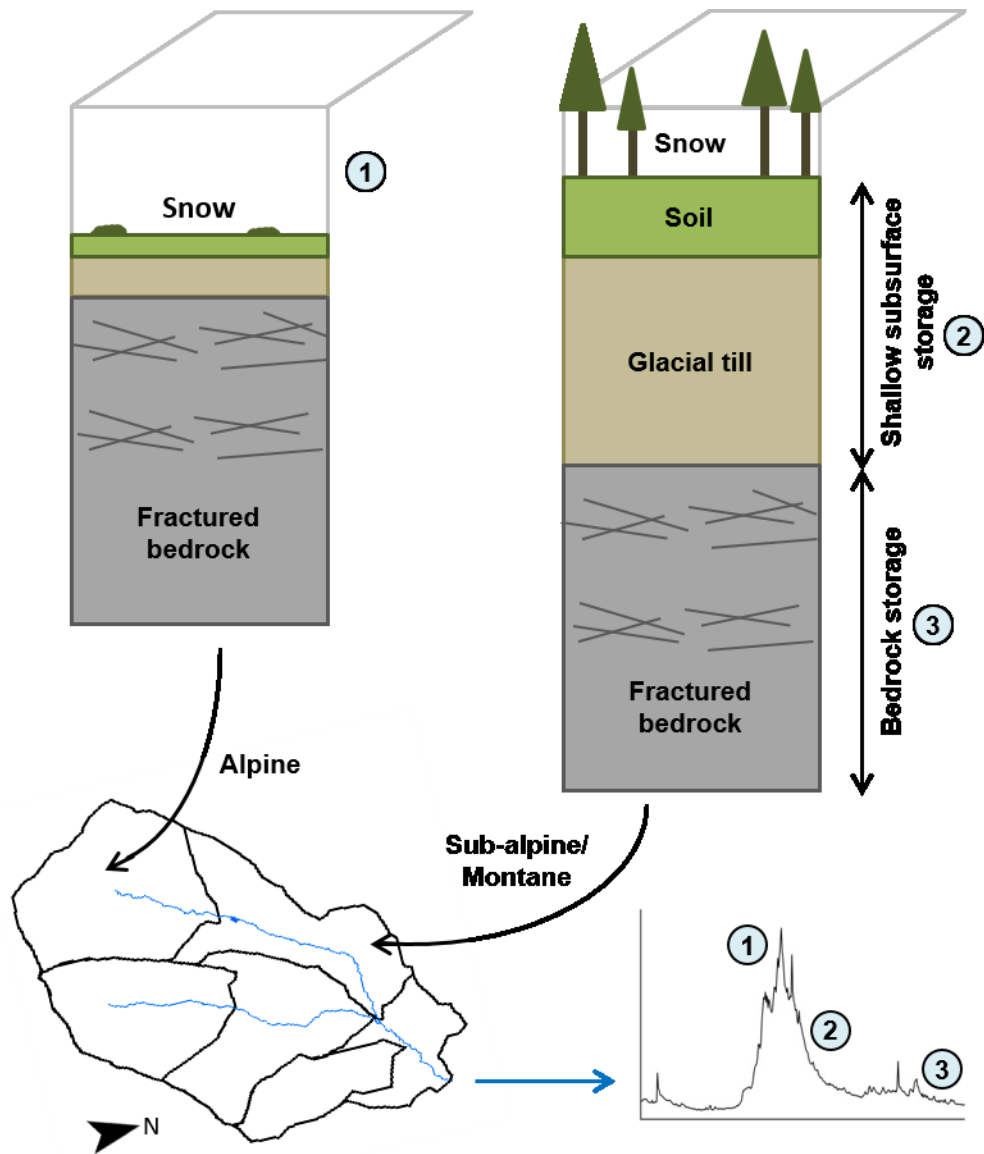


Figure 2.8: Conceptual block diagram of storage zones for alpine and sub-alpine regions in Star Creek watershed and the eastern slopes of the Rocky Mountains. Hydrograph was compiled from mean daily discharge at SM station at the outlet of Star Creek. Numbers on block diagrams and hydrograph refer to the portion of the landscape that is driving the corresponding portion of the hydrograph.

Chapter 3. The influence of watershed structure and climatic regimes on subsurface streamflow contributions in a steep watershed in Alberta's southern Rocky Mountains

3.1. Introduction

The eastern slopes are a critical source area for Alberta's drinking water supply (Emelko et al., 2011) and a key habitat zone for threatened and endangered fish, such as Westslope Cutthroat Trout (*Oncorhynchus clarkii lewisii*) (Fisheries and Oceans Canada, 2014). This area is heavily impacted by forest disturbance (e.g., forestry, wildfire, insect outbreaks), which can alter streamflow quantity at the watershed scale (Stednick, 1996), heightening the need to understand the effects of disturbance on local hydrology. Runoff in steep mountain watersheds is often dominated by subsurface flow due to highly conductive soils (Weiler et al., 2005) and hydrologic connectivity, the connection of the hillslope to the stream along a subsurface saturated layer (Jencso et al., 2009; Blume and van Meerveld, 2015). Hydrologic connectivity is controlled by watershed structure such as topography, soil characteristics, bedrock geology, and surficial geology (Uchida et al., 2006; Jencso et al., 2009; Jencso and McGlynn, 2011) and climate characteristics such as rainfall intensity, snow accumulation, and snowmelt (Detty and McGuire, 2010a; Tromp-van Meerveld and McDonnell, 2006b; Jost et al., 2007). However, many of these studies have been conducted in watersheds with shallow soils and impermeable bedrock so it is not clear how or when hydrologic connectivity occurs in a steep watershed with glacial till and permeable bedrock.

Topographic controls

Topography has long been used to describe throughflow contributions on hillslopes and scale these relationships to conceptualize watershed runoff mechanisms (Anderson and Burt, 1978). Many studies continue to use topographic indices, such as the Topographic Wetness Index, as an indicator of throughflow contributions because they can be effective in determining soil

moisture dynamics, groundwater levels, vegetation patterns, and hydrologic connectivity (Sørensen et al., 2006; Ali et al., 2014). Upslope Accumulated Area (UAA) (Grabs et al., 2010) has also been used as an index of hydrologic connectivity and to upscale the relationships to the watershed (Jencso et al., 2009). A key assumption for topographic indices, however, is that surface topography is a good proxy for bedrock topography and subsurface flow dynamics, which is not always the case. Watersheds with deep soils, glacial till, or permeable bedrock do not function with the same runoff processes as watersheds with shallow soils and, as a result, the water table does not always follow surface topography (Ocampo et al., 2006; Kuras et al., 2008; Smith et al., 2014). Rather, the structure of the watershed and its position in the landscape may determine the dominant subsurface flow pathways that should be considered in conceptual models and confirmed with field observations.

Geologic controls

Multiple permeable subsurface layers complicate the runoff response and make it challenging to characterize hillslope throughflow contributions because stream water can be lost to groundwater and groundwater can contribute to the stream along the stream length (Covino and McGlynn, 2007; Payn et al., 2012). In addition to stream and groundwater interactions, recent studies have also raised the importance of groundwater storage as a factor that can control the contributions of water to streamflow in alpine headwaters (Hood and Hayashi, 2015; Cowie et al., 2017). Geographical indices may be better suited to identify groundwater gradients and upscale streamflow contributions in watersheds where groundwater inflows dominate streamflow contributions (Hjerdt et al., 2004; Ali et al., 2014). For example, the Downslope Index (DI) identifies “how far a parcel of water has to travel along its flow path to lose a given head potential, d (m)” and has been used to identify convergent areas in the watershed as a proxy for groundwater discharge zones (Hjerdt et al., 2004). Transitions in slope from steeper to flatter

(identified by the DI) could create a hydrologic knickpoint where groundwater discharge may occur.

Climatic controls

While watershed structural characteristics have a large impact on runoff dynamics, climate characteristics and the variability in surface water inputs are also important. Snow-dominated watersheds differ from the more commonly studied rainfall-dominated watersheds due to the desynchronization and uneven distribution of snow accumulation and snowmelt across the landscape (Jost et al., 2007). While Jost et al. (2007) showed that elevation, aspect, and forest cover explained 80-90% of the variability in snow accumulation, elevation was the most important predictor of snow water equivalent across the watershed in both of their sampling years. Elevational gradients control atmospheric temperature, so snowmelt may occur in lower elevations in early spring, while snow still accumulates in upper elevations (Jost et al., 2007). Variability in snow accumulation and snowmelt and the subsequent variability in landscape wetness and antecedent conditions (Smith, 2011) may be more important than topography in determining hydrologic connectivity (Smith et al., 2014). Snowmelt can overwhelm percolation rates to create a perched water table and throughflow (Smith et al., 2014; Redding and Devito, 2008; 2010) or contribute to groundwater recharge or storage (Hood and Hayashi, 2015). The delayed release of snowmelt that is stored in alpine regions has been shown to dominate fall baseflows and maintain winter streamflow (Hood and Hayashi, 2015; Paznekas and Hayashi, 2016). While some progress has been made in understanding runoff in snow-dominated alpine watersheds, more work is required to link groundwater or throughflow contributions to hydrologic connectivity and the use of topographic or geomorphic indices at the watershed scale.

The objective of this chapter was to identify throughflow and groundwater contributions to streamflow in a snow-dominated watershed that spans from upper montane to alpine zones.

These results were used to determine if a) UAA can be used to identify the relative magnitude of

throughflow contributions to the stream, b) geology or surficial geology control groundwater upwelling and contributions to streamflow, or c) snow accumulation and snowmelt control throughflow contributions and streamflow timing. This information will help us understand how and when hydrological connectivity occurs in watersheds with deep glacial till and permeable bedrock and provide insights into how these watersheds may respond to disturbance (Green and Alila, 2012).

3.2. Study site

Star Creek is a snowmelt-dominated watershed (10.4 km²) located in the eastern slopes of Alberta's Rocky Mountains (Figure 3.1); peak streamflow occurs on average in late May. Precipitation falls as snow from October to April/May and summer convective storms and autumn rains dominate the warmer seasons (June to September). Average precipitation (2005-2015) is 990 mm in the sub-alpine (1732 m a.s.l.) and 720 mm lower in the watershed at Star Main (1482 m a.s.l.); 50-60% of precipitation falls in the form of snow. Mean monthly temperatures range from 15 °C in July to -6 °C in December. The stream is comprised of two main forks (Star East and Star West) and a smaller ephemeral stream (McLaren). Regional geology is composed of sedimentary bedrock from three geologic formations: Upper Paleozoic formation, Belly River-St. Mary Succession, and Alberta Group formation which transition perpendicular to the stream. In general, all formations are composed of shale and sandstone, with carbonaceous layers present (AGS, 2004). The landscape has undergone glacial erosion and deposition as recent as the Wisconsin Glaciation (Gov. AB., 1996). Surficial geology is primarily composed of colluvium, talus slopes, and glacial till and soils are brunisols. For a more extensive site description see Chapter 2.

3.3. Methods

Throughflow and groundwater contributions to the stream can be difficult to measure. Often longitudinal streamflow measurements are combined with natural water chemistry or isotopes to help quantify groundwater dynamics and conceptualize subsurface flow (Covino and McGlynn, 2007; Cowie et al., 2017). The methods below were used to quantify streamflow contributions, determine the potential sources (throughflow, groundwater, snowmelt) of these contributions, and link streamflow contributions to topographic and geomorphic indices, timing of snowmelt, and hydrograph response.

3.3.1. Differential gauging

Differential streamflow gauging is a technique used to define gains and losses of streamflow along stream lengths (Cey et al., 1999; Ruehl et al., 2006; McCallum et al., 2012). Streamflow is measured at one site at a time moving from site to site in the upstream direction over a short period of time, such as one day (e.g., McCallum et al., 2012; Kuras et al., 2008; Ruehl et al., 2006). The difference in flow between measurements are the net gains or losses for each reach, which can provide insight into how watershed structure (e.g., geology, surficial geology, and topography) or snowmelt control streamflow contributions (Ruehl et al., 2006; Payn et al., 2009). Diurnal fluctuations in streamflow across the experiment day(s) can add uncertainty to these measurements (Payn et al., 2012). Simultaneous discharge measurements would decrease the error associated with diurnal fluctuations and optimize the potentially small differences in discharge between sites.

In this study, dilution gauging was conducted simultaneously at up to eight locations with seven technicians and eight electrical conductivity (EC) probes for a total of 12-13 sites in one day (Figure 3.1). The uppermost location in the first set of streamflow measurements was repeated on the second set of streamflow measurements to account for diurnal changes in streamflow from morning to afternoon (Payn et al., 2009). The differential streamflow gauging locations

were established every 600 m on average (range 300 - 825 m) from the Star Main continuous streamflow gauging site up to the headwaters of Star West, Star East, and McLaren forks (Figure 3.2). Locations were adjusted slightly to separate large UAAs and other watershed features. The streams went dry mid-summer at four locations and were therefore not included in the recession or baseflow periods. Streamflow measurements were conducted during baseflow conditions in 2014 (August 25th) and three streamflow conditions in 2015, high flow (June 5/6th), recession flow (July 22nd), and fall baseflow (August 25th), to capture a range of hydrologic connectivity conditions across the year. High flow and baseflow represent the periods when hydrologic connectivity is greatest and least likely to occur, respectively (Jencso et al., 2009), and correspond to potentially different contributing sources (e.g., throughflow or groundwater). The recession limb represents the transition between the two extremes.

Saltwater solutions (167 g NaCl/l water) were poured into the stream at an upslope location to increase EC and the saltwater plume was measured at a downstream location (approximately 25 times the stream width apart to ensure mixing; Day, 1976) using an EC probe (YSI Model 85, Sonde, or Professional Plus; YSI Inc./Xylem Inc., Ohio, USA). The volume of saltwater solution was adjusted per site and per flow condition to ensure the EC increased by 50% above background levels (Moore, 2005). The short duration of these experiments and instream calibration at each site helped to ensure changes in background EC did not have an impact on discharge results. Uncertainty associated with the dilution gauging method is approximately 5% (Leach and Moore, 2011; Moore, 2005; Day, 1976). Small differences in discharge between gauging locations can result in larger compound uncertainties in the streamflow differential contributions and should be considered when interpreting the results.

3.3.2. Longitudinal stream water chemistry

Water chemistry can be used to identify changes in source contributions through time and along the stream length (Jencso et al., 2010; Ruehl et al., 2006). Stream water chemistry was

measured every approximately 100 m along the length of Star Creek (orange points and half-way between each point in Figure 3.1) to the origin of all 3 forks (McLaren, Star West, and Star East). Sampling points were chosen based on the location of known seepage points, tributaries, and large UAAs to isolate possible effects of these contributions on stream water chemistry. Measurements were taken at the same three flow conditions as the differential gauging measurements (high flow, recession flow, and baseflow) in 2014 and 2015, again, to cover a range in hydrologic connectivity and dominant contributing sources. Temperature and EC were measured instream with a handheld YSI Model 85 probe (YSI Inc./Xylem Inc., Ohio, USA). EC was converted into specific conductivity (SpC), EC standardized to 25 °C, and used to identify potential sources of streamflow contributions because longer contact time with the subsurface (e.g., groundwater) increases the concentration of ions in the water, which would result in greater EC than in surface water that has shorter contact times (Castro et al., 1991). As a result, groundwater inflows would increase the specific conductivity in stream below the inflow zone.

3.3.3. Landscape controls on flow contributions

3.3.3.1. Upslope Accumulated Area

UAA (m²) was calculated in SAGA GIS software (Conrad et al., 2015) for a 1 m Digital Elevation Model (DEM), derived from airborne LiDAR, for the left and right sides of the stream based on the methods of Grabs et al. (2010). These flow contributions were used to identify high contributing reaches along the stream that should measurably affect the instream flow contributions. UAA were aggregated into total reach UAA for differential gauging reaches and categorized based on the range of UAA sizes in the reaches to determine if UAA could be scaled-up as an indicator of relative streamflow contribution.

3.3.3.2. Downslope Index

The DI was calculated in Whitebox Geospatial Analysis Tools (version 3.4; Lindsay, 2017) using a 1 m DEM. The equation for the DI is as follows (Hjerdt et al., 2004):

$$\tan \alpha_d = \frac{d}{L} \quad (3-1)$$

where, α_d is the slope angle between the start point and the target point, d is the elevation distance, and L is the horizontal distance to the point with elevation d below the elevation of the starting cell. Equation 3-1 was processed with $d = 10$ m and solved for L to filter out smaller local topographic features (Lanni et al., 2011). A smaller L would represent steeper slopes; the transition to a larger L (flatter slopes) would represent a hydrological knickpoint with a greater likelihood of groundwater discharge.

3.3.3.3. Potential solar radiation

Potential solar radiation was calculated in ArcGIS using the Area Solar Radiation tool. A 1 m resolution DEM was used to estimate the potential distribution of solar radiation across Star Creek for the snowmelt season (April 1 to June 20, 2014). Although the angle of the sun would change slightly over remaining summer months, these estimates were used to infer differences in potential evaporation throughout the rest of the summer.

3.3.4. Watershed-scale precipitation and streamflow

3.3.4.1. Precipitation

Snow depth was measured with a sonic ranging sensor (SR50, Campbell Scientific; Edmonton, AB) at two locations within the watershed over the 2014 and 2015 snow seasons. Star Alpine (elevation 1874 m a.s.l.) and Star Main (1482 m a.s.l.; Figure 3.1) sites were chosen to represent the minimum and maximum range of snow depths observed. Precipitation (rain and snow) was measured at the sites indicated above and at a mid-elevation site (Star Bench; 1645 m) with a Jarek tipping bucket gauge (Geoscientific, Vancouver, Canada) with an alter shield to estimate average watershed precipitation. Tipping buckets had an anti-freeze overflow system for measuring snow (mm of water equivalent) in winter months.

3.3.4.2. Streamflow

Continuous streamflow was measured at six sites within Star Creek: Star Main, Star West Lower, Star East Lower, Star West Upper, Star East Upper, and McLaren (Figure 3.1). Stage was measured with a Hobo U20 pressure transducer (Onset Computer Corporation; Bourne, MA) or a WaterLOG bubbler system (Xylem Inc.; Yellow Springs, Ohio). Discharge was measured with a Sontek velocity meter (Xylem Inc.; San Diego, CA) every two weeks through the ice-free period (March to October). Stage-discharge relationships were created for each sub-watershed every year to account for changes in the channel morphology.

3.3.5. Hillslope groundwater wells

Hillslope (shallow) groundwater wells were installed to depth of refusal or maximum auger depth (average 1.1 m) in five locations within the watershed (Star Lower, Star West Lower, Star East Lower, Star West Upper, Star East Upper; Figure 3.1) to provide insight into water table dynamics in relation to snowmelt, rainfall, and streamflow responses. Three wells were installed on one side of the stream at each site – riparian zone, toe of the hillslope, and upper hillslope – for a total of 15 wells to determine the timing of hydrologic connectivity. Sites were selected to represent a range of UAA (see Jencso et al., 2009) on the left or right side of the stream. Odyssey capacitance recorders (Dataflow Systems Ltd., New Zealand) were used to measure water level every 10 min for the duration of the study.

3.4. Results

3.4.1. Differential gauging

3.4.1.1. High flow

Differential gauging was conducted four times over three discharge periods (indicated by yellow circles in Figure 3.3) to cover a range in potential hydrologic connectivity. Stream discharges measured during differential gauging are expressed as a percent contribution of the overall

streamflow measured at the stream outlet (Star Main; Figure 3.1). During high flow (June 5/6), the highest contribution of streamflow came from the alpine reaches in Star West Upper (Q8) and Star East Upper (Q13) (29% and 22%, respectively; Figure 3.4). Combined, this represents just over half of the flow contribution for the whole watershed. In contrast, the uppermost reach in McLaren (Q16) only contributed 4% of flow during high flow periods. The lower two reaches (Q1 and Q2) in the Star Lower sub-watershed (below the confluence of Star West, Star East and McLaren) and the lower reaches in McLaren (Q14) and Star West sub-watersheds (Q3) contributed 0% and 4%, 0%, and 1%, respectively, of the flow in the watershed; comparatively far less than the upper reaches (Figure 3.4).

3.4.1.2. Recession flow

During recession flow (July 22), McLaren became intermittent, with no streamflow at the outlet or the two other differential gauging sites (Figure 3.4), although there were small portions of the stream where flow was present. The highest differential gauging reach in Star East Upper (Q13) also became intermittent with no streamflow at the measurement site, although, again, there were small reaches above this differential gauging site where the stream was flowing or water was standing in pools. The highest differential gauging reach in Star West Upper (Q8) contributed the most flow contribution (48%). However, there may have been an error in this flow measurement because discharge at the two downstream sites (Q7 and Q6) were considerably lower than at this site, which resulted in a 12% net loss in streamflow over the Q7 reach. If discharge from Q8 was removed, together the sites would have contributed 35% which is consistent with contributions at high flow and baseflow. The lower two reaches in Star Lower (Q1 and Q2) and the lowest reach in Star West Lower (Q3) and Star East Lower (Q9) contributed more flow than during high flow conditions (10%, 9%, 4%, and 7%, respectively; Figure 3.4). Star Lower, in particular, produced considerably more flow during recession conditions compared to high flow conditions.

3.4.1.3. Baseflow

The Star East Lower differential gauging reaches were consistent contributors of flow regardless of hydrograph phase (~5%; Figure 3.4). The Star East Upper reaches were also consistent from recession to baseflow (August 25) conditions. The Star West Upper reaches were consistent between high flow (29% and 9%) and baseflow conditions (32% and 7%; Figure 3.4). At baseflow, the lowest and highest reaches in Star West Lower (Q3 and Q6) increased flow contributions (to 13% and 7%, respectively) compared to high flow and recession flow conditions. The Star Lower reaches decreased in flow to 8% and 0%. McLaren continued to have small reaches upstream where water flowed above ground, but much of the stream length was dry by August.

3.4.1.4. Baseflow comparison (2014 -2015)

Differential gauging contributions were measured at baseflow (August 25) in 2014 and 2015. Stream discharge (m^3/s) was greater in 2014 than in 2015, and baseflow discharge in 2014 was more comparable to recession flow discharge in 2015 (Table 3.1). Although 2014 baseflow is quantitatively comparable to 2015 recession flow, those flow contributions were not compared because active flow pathways may differ between recession and baseflow due to differing time since the snowmelt period. Despite differences in baseflow discharge from 2014 to 2015, flow contributions as a percent of flow at the watershed outlet were consistent between years at the Star West Upper, Star East Upper, Star Lower, and McLaren reaches (Figure 3.5). Conversely, there were considerable differences between flow contributions in the Star West Lower reaches and small differences between flow contributions in the Star East Lower reaches. The differences at Star East Lower are likely within the margins of error of these measurements but Star West Lower displayed larger variations. Some of the differences between sites or flow conditions would be attributed to the 5% uncertainty in discharge measurement associated with the dilution gauging method, particularly the discharge results at sites Q3 and Q4 in 2014.

However, the differences in these two lowest reaches were particularly large (27% increase and 18% decrease) and may signal a larger effect than measurement uncertainty alone.

3.4.2. Longitudinal water chemistry

SpC decreased from the watershed outlet (Star Main) to the origins in Star West and Star East forks but increased from the confluence to the origin of McLaren (Figures 3.6 and 3.7). The spatial patterns may be due to a difference in stream origin between forks. Star East and Star West are made up of large (size) alpine basins and runoff originated from snowmelt, whereas McLaren is completely forested to the top of the watershed and, instead, runoff appeared to originate from springs. SpC also generally increased in time from high flow to baseflow for all sub-watersheds except McLaren, which was generally similar across time. Although differential gauging locations in McLaren were dry at recession flow and baseflow, water samples were taken from longitudinal water chemistry sampling sites where the stream was flowing above ground. No meaningful differences in spatial or temporal patterns of SpC were observed between 2014 and 2015.

Changes in SpC can be analyzed across each differential gauging reach, where large increases in SpC in the downstream direction may represent subsurface inflows (groundwater or throughflow) to the stream. During high flows (June), SpC increased consistently across all reaches in Star East and reach Q4, Q7, and Q8 in Star West (Figures 3.6 and 3.7). These reaches also contributed much greater streamflow in Star West (Table 3.1 and Figure 3.4). During recession flow, SpC increased across reach Q9, Q10, and Q12 in Star East and represented the largest streamflow contributions in the east fork. In Star West, stepwise changes occurred across all reaches; however, not all reaches had large streamflow contributions. For instance, the stepwise increase of SpC across reach Q6 occurred due to a small pond where SpC above and below the pond were different. Further, reach Q7 contributed -12% (net outflows) yet SpC suggested there were groundwater inflows over that reach.

Although water chemistry can inform locations of inflows, there may be gross inflows and gross outflows across the reach, which in turn represents a net outflow/inflow (Payn et al., 2009). At baseflow in 2015, SpC increased across reach Q3 and Q4 (Star West), with relatively weaker changes for the rest of the watershed despite strong streamflow contributions. Similar inconsistencies were also observed in Star West at baseflow in 2014 because SpC remained fairly consistent above reach Q4 despite large contributions to discharge. Comparatively, baseflow contributions in Star East were more consistent with changes in SpC in 2014 and 2015 (e.g., reach 9).

3.4.3. Topographic indices

3.4.3.1. Upslope Accumulated Area

UAA was calculated for 1 m segments along Star Creek and the largest UAAs were field verified by inspections of the surface topography. The largest UAA often corresponded with visible seeps or large draws (locations of topographic convergence on a hillslope) that had evidence of historical surface flow, though had no surface flow in 2014 and 2015. There was a positive relationship between total UAA (summed within a differential gauging reach) and flow contribution for all flow conditions (Figure 3.8). However, this relationship was largely driven by the uppermost alpine reaches that were more than twice as large as the next largest reach. When these outliers were removed, the relationship between total UAA and flow contribution no longer existed for any flow condition (Figure 3.9).

3.4.3.2. Downslope Index

DI (solved for L) was used to assess if streamflow contributions corresponded to the area predicted to have groundwater discharge. Large L corresponded with visible seeps and topographic draws with visible water (Figure 3.10). In several cases, the origin of topographic draws aligned with a L of at least 65 m or 80 m. A threshold of $L > 80$ m was used to be conservative. The reaches with the largest percent area with $L > 80$ m were in the lower portion

of the watershed (Q3, Q4, Q1, Q14, Q2, Q5, and Q9, in descending order; Table 3.2). All other reaches had considerably less area with $L > 80$ m. The large L reaches corresponded with the portion of the watershed with slightly leached glacial till surficial geology but did not correspond with a particular bedrock formation (Figure 3.11). Regions with $L > 80$ m also corresponded with the most complex reaches for flow contribution variability (Section 3.4.1; Figure 3.4 and 3.5).

3.4.3.3. Solar radiation index

The estimated potential solar radiation on the west portion of Star West was the highest in the watershed (Figure 3.12), which could cause faster snowmelt, greater evaporation, and thus, larger shallow subsurface storage opportunity than in the rest of the watershed. This area corresponded with casual field observations of dry soils and shallower spring snowpack depths. The potential storage opportunity may reduce the amount of throughflow that contributes to the stream, which could explain some of the variability and losing reaches reported for Star West Lower sub-watershed. Star West alpine region had the lowest potential solar radiation, which could lead to slower snowmelt, less evaporation, and thus, lingering streamflow contributions later in the summer. Star East showed similar patterns of greater potential solar radiation in the lower reaches than in the upper reaches but not to the extent as in Star West. This could lead to a less prolonged streamflow contribution than in Star West.

3.4.4. Snow and stream response

Maximum snow depth at Star Alpine was more than twice as deep and persisted for 6-7 weeks longer compared to at Star Main in 2014 and 2015 (Table 3.3; Figure 3.3). The Star Main hydrograph started to rise at the same time as the lower elevation snowmelt in 2014 and 2015; Star West Upper and Star East Upper streamflow did not respond at that time. Peak streamflow in 2014 occurred after the snow-free date at Star Main, likely corresponding to the snowmelt at Star Alpine. A second peak occurred due to a rain-on-snow event in mid-June. Warm

temperatures and poor snow conditions resulted in a lack of spring freshet in 2015; instead, peak streamflow occurred just after the snow-free date due to a large precipitation event.

Hillslope groundwater wells started to respond at the same time as snowmelt occurred at the lower elevations but prior to the main discharge peak at all locations in spring 2014 (Figure 3.3). Amongst wells, the upper hillslope well often responded after the toe of the hillslope and riparian wells. Peak water level in most wells occurred within days of peak streamflow in 2014. In 2015, numerous warming events throughout the winter resulted in complicated hillslope groundwater well responses. In general, upper hillslope wells still responded later than toe of the hillslope and riparian wells. However, a large rain event caused the peak hillslope groundwater level to be concurrent with peak streamflow. At all sites, the upper hillslope well responded only during the intense snowmelt periods or during some large rainfall events in 2014 and 2015, which indicates these were the only times the upper hillslopes were connected to the stream.

3.5. Discussion

Multiple lines of inquiry were used to identify throughflow and groundwater contributions along Star Creek and to infer potential controls of hydrologic connectivity at the watershed scale. Contrary to other studies (Jencso et al., 2009; Anderson and Burt, 1978; Detty and McGuire, 2010b), topography was not the primary driver of subsurface streamflow contributions (throughflow or groundwater) or hydrologic connectivity. Rather, the results suggest that streamflow contributions in Star Creek watershed were largely driven by other elements of watershed structure (e.g., surficial geology, watershed elevational gradient, alpine basin) and snow accumulation and snowmelt dynamics. Snowmelt in the alpine region was the main driver of high flows and the glacial till beneath the soil layer likely controlled the storage and release of subsurface flow. Results are discussed in the context of the potential drivers of subsurface flow

(e.g., topography, geology, and precipitation inputs) and how land use changes may affect streamflow in the eastern slopes of Alberta's Rocky Mountains.

3.5.1. Topography

Topography (UAA) has been used to explain the subsurface contribution of hillslope runoff (throughflow) to the stream in regions with shallow soils and impermeable bedrock (Jencso et al., 2009; 2010; Detty and McGuire, 2010b). However, topography or UAA is not always the primary control on throughflow or shallow hillslope groundwater response in regions with very transmissive soils or deep glacial till deposits (Kuras et al., 2008; Smith et al., 2014; Penna et al., 2015). In Star Creek watershed, deep, unconsolidated glacial tills result in primarily vertical flow and water table dynamics that do not explain the observed runoff patterns. Hydrologic connectivity occurred during the snowmelt period but was largely disconnected afterwards; indicated by the lack of water table in the hillslope wells (Figure 3.3). The sub-watersheds with many large UAAs should be connected to the stream for the longest time (Jencso et al., 2009) and, thus, have the largest effect on flow contribution, particularly during the snowmelt season. However, there was no relationship between the UAA and the length of time of hydrologic connectivity, or between the UAA and flow contribution (Figure 3.9).

The lack of relationship at the sub-watershed scale in Star Creek may be because of multiple reasons. First, each streamflow measurement has a 5% uncertainty associated with it and is compounded when the streamflow differentials were calculated (subtracted discharges from the upper streamflow sites). These uncertainties can add substantial noise to the discharge contribution estimates. Second, differential gauging is a measure of net gains and losses, rather than gross gains and losses (Payn et al., 2009; Blume and van Meerveld, 2015). For instance, a net gain of 5% could be comprised of 10% gain and 5% loss in streamflow; the UAA could be associated with a 5% gain rather than the 10% gain that the reach actually contributes, which would misrepresent the contributions in Figure 3.9. Third, UAA was calculated at the hillslope

scale (every 1 m stream segment) not at the reach scale (Jencso et al., 2009) but were summed to the reach scale in this study. It is possible that there were multiple important high UAA draws that contributed flow to the stream throughout the year and yet, the total UAA for the reach may have been small in comparison to other reaches. To incorporate the variability in the individual UAAs that were summed across the reach, points in Figure 3.9 were colour-coded based on the number of UAA points in 10,000 m² categories. Dark green indicates one end of the spectrum, a reach with many large draws (>100,000 m² or between 30,000 and 60,000 m²) and few smaller draws (10,000 - 20,000 m²); red indicates the other end of the spectrum, a reach with mostly small draws (10,000 - 20,000 m²) and only one slightly larger draw (>30,000 m²). Reaches with more large draws (green reaches) could have had greater flow contributions than reaches with smaller draws (red or yellow reaches) but have the same total UAA. However, despite taking into account the individual draws in each reach, no pattern was observed. Finally, UAA should be applied to regions where the water table mimics topography and where shallow soils and an impeding layer results in a responsive watershed (Jencso et al., 2009). It is likely that subsurface characteristics, and the resultant groundwater flow pathways, complicated this pattern or that the mechanisms driving runoff were complex and could not be explained by topography alone.

Similar results have been reported during the early freshet period in southeastern British Columbia (Cotton Creek Experimental Watershed), where water table response was driven by the spatial distribution of snowmelt quantity and intensity rather than topographic convergence due to deep glacial tills with variable saturated hydraulic conductivity (Smith et al., 2014; Smith, 2011). However, there was a shift in the dominant runoff processes later in the melt freshet and through the low flow period that could be explained by topographic controls (Smith et al., 2014). In Star Creek, UAA and sub-watershed flow contributions were not correlated at any flow condition so a shift to topographically controlled runoff processes was not evident (Figure 3.9).

The effects of plant water uptake and the variability in solar radiation (a proxy for potential evaporation and snowmelt processes) across the watershed may also be partially responsible for the lack of apparent trends and complexity in sub-watershed flow contributions (Figure 3.12; Section 3.4.3.3). Regions of high potential solar radiation in Star West and Star Lower (Figure 3.12) could create a shallow subsurface storage opportunity, decrease runoff responses (Detty and McGuire, 2010a), or accelerate the timing of flow contributions from snowmelt on those hillslopes. Similarly, Nippgen et al. (2015) modelled watershed storage and runoff areas in Tenderfoot Creek Experimental Forest in Montana and showed that plant water uptake decreased the correlation between UAA and storage.

3.5.2. Watershed structure

Bedrock geology of montane watersheds is an important contributor to subsurface flow contributions in low flow conditions (Jencso and McGlynn, 2011; Oda et al., 2013). For instance, sandstone regions in the Tenderfoot Creek Experimental Forest in Montana became the largest contributor to streamflow during low flows (Jencso and McGlynn, 2011). Geology in Star Creek is consistent across the watershed, with shale as the primary component of all three formations present in the watershed. The Lewis Fault, which separates the Upper Paleozoic formation from the Belly River-St. Mary River Succession in the upper alpine region (Figures 3.1 and 3.11), could be a potential downwelling point. Another geologic transition (to Alberta Group formation) occurs in the Star Lower sub-watershed along the mainstem. While the various geologic formations and the transitions between formations provide an opportunity for groundwater upwelling and downwelling, respectively, it is unlikely that they provide a dominant control on subsurface streamflow contributions. The Belly River-St. Mary River Succession is too large to determine whether it specifically contributed a different quantity of groundwater to the stream than other formations and most differential streamflow gauging sites were located below the Lewis Fault and above the Alberta Group formation. Furthermore, if there was a preferential flow

pathway associated with the bedrock, it would be reflected in the stream water chemistry as groundwater, with theoretically much greater conductivity, mixed with stream water. The stream water chemistry did not show any large changes in SpC that would be associated with a deep, old, groundwater flow pathway (Figure 3.7). Smaller changes in water chemistry were present at multiple points in the stream that were not associated with thrust faults or geological transitions, so these were likely younger groundwater or throughflow contributions.

Others have suggested that watershed structure (Ali et al., 2014) and subsurface storage (Bracken et al., 2013) may influence hydrologic connectivity and subsurface flow contributions. Surficial geology and subsurface storage appear to influence the storage and release of groundwater to the stream in Star Creek (Figure 3.11). Despite the lack of snowmelt during recession flow and baseflow periods, Star West alpine continued to contribute most of the flow to the overall watershed (Figure 3.4). In contrast, Star East alpine stopped flowing in the uppermost reaches in July and through the rest of the season. Star West and Star East both have large alpine areas above the tree line but are structurally different. Star West alpine has cirque tills, with a permanent marshland, and the stream is dominated by bedrock. Star East alpine has accumulated much talus and colluvial deposits, so the stream is dominated by pool-riffle sequences flowing over rocky material. Similar to Hood and Hayashi (2015), the cirque tills in Star West alpine may serve as a storage zone where snowmelt was held temporarily and slowly released throughout the dry summer months. The moraine in the Opabin headwaters in Yoho National Park, Canada stored 64-95 mm of water during snowmelt and was subsequently released during low flows (Hood and Hayashi, 2015). McLaren is structurally different than the other two sub-watersheds as it is forested to the top of the watershed and does not have a bedrock outcrop; the stream appears to originate from springs in the upper hillslopes. This difference was reflected in the stream water chemistry, with consistently greater ion concentrations in McLaren than in Star East and Star West forks (Figures 3.6 and 3.7). Seeps

may have more contact time with the subsurface material than streamflow originating in the alpine, and thus increase the ion concentrations in the water (Castro et al., 1991).

At baseflow, groundwater flow contribution (longer flow pathways) becomes a more important contributor to streamflow (Rademacher et al., 2005) and may explain some of the seemingly complicated patterns in flow contribution. Many of the lower reaches contributed more flow as a portion of the overall discharge at the watershed outlet at baseflow than at high flow (Figure 3.4), likely due to the reduced dominance of snowmelt at higher elevations and the change in flow pathways to slower draining groundwater. This was evident in the lowest reach in Star West Lower (Q3), which contributed the most flow to the watershed (13%) at baseflow aside from the Star West Upper alpine reach (Q8; 32%) (Figure 3.4). This region of the watershed corresponded to the region with the highest percent of $L > 80$ m (32%) (Figure 3.11; Table 3.2). Hjerdt et al. (2004) suggested that areas with large L values were responsible for high groundwater discharge based on the McDonnell (1990) model of the “backing up of water” in concave watershed scale topographic zones. Ali et al. (2014) also suggested that watershed structure may influence hydrologic connectivity and thus, geomorphic indices should be considered. The large increase in flow in the lowest reach in Star West Lower were corroborated with small steps in specific conductivity in the stream water (Figure 3.7) and were likely due to groundwater discharge. However, it is also possible that the transition in surficial deposits from colluvium to glacial till created a zone of storage that was recharged during snowmelt and slowly released through the summer season. The glacial till is composed of fine to coarse grained material that may increase the storage capacity and decrease the drainage rate compared to the colluvium. Most of the large L values (>80 m) were associated with the glacial till so it was not possible to determine which mechanism influenced the groundwater contributions from the current dataset. However, it is clear that this was a region where groundwater flow was important to streamflow contributions during low flow conditions.

3.5.3. Snowpack and snowmelt distribution

Snow depth in the alpine zone was two times as deep as in the lower elevation site and took 6 - 7 weeks longer to melt (Table 3.3). Snowmelt from the alpine region occurred at the same time as high flow and hydrologic connectivity in 2014 (Figure 3.3). A small snowpack and mid-winter snowmelt in 2015 resulted in high flows that were driven by a large rain event rather than snowmelt. Regardless of low snow conditions, the uppermost alpine reaches in Star West and Star East forks contributed the majority of streamflow at the watershed outlet (Figure 3.4). The volumetric addition of inflows over low elevation reaches were so much smaller than the flow contributions in the alpine that they were not visible in comparison (Table 3.1; Figure 3.4). Conversely, during recession flow and baseflow, subsurface contributions to some of the lower reaches represented larger contributions to the overall flow as groundwater pathways began to dominate. While subsurface characteristics are dominant controls on runoff generation, the location, distribution and rate of precipitation inputs can also influence the temporal shift of runoff dynamics and hydrologic connectivity (Nippgen et al., 2015; Hood and Hayashi, 2015; Smith et al., 2014). The evolution of watershed connectivity was monitored in the Tenderfoot Creek Experimental Forest in Montana to characterize how elevation affects connectivity and flow contributions (Nippgen et al., 2015). They also showed that runoff was generated mostly in the higher elevations and from larger drainages in lower elevations.

Baseflow in August 2014 was greater than baseflow in August 2015 and was more equivalent to recession flows in July 2015 (Table 3.1). Chapter 2 showed that seasonal precipitation patterns can influence streamflow discharge in later seasons. The differences in baseflow between 2014 and 2015 might be due to differences in snow accumulation rather than summer precipitation (May 20-Aug 31). Maximum snow depth in 2014 (2.45 m) was almost twice as much as that in 2015 (1.45 m; Table 3.3), whereas summer rainfall was very similar between 2014 (~300 mm) and 2015 (~280 mm). However, the timing of storms in proximity to snowmelt and baseflow

differed. A large rain-on-snow event occurred after the snowmelt peak (June 17) in 2014 and created a second hydrograph peak that continued into July (Figure 3.3). Greater stream discharge in July would result in greater discharge in August. Whereas the rain event that caused the peak in 2015 occurred earlier in the year (June 2) and on a less saturated landscape. In turn, high flows were shorter in duration and the resultant July flows were lower, which would result in lower baseflow than in 2014. However, rainfall from the previous fall (Sept 1-Oct 14; 152 mm in 2013) may have also partially filled storage before the 2014 winter compared to the fall rainfall before the 2015 winter (105 mm in 2014). As suggested in Chapter 2, snowmelt likely recharges the glacial till and bedrock storage, which could sustain baseflow later in the year. Others have shown that a larger snowpack can increase groundwater levels (Deng et al., 1994) and, in turn, increase summer baseflow as snowmelt recharge sustains flows in the late summer (Hood and Hayashi, 2015). Dense glacial till, with a large storage capacity and low permeability, can also sustain baseflow as groundwater is slowly released (Shanley et al., 2015).

3.5.4. Sensitivity to change

Rather than topographic indices explaining the distribution of flow across the watershed as in other regions, it appears that snow accumulation, snowmelt, and watershed structure (e.g., surficial geology and alpine basin) were the primary controls on flow contribution in Star Creek. This is important for the fundamental understanding of how water moves through and is stored in steep watersheds in Alberta's southern Rocky Mountains and how sensitive this region may be to climate and land use change. Land managers should consider locations of major streamflow contribution because changes to the landscape in these areas may have the largest impacts on streamflow. Although the Alberta government historically protected the areas with water (e.g., Zone 1 – higher than 1829 m in elevation) in the eastern slopes policy (Alberta Energy and Natural Resources, 1984), these areas continue to be impacted by natural

disturbance (e.g., wildfire and climate change). Our data show that the alpine regions of Star Creek dominate high flows and summer low flows. Talus slopes in alpine basins have been attributed to sustained baseflow in the Colorado Front Range (Clow et al., 2003) and in the eastern slopes (McClymont et al., 2010). Large headwater areas with large UAA have also been linked to high flow conditions in Montana because these areas were often hydrologically connected for most of the year (Jencso et al., 2009). Changes to these regions would cause significant impacts on the streamflow regime and should be the focus of environmental protection. However, considering the alpine region appears to dominate so much of the hydrograph, the overall streamflow regime would likely be resistant to changes in forest cover at lower elevations.

Changes in climate may pose the greatest risk to the streamflow regime because snowmelt not only dominates high flows, it can also be the primary source of groundwater recharge and late summer flows (Cowie et al., 2017). Increases in air temperatures have been observed globally (Jiménez Cisneros et al., 2014) and increases in minimum temperatures in mid-elevations of the Canadian Rocky Mountains (3.6 °C increase since 1960s) have exceeded global averages (Harder et al., 2015). While warming has occurred at all elevations, the extent of the impact on SWE was larger in lower elevation sites (<1900 m) than in upper elevation sites (>1900 m) in Marmot Creek Research Basin. SWE decreased by 55% between 1967-2013 at the lower elevation sites and showed no change at the upper elevation sites (Harder et al., 2015). However, simulations based on a 5 °C temperature increase (maximum predicted climate change estimate) predicted more rainfall than snowfall in alpine and forested regions, which changed the flow regime from snow-dominated to rainfall-dominated regardless of elevation (Pomeroy et al., 2015). Although the amount of mid-winter snow did not change in the alpine, the timing of melt was advanced in both alpine (37 days earlier) and forested regions (32 days earlier).

Snowmelt can be stored in talus slopes (Clow et al., 2003; McClymont et al., 2010) and deep glacial till or moraines (Shanley et al., 2015; Hood and Hayashi, 2015) and slowly released through the season. Snowmelt storage may be able to buffer streamflow in dry summers, but it is likely not enough to buffer many years of drought or climate change extremes (Hayashi et al., 2010). Hood and Hayashi (2015) called for more groundwater research in alpine watersheds to develop a conceptual framework of alpine groundwater processes. Although Star Creek is not a fully alpine watershed, this study contributes further understanding of the controls of groundwater-surface water interactions in alpine zones of Rocky Mountain watersheds and the resistance of this region to change.

3.6. Conclusion

In this study, instantaneous discharge measurements made at 16 locations along Star Creek were used to explore hydrologic connectivity to the watershed scale. The structural controls (e.g., deep glacial till, fractured bedrock, and alpine basin) in Star Creek create conditions in which streamflow contributions did not correlate with UAA. Rather, snow accumulation and snowmelt dynamics, complex groundwater flow pathways, and surficial geology were the likely drivers of temporal trends in flow contributions. The annual snowmelt pulse saturated the landscape and created the main period of hydrologic connectivity in the watershed and recharged groundwater storage. Stream water chemistry suggested that groundwater was an important source of streamflow for much of the year. Snowmelt from the alpine region dominated streamflow contributions (as a percent of flow at the watershed outlet) during high flows. The slow release of water from glacial till and the alpine cirque and rainfall runoff likely sustained flow for the rest of the season. The overall watershed structure and the distribution of snowmelt processes should also be considered when conceptualizing subsurface flow contributions. Together, these characteristics suggest that the eastern slopes of the Alberta's

southern Rocky Mountains are likely resistant to land disturbance, yet climate change driven snow-rain contributions will likely have long-term impacts on runoff generation mechanisms.

3.7. Tables

Table 3.1: Stream discharge at differential gauging point locations within Star Creek sub-watersheds. Discharges were estimated by differential calculations. Blank values for McLaren (14, 15, 16) and Star East Upper (13) indicate no flow at those stations.

			Baseflow	High flow	Recession flow	Baseflow
Sub-watershed	Reach	Area (km ²)	August 2014	June 2015	July 2015	August 2015
			Q (m ³ /s)			
Star Lower	Q1	0.61	0.108	0.691	0.102	0.078
	Q2	0.23	0.101	0.650	0.091	0.072
McLaren	Q14	0.24		0.040		
	Q15	0.46		0.043		
	Q16	0.25		0.028		
Star West Lower	Q3	0.6	0.072	0.337	0.052	0.052
	Q4	0.19	0.087	0.333	0.048	0.042
	Q5	0.70	0.062	0.281	0.042	0.038
	Q6	0.34	0.050	0.277	0.037	0.036
Star West Upper	Q7	0.71	0.052	0.269	0.036	0.031
	Q8	2.04	0.041	0.203	0.048	0.025
Star East Lower	Q9	0.81	0.028	0.288	0.030	0.021
	Q10	0.54	0.018	0.245	0.023	0.016
	Q11	0.65	0.015	0.211	0.015	0.011
Star East Upper	Q12	0.36	0.011	0.177	0.011	0.008
	Q13	1.54		0.150		

Table 3.2: UAA and L for all differential gauging reaches. Ordered in decreasing UAA.

Sub-watershed	Reach	UAA (m ²)	L > 80 m (% of reach area)
SWU	Q8	2,092,518	0.5
SEU	Q13	1,572,171	1.2
SEL	Q9	832,017	11.6
SWL	Q5	685,978	12.4
SWU	Q7	676,094	0.2
SEL	Q11	657,361	4.6
SL	Q1	635,901	19.3
SWL	Q3	603,875	32.1
SEL	Q10	534,285	5.9
McL	Q15	449,503	4.6
SEU	Q12	335,183	1.6
SWL	Q6	318,879	2.7
McL	Q16	253,043	1.4
McL	Q14	239,652	16.6
SWL	Q4	199,288	21.1
SL	Q2	184,761	15.7

Table 3.3: Maximum snow depth (m) and the snow-free date for Star Alpine and Star Main stations in 2014 and 2015.

Station	Maximum snow depth (m)		Snow-free date	
	2014	2015	2014	2015
Star Alpine	2.45	1.45	June 23	May 31
Star Main	1.11	0.42	May 11	April 11

3.8. Figures

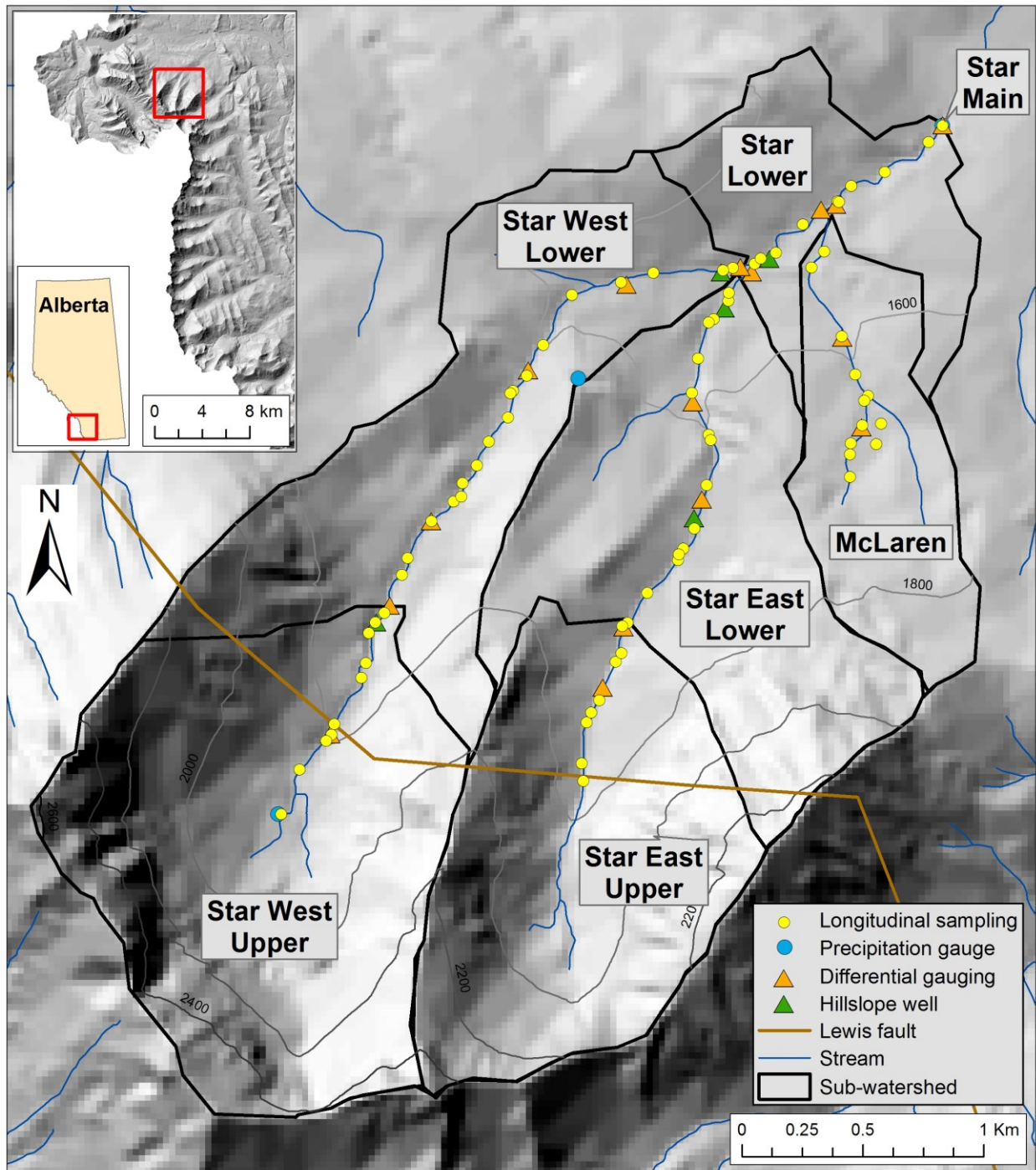


Figure 3.1: Star Creek watershed. Inset 1 shows watershed location within Alberta, Canada. Inset 2 shows watershed location within the Rocky Mountains, on the east side of the Continental Divide.

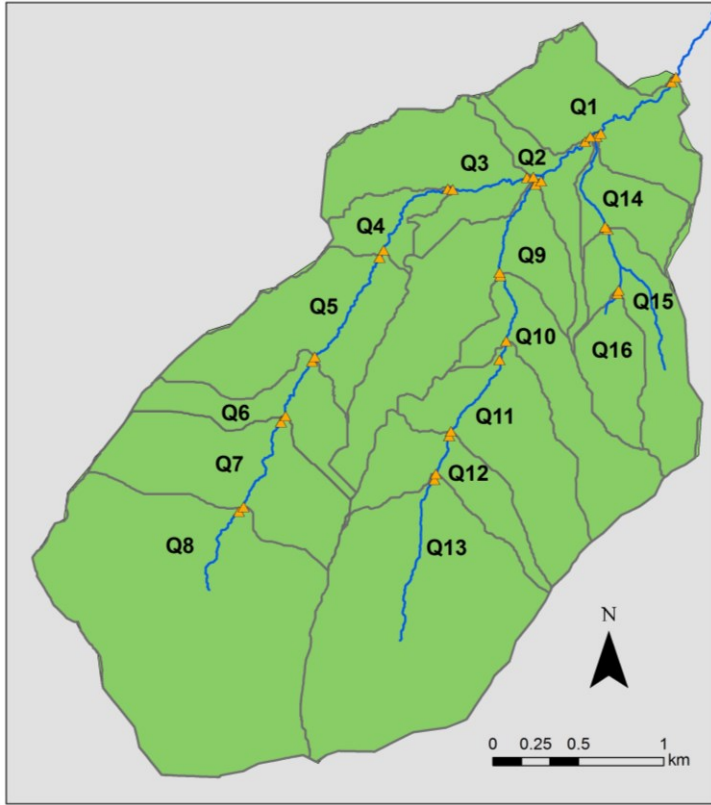


Figure 3.2: Stream reaches (Q1-16) and delineated watersheds for differential streamflow gauging in Star Creek.

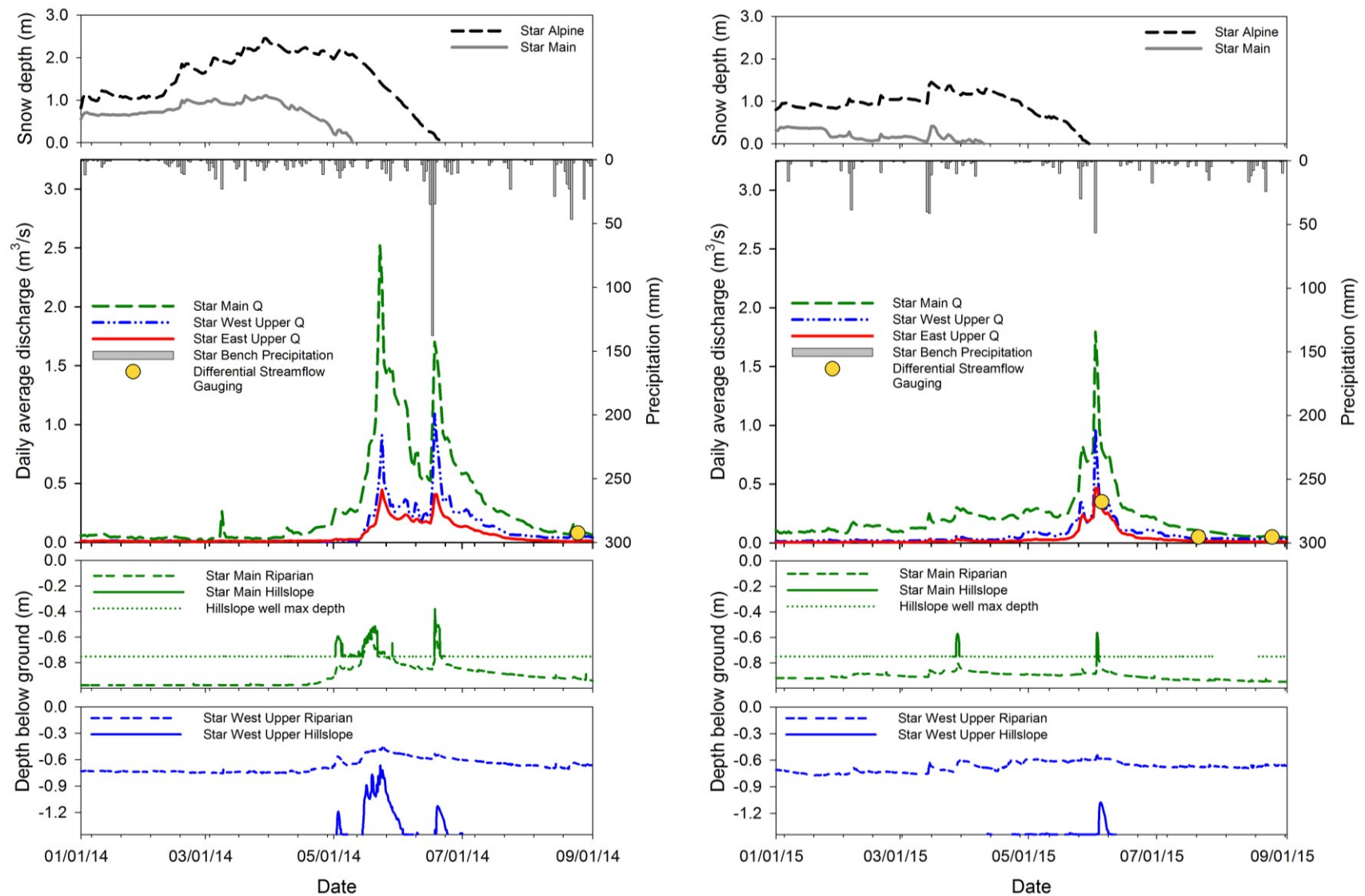


Figure 3.3: Stream hydrographs for 2014 (left plots) and 2015 (right plots). Yellow circles on the hydrographs indicate dates of differential gauging. Precipitation is shown with a reverse secondary axis. Top sub-plot shows snow depth at alpine and lower elevation sites. Bottom sub-plots show groundwater responses in riparian and hillslope wells for Star Main and Star West Upper as representative wells for the lower and upper watershed.

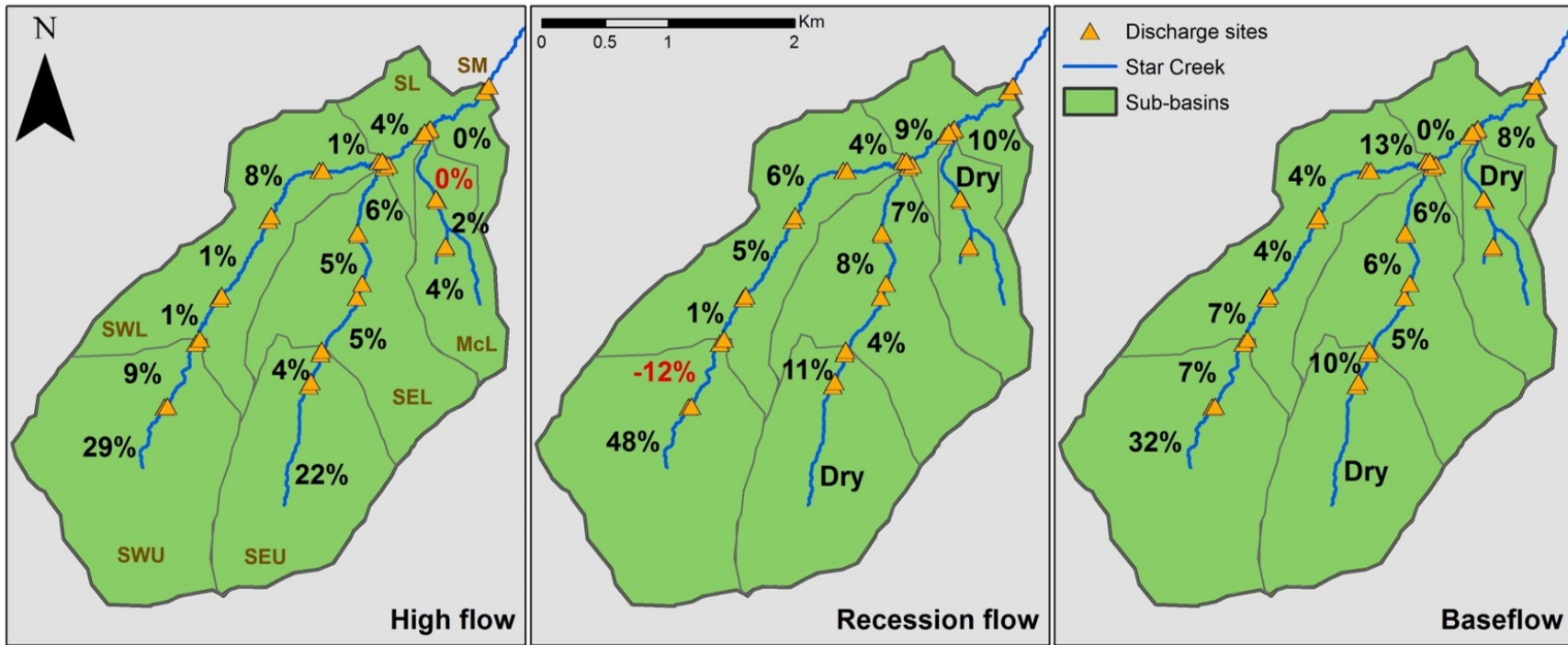


Figure 3.4: Streamflow contributions as a percent of flow at the outlet at the reach scale (average 600 m sections) for three flow conditions in 2015: High flow (June 5/6), recession flow (July 21), and baseflow (Aug 25).

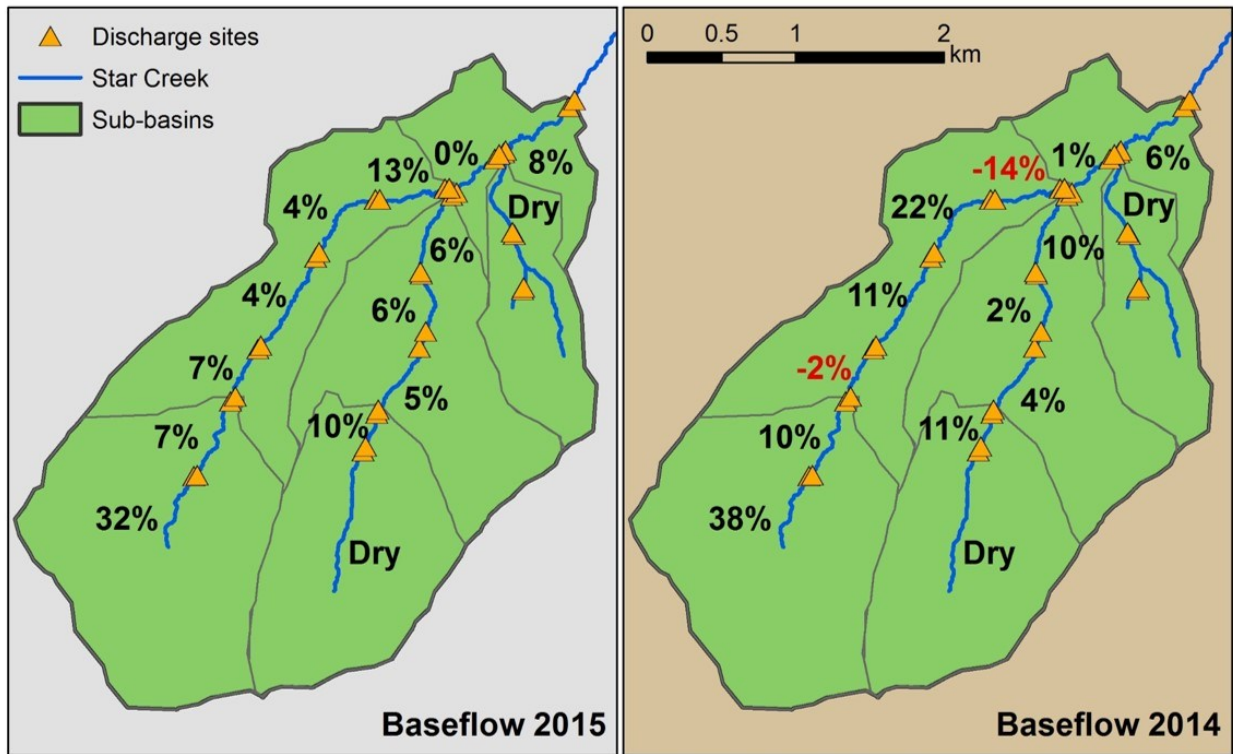


Figure 3.5: Streamflow contributions as a percent of flow at the outlet for baseflow in 2015 (Aug 25) and 2014 (Aug 25).

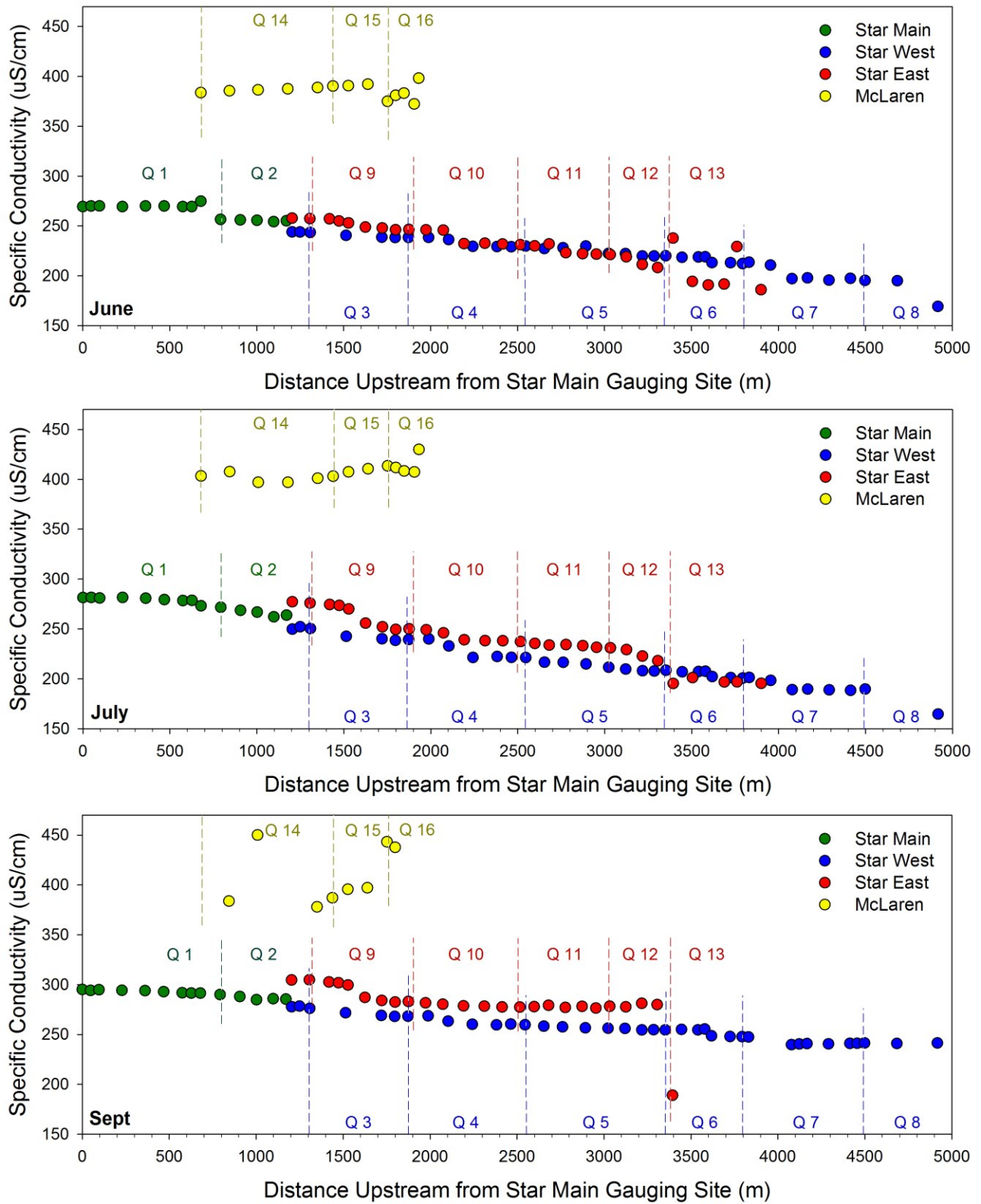


Figure 3.6: Specific conductivity of stream water from outlet at Star Main (0 m) to upper reaches of all forks for 2014 season: High flow (June 6), recession (July 17), and baseflow (Sept 19). Q1-16 correspond to the differential gauging reach numbers in Table 3.1.

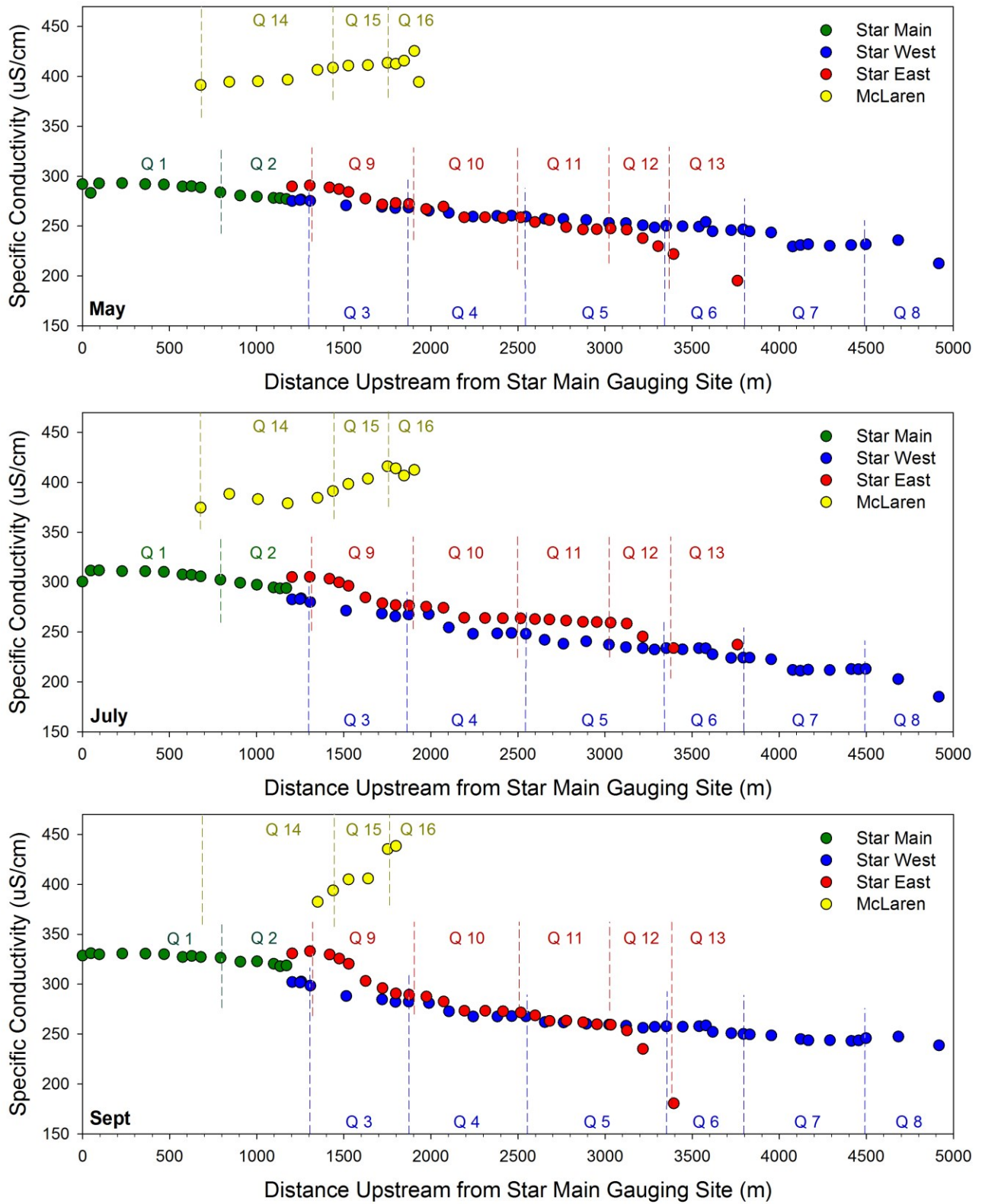


Figure 3.7: Specific conductivity of stream water from outlet at Star Main (0 m) to upper reaches of all forks for 2015 season: High flow (May 21), recession (July 7/8), and baseflow (Sept 8). Q1-16 correspond to the differential gauging reach numbers in Table 3.1.

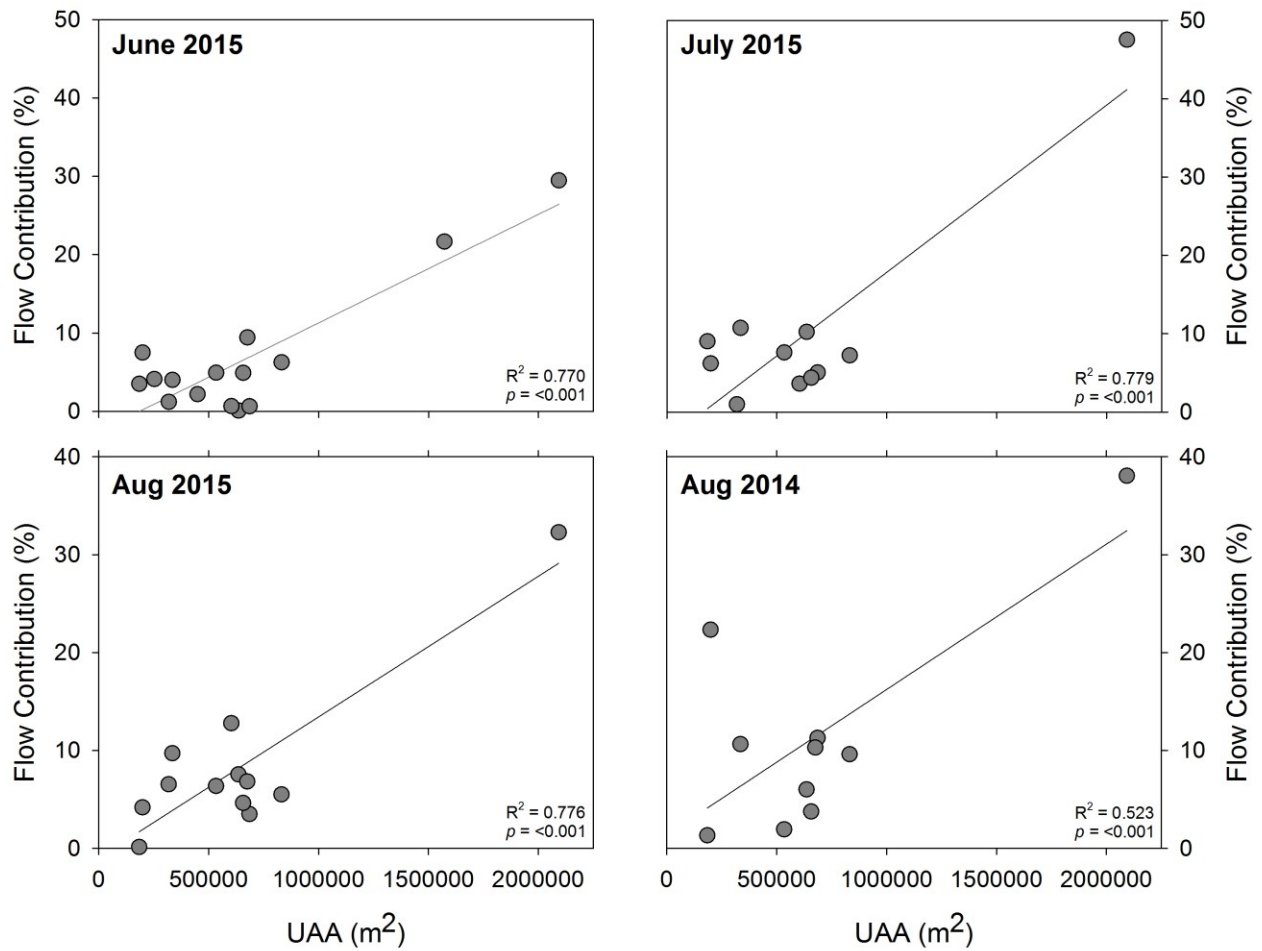


Figure 3.8: Flow contribution (as a percent of flow at the outlet) as a function of UAA. Flow contributions were calculated from differential gauging experiments at three flow conditions in 2015 and for baseflow in 2014. UAA for 1 m stream lengths were upscaled to total sub-reach contribution for each differential gauging sub-reach. All sites, including large alpine reaches, were included in the plots.

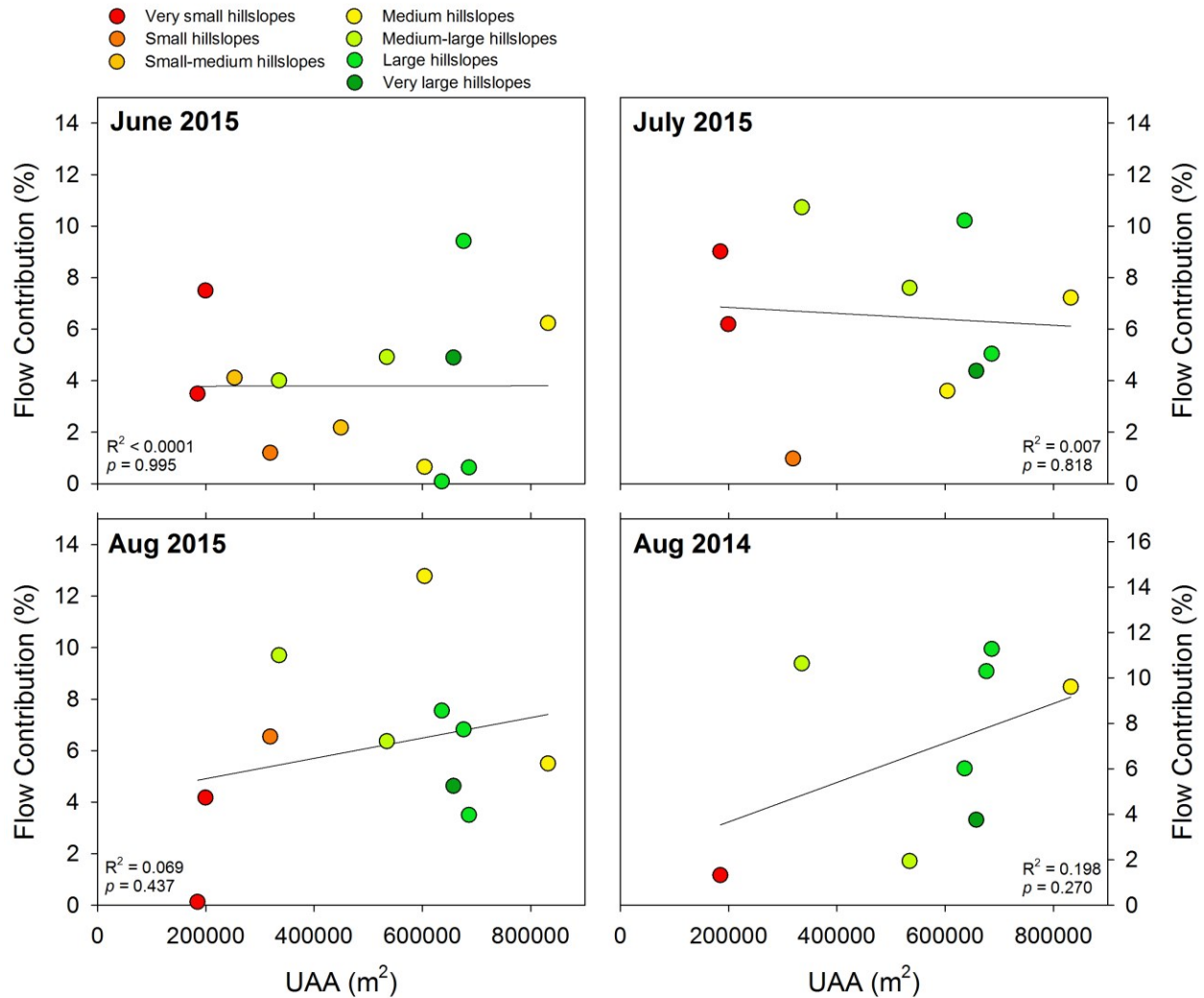


Figure 3.9: Flow contribution (as a percent of flow at the outlet) as a function of UAA. Alpine reaches were excluded from the plots. Colours indicate the contribution of hillslope sizes (>10,000 m²) within each differential gauging reach and transition from red to dark green represent only small hillslopes to many large hillslopes, respectively: Red - few sections were 10,000 - 20,000 m² and one > 30,000 m², Yellow - eight sections were 10,000 - 30,000 m² and one large draw > 100,000 m², Dark Green – few sections were 10,000 - 20,000 m², two sections 30,000 - 60,000 m² and two large draws > 100,000 m².

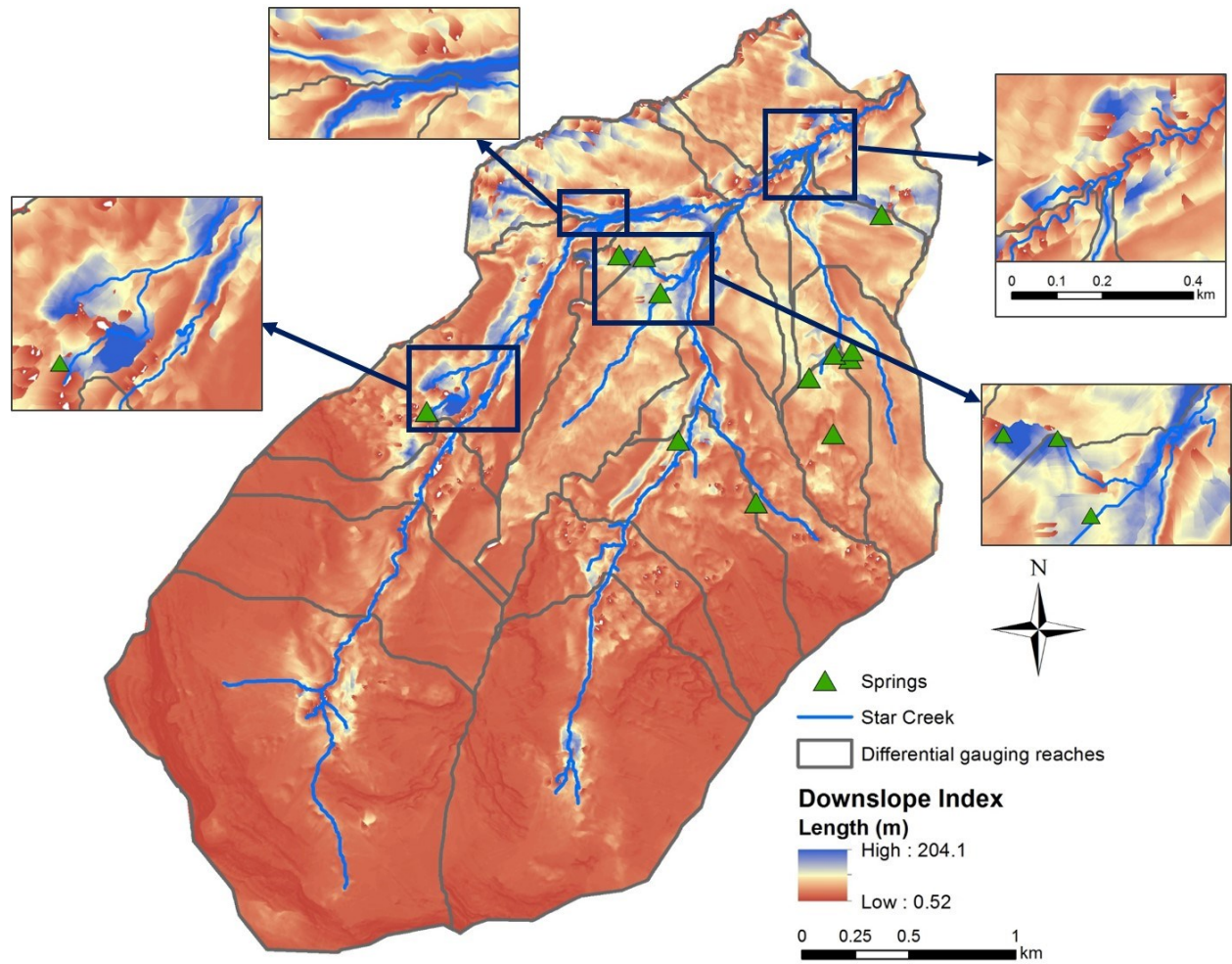
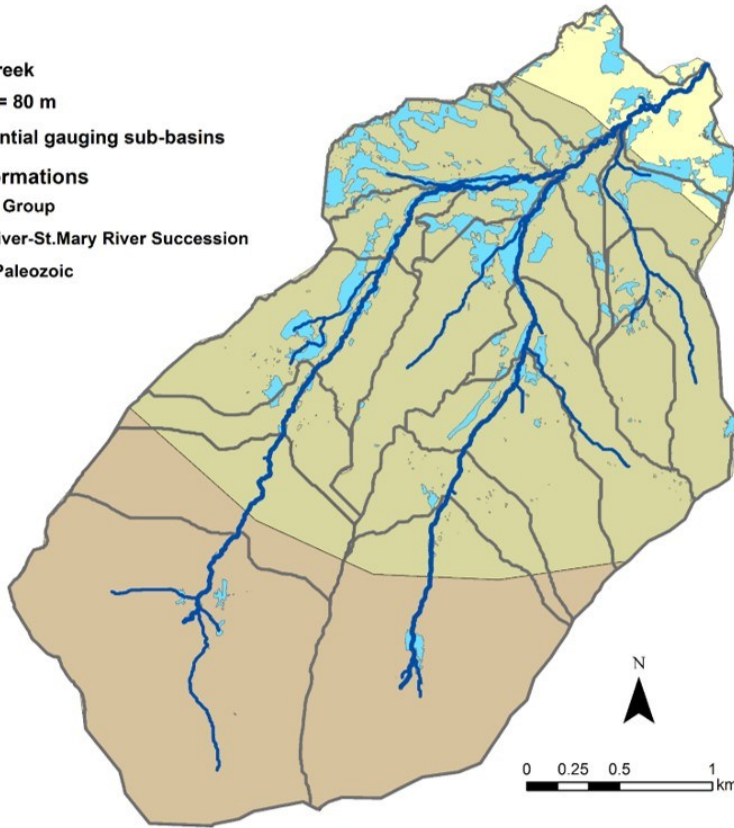


Figure 3.10: DI (solved for L) map with scaled colours. Red represents small L and shorter distances water must travel to decrease 10 m. Blue represents large L and longer distances water must travel to decrease 10 m. Insets were focused areas with identified seeps or tributaries and have a separate scale.

Legend

- Star Creek
- L > or = 80 m
- Differential gauging sub-basins
- Geologic Formations**
- Alberta Group
- Belly River-St.Mary River Succession
- Upper Paleozoic



Legend

- Star Creek
- L > or = 80 m
- Differential gauging sub-basins
- Surficial Geology**
- Bedrock
- Cirque tills
- Colluvium
- Slightly leached till
- Talus

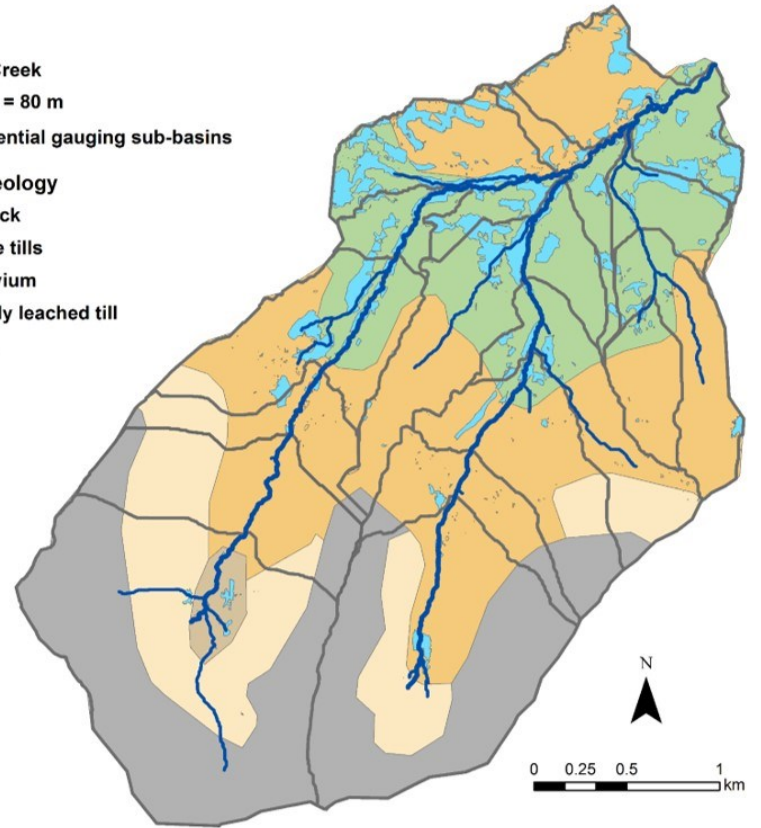


Figure 3.11: Correspondence of regions with L >80 with surficial geology and bedrock geology.

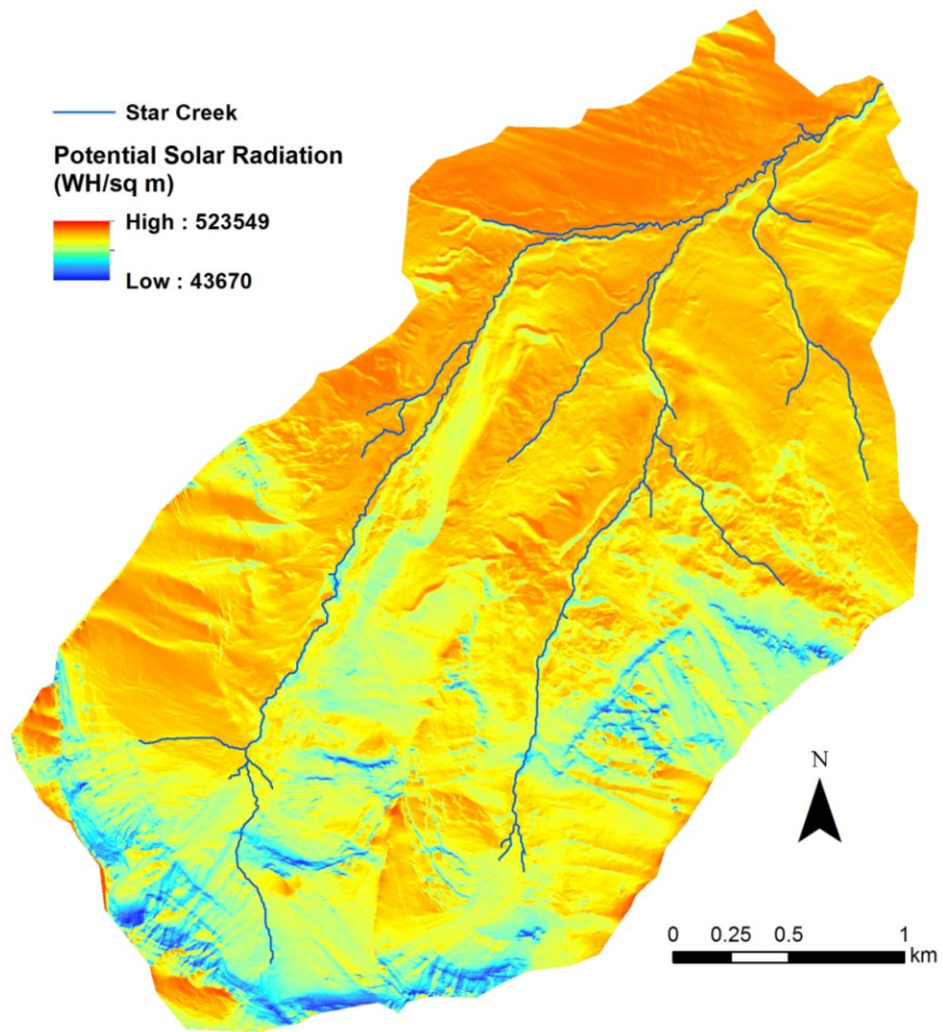


Figure 3.12: Potential solar radiation for the 2014 melt season (April 1 - June 20). Processed using Area Solar Radiation in ArcGIS.

Chapter 4. Source water contributions in a glacial till and fractured sedimentary bedrock dominated Rocky Mountain watershed

4.1. Introduction

Forest disturbance (e.g., wildfire, pine beetle infestation, forest harvesting) removes the forest canopy which increases the total precipitation that reaches the forest floor (Williams et al., 2014; Burles and Boon, 2011; Boon, 2012; Varhola et al., 2010) and can subsequently increase streamflow quantity, change the timing of flows, and alter the dominant flow pathways in a watershed (Stednick, 1996; Scott, 1993; Winkler et al., 2017). However, large variability has been observed in streamflow responses following disturbance due to differences in disturbance type and timing, vegetation type, precipitation regimes, and soil moisture storage (Brown et al., 2005; Stednick, 1996). Some studies have reported little, if any, change in streamflow following disturbance (Williams et al., 2015; Harder et al., 2015) but the mechanisms or features potentially responsible for that lack of change are unclear. Regardless, some authors have used hydrological resistance, a measure of synchronicity between precipitation and runoff (Carey et al., 2010), to explain the lack of change in streamflow following disturbance (Harder et al., 2015). Watersheds exhibiting resistance are associated with a large storage capacity, where water can be stored for months or years and then subsequently released to the stream gradually (Carey et al., 2010).

High bedrock permeability is a watershed feature that is often associated with different streamflow runoff behaviour and watershed resistance. Uchida et al. (2006) showed that a watershed with greater bedrock permeability had larger aquifer storage, and the subsequent release of stored water maintained baseflow later in the year. Similarly, Liu et al. (2004) showed that the recession limb of the annual hydrograph in the Colorado front range Rocky Mountains was driven by baseflow released from fractured bedrock. While streamflow responses to

increased net precipitation after canopy removal may be muted by high storage capacity, climate related changes to the proportions of snow and rain may reduce the magnitude of baseflow. Tague and Grant (2009) cautioned that although slow draining groundwater systems in high mountainous regions may be buffered against climate change because late season baseflow may be maintained, the absolute decrease in streamflow may be substantial due to reductions in snow accumulation, and thus, concomitant reductions in groundwater recharge.

Deep soils and till deposits also have a large storage capacity, which can sustain baseflows and lead to increased hydrologic resistance. For instance, deep basal till in Sleepers River watershed in Vermont was associated with large storage capacity and low permeability; properties that were able to maintain baseflow (Shanley et al., 2015). Deep sediment deposits in the Poschiavino watershed, in Switzerland, created greater storage capacity and greater winter baseflows compared to watersheds with shallow sediment deposits (Floriantic et al., 2018).

In the eastern slopes of Alberta's Rocky Mountains, a region with fractured and faulted sedimentary bedrock overlain by deep glacial tills, Harder et al. (2015) modelled climate and disturbance driven changes in streamflow and reported a lack of change in streamflow. The authors suggested this was due to complex subsurface flow pathways and large storage capacity, but they did not quantify these components. To address this knowledge gap for the eastern slopes of the Rocky Mountains, storage-discharge relationships were developed in Chapter 2 and results indicated that this region has a large storage capacity compared to regions with shallow soils and impermeable bedrock. Storage was found to be similar to other regions with deep surficial materials and permeable bedrock (Hale et al. 2016; Sayama et al. 2011). Two zones of storage were conceptualized as shallow subsurface storage (soil and glacial till) and bedrock storage, which likely contributed to streamflow during the hydrograph recession and baseflow, respectively. While the importance of groundwater upwelling during hydrograph recession and baseflow was corroborated in Chapter 3, the distinct separation

between bedrock groundwater and glacial till groundwater and their contributions to streamflow were less clear.

Chemical signatures of source water (e.g., glacial till groundwater, bedrock groundwater, soil water, and precipitation) and stream water can be used to determine which sources are contributing to streamflow during different flow conditions using end-member mixing (Christophersen and Hooper, 1992). This should improve our understanding of which geologic formations (bedrock or glacial till) are associated with baseflow and, in turn, hydrologic resistance. Thus, the objectives of this chapter were to: 1) characterize how stream water sources (precipitation, soil water, hillslope groundwater, till groundwater, bedrock groundwater, and seeps) vary across four sub-watersheds in Star Creek and from spring snowmelt to fall low flows, and; 2) determine the relative contributions of stream water sources to the stream from spring to fall for each sub-watershed. By characterizing source water contributions to streamflow, we will better understand runoff generation and the hydrological processes controlling watershed resistance on the eastern slopes.

4.2. Study Site

Star Creek watershed (10.4 km²) is located in the eastern slopes of Canada's Rocky Mountains. Average precipitation ranges from 720-990 mm varying with elevation, with 50-60% in the form of snow. There are two main sub-watersheds (Star East and Star West) that span approximately the same elevation (1540-2600 m) but differ structurally. Star West has a larger alpine region with till deposits that holds water throughout the summer. This marshy area drains into the main channel that is primarily bedrock in the upper reaches; in contrast, alluvium and colluvium form the channel in the lower reaches. Star East has a smaller alpine region than Star West and is comprised of colluvial material and a grassy meadow. The stream appears to originate from springs where the water table reaches the soil surface. The upper reaches of the main channel

are colluvial with large boulders, becoming a series of step-pools further downstream. Star West has a larger zone of storage than Star East and a more consistent baseflow discharge (Chapter 2). Two historical continuous streamflow gauging sites exist in each sub-watershed – a lower site (Star West Lower (SWL) and Star East Lower (SEL)) near the confluence of the two sub-watersheds (1530 m elevation) and an upper site (Star West Upper (SWU) and Star East Upper (SEU)) located at approximately 1690 m elevation in the sub-alpine zone. For a more detailed description of Star Creek watershed see Chapter 2.

4.3. Methods

4.3.1. Stream water chemistry

Stream water samples were collected from the four hydrometric stations (SEL, SEU, SWL, SWU; Figure 4.1) every two weeks from April to October in 2014 and 2015 to capture the full range in streamflow chemistry. One litre plastic bottles were triple rinsed prior to sample collection. Samples were analyzed in the Biogeochemical Analytical Service Laboratory (University of Alberta) for major cations and anions (Na^+ , Mg^{2+} , Ca^{2+} , K^+ , Cl^- , SO_4^{2-}) and Si (as SiO_2). Analytical precision for each ion analysis was 1.9, 3.0%, 1.9%, 2.4%, 2.4%, 3.1%, and 3.4%, respectively.

4.3.2. Source water chemistry

Stream water sources were initially hypothesized to be rain, snowmelt, soil water, hillslope groundwater, and groundwater seeps. Installation of sample collection equipment and sampling methods for each source are detailed below. However, in each case, 50 ml plastic vials were triple rinsed by source water prior to sampling. All samples were analyzed for the same ions and by the same methods as the stream water samples.

4.3.2.1. Rainfall and snowmelt

Rain samples were collected in a clean bucket rinsed with deionized water. Buckets were placed in open areas throughout the watershed or in the nearby townsite (Coleman, AB) after a rainstorm began. Locations were chosen opportunistically depending on storm timing and site access. Samples were collected once there was enough water in the bucket to sample to prevent changes in chemical composition due to dry deposition of dust or evaporation. Five, four, and three samples were collected throughout the summer of 2013, 2014, and 2015, respectively.

Eleven snowmelt samples were collected from alpine and sub-alpine regions of Star Creek and North York Creek (an adjacent watershed, Figure 4.1 inset) throughout spring and early summer in 2014. Only three additional samples were taken in spring 2015 because mid-winter melt of snowpacks hindered the collection of more snowmelt samples. Eavestroughs 3 m in length were installed parallel to the hillslope with a small overhang off the edge of the hillslope in Star Creek and North York Creek watersheds prior to snow accumulation. Samples were taken directly from snowmelt troughs and from snowbanks or snow bridges with clearly visible melt. Snowmelt was sampled instead of snow for a better signature of the water that flows through the watershed during the snowmelt period (Johannessen and Henriksen, 1978).

4.3.2.2. Soil water

Suction lysimeters were installed between 30-60 cm depth using a hand auger in two locations near the toe slope groundwater wells (see below) in early spring 2014 (2015 for SEU; Figure 4.1). Suction lysimeters were built with a 0.5 bar ceramic cup and 3.81 cm PVC pipe to ensure that there was ample water collected for subsequent chemical analyses. Water from the suction lysimeter was sampled using a hand pump every two weeks between April and October in 2014 and 2015. Suction lysimeters were pumped dry following sampling and vacuum was reapplied. Thus, soil water was composed of water that was able to pass through the ceramic cup over the

two-week period until the lysimeter was at equilibrium pressure with the surrounding soil.

Shallow depths were targeted with the intention to collect the unsaturated soil water above the saturated hillslope water (see below).

4.3.2.3. Hillslope groundwater

Hillslope wells were dug with a shovel or hand augered to depth of refusal or maximum auger depth (1.5 m) near the hydrometric gauging stations at SEL, SEU, SWL, SWU and on the mainstem of Star Creek below the confluence of the east and west forks (Figure 4.1). A site was added at SEU at the end of the summer in 2014, whereas the other sites were established during summer 2013. Wells were installed in three locations at each site: riparian, toe slope, and hillslope positions to determine the full range in hillslope groundwater. Well depths ranged between 0.5 m (riparian wells) and 1.6 m. Wells were purged using a hand pump prior to sampling. Samples were collected approximately every two weeks, as available, between April and October in 2014 and 2015. Samples from the upper hillslope wells were generally only obtained during the snowmelt or high flow period; at all other times, these wells were dry. Riparian and toe slope wells contained water for all or most of the year, respectively.

4.3.2.4. Groundwater seeps

Seeps were identified on side banks during reach walks that were conducted along the lengths of the east and west forks from the confluence to the stream origins. Samples were taken during three flow conditions: high flow (May/June), recession flow (mid-July), and baseflow (early Sept prior to fall rains), in both 2014 and 2015.

4.3.2.5. Bedrock and till groundwater

Preliminary analysis suggested that a source was missing from those initially collected. Forestry roads were constructed into Star Creek in 2015 to facilitate forest harvesting, which created access for a drill rig. Due to time and monetary limitations, a single hole was drilled to 12 m

depth (15.24 cm in diameter) in the ridge between SEL and SWL (approx. 500 m upstream from gauging sites) in October 2015 (Figure 4.1). Two wells were installed in the borehole, one well in a water-bearing formation in the bedrock at 11 m depth and a second well in the glacial till deposits at 4.5 m depth, to characterize the differences in bedrock and till groundwater chemistry. Both wells had screens that were 1.5 m in length. Sand was used to backfill the borehole around screened section of the bedrock groundwater well and was capped with bentonite clay. Local material removed during drilling was used to backfill the borehole up to the till layer. The same method of back filling (sand, bentonite clay, local material) was used for the till groundwater well. Bedrock and till wells were sampled every two to four weeks in 2016 and 2017. Water in the till well was purged until dry prior to sampling. Water in the bedrock well was purged for 2-5 minutes prior to sampling because the recharge rate was faster than the pump rate.

4.4. Data Processing

End-member mixing analysis (EMMA) was used to visualize multi-variate source water and stream chemistry by reducing the dimensionality of the data with principal component analysis (PCA; Christophersen and Hooper, 1992). The key assumptions for EMMA are: 1) the tracers are conservative; 2) the mixing process is linear; 3) source chemistry does not change temporally or spatially over the period or area studied (Inamdar et al., 2011; Hooper, 2003); and 4) all sources have been identified and have the potential to contribute to streamflow. In addition, there were multiple subjective decisions required prior to running EMMA, such as choosing tracers/ions and defining sources. Two methods were used to determine if tracers were appropriate to use in the analysis. A matrix of bivariate plots of stream chemistry data (ion concentrations), used most commonly in geographical hydrograph separations, was used to determine if ions were conservative in nature (Hooper, 2003). The tracer variability ratio (TVR), used most commonly in sediment apportionment studies, was used to determine if the

difference in ion concentrations between groups is larger than the variation within a source group (Pulley et al., 2015). The TVR was calculated for each tracer pair and compared between each group as the percent difference between source group medians divided by the average coefficient of variation between group pairs (Pulley et al., 2015). TVR should be greater than 2 to be considered appropriate for use in mixing calculations (Pulley and Collins, 2018), although depending on the dataset in question, a greater threshold may be adopted to make the tracer selection more stringent and to help reduce the numbers of tracer/ions included in further data processing.

Box and whisker plots and linear discriminant analysis (LDA) were used to remove the subjectivity of defining sources (Ali et al., 2010; Pulley and Collins, 2018). Box and whisker plots were used as a visual means of discriminating between sources. LDA was then used to determine if the combined sources demonstrated sufficient robust statistical separation (Pulley and Collins, 2018). Other statistical classification methods, such as hierarchical clustering or k-means clustering, were not appropriate because source categories were known a priori. Sources were scaled between 0-1 to satisfy the assumption of equal variance between groups. The data were processed using LDA in the MASS ('lda' function; Venables and Ripley, 2002) and klaR ('stepwise' function; Weihs et al., 2005) packages in R (R Core Team, 2014). The 'stepwise' function was used with the 'backwards' direction in an attempt to maintain the most tracers, 'lda' method, and 'ability to separate' criterion.

After the sources were characterized, the stream water was processed using PCA ('prcomp' in R; R Core Team, 2014) as a method of dimensionality reduction to create a two-dimensional (2D) mixing space (Christophersen and Hooper, 1992). Stream water was standardized (subtracting the mean and dividing by the standard deviation for each sampling point) for each tracer to create equal variance between chemical components and used to create a correlation matrix. PCA was conducted on the correlation matrix to calculate eigenvectors and eigenvalues.

Standardized stream water was then projected into the end member mixing-space by multiplying by eigenvectors. Ideally, two principal components (PCs) explained most of the variation in the data and were used to generate a 2D mixing space, which corresponds to three sources in EMMA (Hooper, 2003). Other studies have used the 'Rule of 1' to determine how many dimensions, and therefore sources, should be used to create the mixing space (Ali et al., 2010; Barthold et al., 2011). For this study, the mixing space was set to two dimensions for ease of visualization but all appropriate sources were used as suggested by Inamdar et al. (2013) to provide a full description of potential source contributions. Source water was then standardized using stream water means and standard deviations for each ion and projected into the 2D mixing space as defined by the stream water (Christophersen and Hooper, 1992; Hooper, 2003). Stream water sources should create an outer boundary or polygon around all stream water samples if all sources were correctly identified and adequately sampled.

4.5. Results

4.5.1. Tracer and source water group selection

Bivariate plots were created and TVR was calculated to determine which tracers were appropriate for use in EMMA. Pearson correlation coefficients were calculated between all stream bivariate plots for stream water at each sub-watershed (Figures 4.2 and 4.3) and showed that all tracers exhibited acceptable linear trends (Pearson's $r > 0.5$) and were thereby likely conservative in nature. Average TVR for almost all tracers at all sites (exception Si at SW and SE) were below 2, which suggested that the within-group variation exceeded the between-group variation and was considered unacceptable. As a result, rather than calculating mixing ratios or percent contributions on the basis of an un-mixing routine, trends in stream water distribution were described in relation to source water dynamics and runoff processes, as suggested by Inamdar et al. (2013).

Sources were initially defined as rain, snowmelt, soil water, riparian water, toe slope water, upper hillslope water, till groundwater, and bedrock groundwater. However, box and whisker plots showed that the distribution of rain and snowmelt were similar as well as the distribution of soil water, riparian water, toe slope water, and hillslope water for most sites. Final source groups are described below for each sub-watershed; box and whisker plots are plotted for final source groups (Figures 4.4-4.7). LDA plots indicated that the first 2 LDs explained 90%, 100%, 100%, and 100% of the variance of the centroids for SWL, SWU, SEL, and SEU sites, respectively. Stepwise analyses were also used in attempt to reduce the redundancy of the tracers and to ensure that samples were well separated; on this basis, 84%, 81%, 81%, and 87% of samples were well separated in SWL, SWU, SEL, and SEU, respectively. In all sites except SEL, the analysis indicated that all tracers should be retained to distinguish between the source groups; Na⁺ was, however, removed to best separate the groups in SEL. Based on these results, it was concluded that there was good separation between source groups as categorized for the individual sites.

4.5.2. Source water characterization

4.5.2.1. Star West Lower

Sources were grouped as precipitation (rain and snow), hillslope groundwater (soil water, riparian water, and toe slope water), till groundwater, and bedrock groundwater and plotted in PCA mixing space (Figure 4.8). Minimal variation across all precipitation samples (standard deviation (SD) of 2.4 and 1.1 for PC1 and PC2, respectively) and overlap of snow and rain samples in the mixing space confirmed that it was appropriate to aggregate all samples (snow and rain) taken across all sites (Star Creek, York Creek, and Coleman). Hillslope groundwater exhibited larger variation across samples (SD of 3.8 and 2.0 for PC1 and PC2, respectively), but no clear temporal pattern was observed. The largest variation in source water was observed in till water (SD of 39.8 and 8.6 for PC1 and PC2, respectively) and the range in values depended

on the year. The 2016 signature of till groundwater became less chemically similar to stream water as it varied from spring to fall, whereas the 2017 signature became more chemically similar to stream water as it varied from spring to fall. The large SD and temporal variation in till groundwater chemistry may have been due to bentonite contamination (Remenda and van der Kamp, 1997). Bedrock chemistry showed slight temporal variation, with more positive values in PC2 in the spring than in the fall (SD of 2.9 and 4.8 for PC1 and PC2, respectively). Seeps were initially considered as a potential source, but of the four features considered, two were chemically similar to hillslope water and two were chemically similar to stream water so none were included as a discrete source.

4.5.2.2. Star West Upper

Sources were grouped as precipitation (rain and snow), hillslope groundwater (soil water, toe slope water, and upper hillslope water), and riparian water (Figure 4.9). Till and bedrock groundwater were collected from a lower elevation in the watershed and were likely not representative of higher elevation groundwater signatures; therefore, they were excluded as potential sources at the upper sites. Precipitation clustered tightly in one location except for a few samples of snow and rain, which increased the SD for precipitation (SD of 4.5 and 2.7 for PC1 and PC2, respectively). All sources showed similar variation as precipitation; hillslope groundwater had a SD of 4.3 and 2.7 for PC1 and PC2, respectively and riparian water had a SD of 3.0 and 2.0 for PC1 and PC2, respectively. No obvious temporal pattern was observed for hillslope water. Conversely, slight temporal variation was observed across months for riparian water, in which SO_4^{2-} concentrations increased from spring to fall. Seeps were initially considered as a potential source, but of the two features considered, one was chemically similar to riparian water and one was chemically similar to stream water so neither were included as a source.

4.5.2.3. Star East Lower

Sources were grouped as precipitation (snow and rain), hillslope groundwater (soil water, riparian water, toe slope water, and upper hillslope water), till groundwater, bedrock groundwater, and seep 27 (Figure 4.10). Precipitation, bedrock and till sources were the same as those used in SWL. Again, precipitation was tightly clustered in the PCA biplot for SEL (SD of 3.0 and 3.1 for PC1 and PC2, respectively). Although hillslope groundwater samples were grouped together as a single source (SD of 10.0 and 8.4 for PC1 and PC2, respectively), there was slight clustering within the group. Riparian and toe slope samples were more chemically similar than soil water and were also more similar to stream water but did not vary temporally. Soil water was most different from stream water and varied from spring to fall (increased Ca^{2+} and Mg^{2+} concentrations). Till groundwater showed the same variation between years and across months as for SWL (Figure 4.8). However, till groundwater did not differ from the stream water as much as in SWL, had some chemical similarities to soil water, and varied less (SD of 5.9 and 5.7 for PC1 and PC2, respectively) than hillslope groundwater. This was likely due to the removal of Na^+ as a tracer (outcome of LDA stepwise procedure) because it showed the most difference between sources when compared to the other source water chemistries in the corresponding box and whisker plots (Figure 4.4). Bedrock groundwater was clustered in a linear pattern, but no temporal variation was observed. Seep 27 was chemically similar to stream water and likely should not be used as an end member but was retained to aid in the explanation of stream water dynamics.

4.5.2.4. Star East Upper

Sources were grouped as precipitation (rain and snow), hillslope groundwater (soil water, riparian water, and toe slope water), and seep 35 (Figure 4.11). Precipitation was clustered in a linear pattern (SD of 4.0 and 1.5 for PC1 and PC2, respectively) but did not vary temporally. Large variation was observed for hillslope groundwater (SD of 9.3 and 7.3 for PC1 and PC2,

respectively). Toe slope water and riparian water had some chemical dissimilarities but were not different enough from each other or soil water to be considered as different groups. Soil water varied temporally and was more similar to riparian water in the spring but less like all other sources in the fall. No temporal pattern was observed for toe slope water or riparian water chemistry. Seep 35 was chemically similar to stream water and should have been removed from the analysis, but again, was retained to aid in the explanation of stream water dynamics.

4.5.3. Stream water characterization

Stream water chemistry for all sites showed temporal variation throughout months with open water flow but not between years. As a result, the temporal pattern of stream water was characterized for each site in general for both years combined. Further, due to the lack of source water samples from winter months, stream water characterization was completed from April to October, which represents the beginning of snowmelt through to the start of the next year's snow period, the main dynamic period of the stream hydrograph.

4.5.3.1. Star West Lower

PCA analysis indicated that 82% of the variation in the data was explained by the first two PCs. Stream water samples were contained within an outer boundary created by source water when the temporal variation in source water was considered (Figure 4.8), but not if median values of source water were considered. As a result, all source water samples were plotted with all stream water samples. In April, stream water was most similar to the hillslope groundwater. Stream water transitioned through May and was most similar to precipitation source water in June. In July, stream water was slightly more similar to hillslope groundwater and bedrock groundwater. In August, September and October, stream water was once again most similar to hillslope groundwater and bedrock groundwater. The temporal pattern associated with stream water variation through the fall was perpendicular to the direction of the bedrock temporal pattern suggesting that hillslope groundwater, rather than bedrock groundwater, was driving

stream water chemistry in the fall. Stream water chemistry did not reflect the high concentrations in till groundwater at any time of the year which could be due to bentonite contamination of till groundwater rather than a lack of contribution to the stream.

4.5.3.2. *Star West Upper*

PCA analysis indicated that 77% of the variation in the data was explained by the first two PCs (Figure 4.9). Sources formed two ends of a spectrum for stream water mixing rather than a triangle or polygon defining the mixing space. It is possible that a source was missed in the sampling campaign but when the variation in sources was taken into account, the stream water was mostly contained between the two points. In April, stream water was most similar to hillslope groundwater. Stream water transitioned through May and was more similar to precipitation in June and July. Stream water was similar to hillslope groundwater again through August, September, and October but did not follow the same pathway as in the early summer months. These temporal differences in stream water between spring and fall are similar to the temporal differences observed in riparian water from April to October. It is possible that there was mixing between riparian water and stream water producing a similar temporal variation in their chemical signature.

4.5.3.3. *Star East Lower*

PCA analysis indicated that 86% of the variation in the data was explained by the first two PCs (Figure 4.10). Stream water samples were mostly contained within an outer boundary created by source water when the temporal variation in source water was considered; however, September/October stream water plotted outside this boundary. In April, stream water was most similar to the hillslope or bedrock groundwater. Stream water transitioned through May and was most similar to precipitation in June. In July and August, stream water became dissimilar from precipitation and was once again similar to hillslope groundwater. In September and October, stream water was less similar to hillslope groundwater and plotted outside the boundary created

by the identified sources. Since stream water was not contained within the boundary created by the source water, it is likely that a source was missed from the analysis. The temporal variation in seep 27 followed the same pattern as the September/October stream water, suggesting the same source water for seep 27 and late fall baseflow. As in SWL, stream water chemistry did not reflect the high concentrations in till groundwater at any time of the year but again could be due to contamination of the till groundwater well.

4.5.3.4. Star East Upper

PCA analysis indicated that 83% of the variation in the data was explained by the first two PCs (Figure 4.11). Similar to SEL, some of the stream water samples were outside the boundary formed by the stream water sources. In April, stream water was most similar to hillslope water. Stream water was similar to precipitation in May and June. In July and August, stream water was similar to hillslope groundwater but not as much as in April. In September and October, stream water became chemically dissimilar from all identified sources and plotted outside the boundary created by these sources. As in SEL, the temporal variation observed in the stream in September and October was also observed in seep 35 (spring to fall). Again, it is likely that there was another source contributing to streamflow in the fall that was not captured by the field sampling.

4.6. Discussion

4.6.1. Temporal and spatial variation in source water

Chemical signatures of source water have been shown to vary seasonally and annually (Rademacher et al., 2005) as well as spatially across sub-watersheds (James and Roulet, 2006). As a result, James and Roulet (2006) suggested that only source water from within individual sub-watersheds of interest should be used in mixing calculations. Inamdar et al. (2013) further argued that mixing proportions should not be calculated because multiple

assumptions are often violated and can lead to significant errors in un-mixing proportions. Rather, temporal and spatial variation in stream water and source water should be examined and used to describe or to develop a physically-based conceptualization of runoff mechanisms.

Two of the key assumptions for EMMA, the chemical composition of sources does not change over 1) the time scale considered or 2) with space (Hooper, 2003; Inamdar et al., 2011), were violated in this dataset. Source water chemistry varies greatly across the watersheds. For example, when all hillslope samples from each sub-watershed were projected into the mixing space created by stream water at the watershed outlet (SM), large variability was evident between sites (Figure 4.12). While there was some overlap between some sites (SWL and SEU), SWU was clearly different than the other hillslope samples. As a result, source water from within individual sub-watersheds was used to reduce the uncertainty associated with large spatial variability. However, the variability within sites was also quite large. The coefficient of variation (CV) of source water was often larger than the CV of the stream water (there should be little to no variation in source water over time; James and Roulet, 2006; Inamdar, 2011), particularly for K^+ . The occasions where source water CV were smaller than stream water CV for most ions were for seeps in SEU and SEL, bedrock groundwater in SWL and SEL, and hillslope and riparian water in SWU.

Despite the violation of assumptions, interesting temporal trends in source water chemistry were observed. For example, temporal variations in riparian water in SWU were observed from spring to fall. Despite most of the stream water ranging between two main points (hillslope and precipitation sources) on the PCA biplot (Figure 4.9), there was a difference in spring and fall stream water chemistry. Riparian water followed the same pattern observed in stream water chemistry in May compared to September/October. It is not clear if the stream chemistry responded to variation in riparian chemistry or if riparian water responded to stream chemistry, but these pools of water were likely mixing to create the same temporal pattern. Not all sources

had clear patterns of variation. Shallow well data presented in Chapters 2 and 3 suggested that the upper hillslope and the stream were only connected during the spring freshet. While this would suggest that hillslope water chemistry should reflect the dilution from snowmelt, no corresponding temporal pattern was observed in hillslope water chemistry in most sub-watersheds. This is likely because snowmelt was not the only precipitation source that mixed with older hillslope water. Large, high intensity convective storms throughout the summer season may have mixed with hillslope water and muted the effect of the snowmelt pulse over a short time period. These effects would be limited due to high soil storage capacity (Chapter 2) and evaporative demands (Chapter 3) but may affect the hillslope water chemistry depending on when the samples were collected compared to large rainfall events.

All sources were consistent between years, except till groundwater which varied greatly across seasons and in opposite directions in 2016 and 2017. The high concentrations of Na^+ , Cl^- , and SO_4^{2-} (Figures 4.4 and 4.6) and the variability between years suggests that the till groundwater well was likely contaminated by bentonite clay used to backfill and seal between layers (Remenda and van der Kamp, 1997). Slow recharge rates (and therefore, low hydraulic conductivity) of glacial till prevented the removal of three pipe volumes when sampling and the corresponding low hydraulic conductivity resulted in little flushing of contaminants. Faster recharge rates (and therefore, higher hydraulic conductivity) of the bedrock groundwater would result in better flushing of contaminants which reduced the contamination effects of bentonite (Remenda and van der Kamp, 1997). Glacial till is also spatially heterogenous and likely has multiple flow pathways within it (Langston et al., 2011). For example, clay lenses can create perched water tables that have different response times than the rest of the till matrix (Evans et al., 2000) or create complex groundwater flow pathways (Freeze and Witherspoon, 1967). As a result, there are limitations to the inferences that can be drawn from a single till groundwater well in the study watershed.

Bedrock groundwater was consistent between years but there is uncertainty around the variability of bedrock groundwater chemistry across the watershed. Although most of the stream is situated within the same geologic formation, there may be differences in bedrock groundwater chemistry associated with heterogeneous sedimentary layers or contact time (Freeze and Cherry, 1979). Seeps that were sampled along the stream length could be used as a potential indicator of groundwater variability because they may come from various formations or flow pathways. Temperature signals from seeps suggested some were groundwater fed (consistent cool temperatures) and others were fed by shallow subsurface water (larger fluctuations in temperature; Taniguchi, 1993). However, ion concentrations of the seeps were not chemically distinct because they were generally similar to stream water or hillslope groundwater. Other tracers such as nitrogen or oxygen and hydrogen isotopes may help differentiate between seeps, hillslope groundwater, and bedrock groundwater. More wells in the bedrock could also characterize the variability in bedrock groundwater more robustly across the watershed and improve the EMMA results.

4.6.2. Temporal variation in stream water contributions

Stream water contributions can be generalized for all sub-watersheds in a number of ways. The water that was stored in the hillslope over winter was likely the first to reach the stream in the early spring prior to high flow as snowmelt started to saturate the landscape. The displacement of old subsurface water has been observed in other regions such as Sleepers River Research Watershed in Vermont (McGlynn et al., 1999). McGlynn et al. (1999) suggested this was due to a small volume of snowmelt being added to the large storage of water already in the subsurface. This initial displacement of old water was likely followed by a dilution effect, where large volumes of low concentration snowmelt mixed with soil water and contributed to streamflow. Snowmelt was the major event that produced a water table response in all wells and connected the hillslopes to the stream (Chapters 2 and 3). The initial snowmelt period was also the only

time overland flow was observed at the study site. Stream water contributions were more similar within Star East (SEL and SEU) and Star West (SWL and SWU) sub-watersheds than between upper (SEU and SWU) and lower (SEL and SWL) sub-watersheds. PCA plots for SEL and SEU showed that stream water was most like precipitation in May and June. Conversely, this dilution effect occurred in June and July in SWL and May to July in SWU. The delayed response in SWL and SWU is consistent with the results in Chapters 2 and 3 that suggested that the west fork sub-watersheds had a larger storage capacity than the east fork sub-watersheds. Accordingly, more water would be required to fill storage before saturation or hydrologic connectivity occurred.

Differences in the east and west forks were also evident later in the year. In SWL and SWU, stream water was chemically similar to hillslope groundwater in the fall. In SEL and SEU, stream water was similar to hillslope groundwater in August but fell outside the boundaries created by the identified sources in September and October (Figures 4.10 and 4.11). A seep in SEL (seep 27) and SEU (seep 35) followed a similar temporal pattern as stream water from spring to fall and may provide insights into the sources of stream water in the fall. In SEL, the temperature of seep 27 ranged between 2.2-3.7 °C throughout the summer, which is indicative of a bedrock groundwater source because the temperature range was muted and was not influenced by radiative warming (Taniguchi, 1993). Similarly, in SEU, the temperature of seep 35 ranged from 2.5-3.5 °C, also indicating a bedrock groundwater source. Temperature records from groundwater wells showed that till groundwater ranged between 2.7-9.7 °C and bedrock groundwater ranged between 5.1-5.8 °C. Both seep 27 and seep 35 had low variability like bedrock groundwater but were cooler suggesting a deeper bedrock groundwater source than in the well. However, the water chemistry of both seeps was different from the bedrock groundwater well lower in the watershed. Star Creek has spatially heterogeneous surficial deposits and geology (Chapter 3) which likely has a large influence on groundwater chemistry

throughout the watershed. It is possible, therefore, that additional bedrock groundwater sources were contributing to streamflow in Star Creek.

4.6.3. Conceptualization of streamflow generation

Contamination of the till groundwater well limits the inferences that can be made about contributions to streamflow. However, the slow recharge rate (and therefore, low hydraulic conductivity) of the till groundwater well suggests there is likely a slow release of water from glacial till and may be important in evaluating resistance of watersheds to disturbance (e.g., wildfire, forest harvesting, insect outbreak). Heterogeneous glacial till deposits with different physical characteristics were linked to the variable release of stored water, and thus the variability in baseflow, in the Scottish Highlands (Blumstock et al., 2015). This delayed or variable release of stored water could mute the impact of disturbance during high flows and subsequently increase baseflows. Chapter 2 showed that the Star Creek sub-watersheds have a large storage capacity (400 or 520 mm in SE or SW, respectively) in glacial till or fractured bedrock. When compared to average annual precipitation (720-990 mm), it is possible that storage can mitigate the effects of the increased net precipitation reaching the ground following disturbance (Williams et al., 2014).

4.7. Conclusion

Stream and source water chemistry in four sub-watersheds of Star Creek showed that old water reached the stream first at the onset of spring melt. This was followed by a dilution effect as the snowmelt saturated the landscape and the hillslope was connected to the stream. Fall baseflows differed between Star East and Star West forks. Star West stream water was once again similar to hillslope water, but Star East was unlike all measured sources. Contamination of the till groundwater well limits the inferences that can be made from the water chemistry. However, slow recharge rates (and likely low hydraulic conductivity) suggest that water

recharged into the till groundwater is slowly released to the stream, thereby muting the effects of disturbance on peak flows. This large storage zone may be an important factor in watershed resistance to disturbance that has been observed in front-range Rocky Mountain watersheds in Alberta.

4.8. Figures

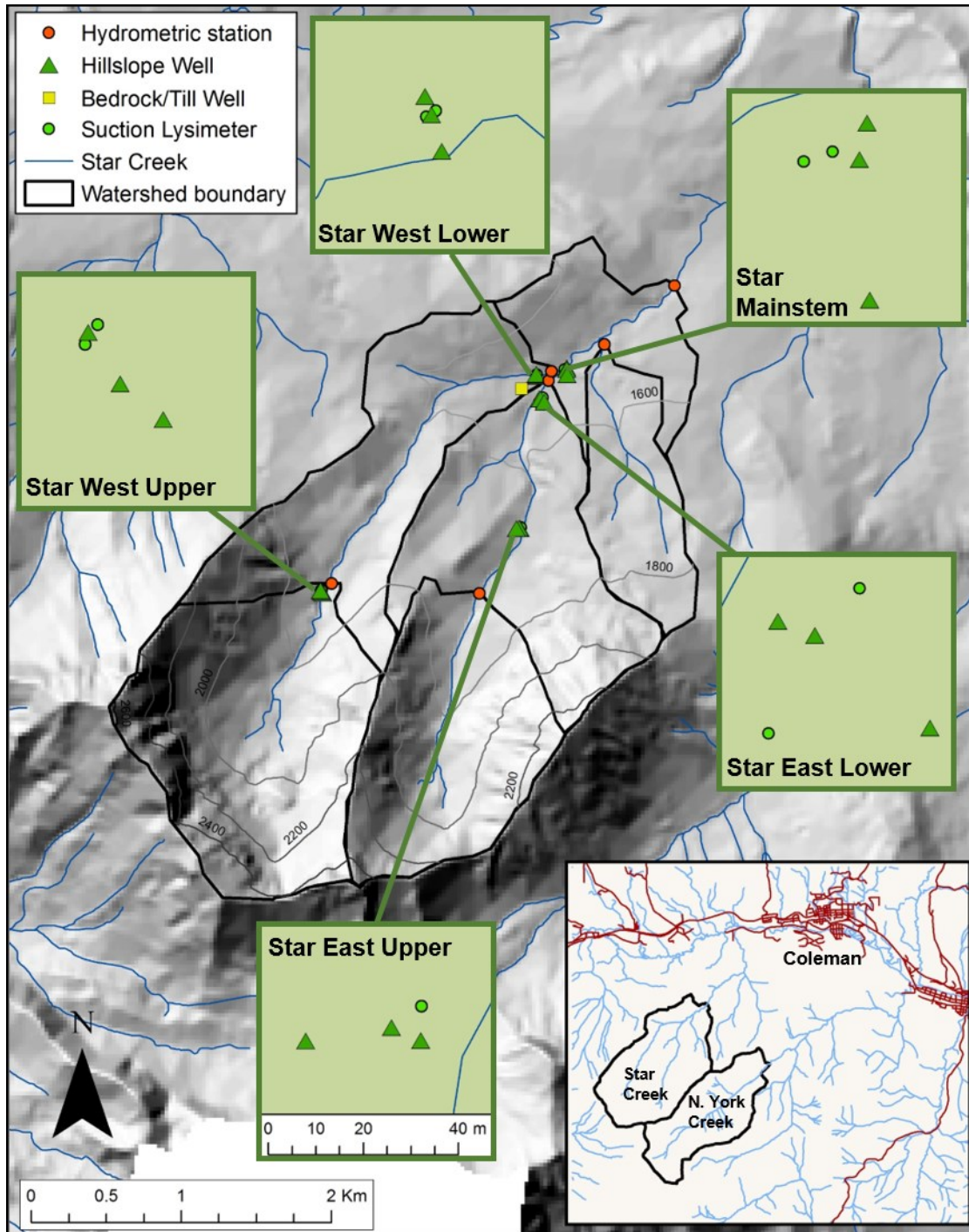


Figure 4.1: Map of Star Creek watershed. Suction lysimeter and hillslope groundwater well locations are magnified in green boxes. Map inset shows location of Star Creek in relation to North York Creek and the town of Coleman, Alberta.

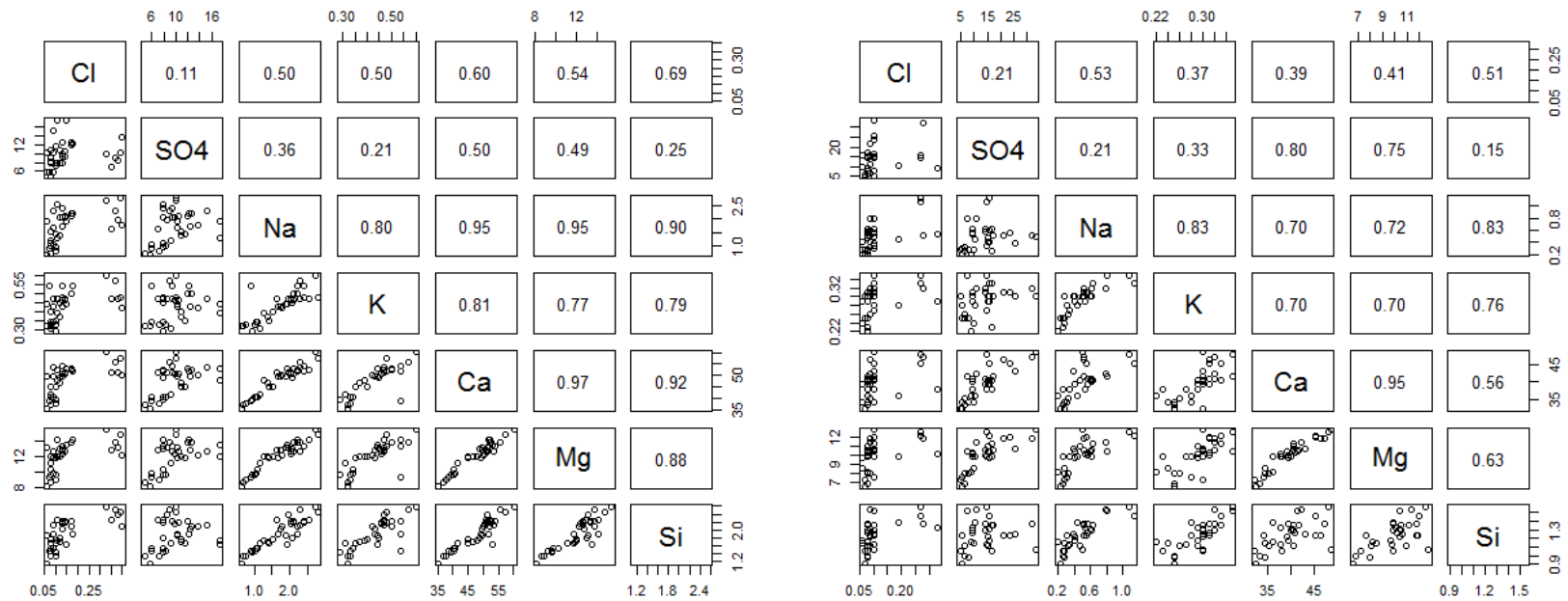


Figure 4.2: Bivariate plots of stream water chemistry at Star East Lower (left) and Star East Upper (right). Ions are measured in mg/l. Top half of plots represents the Pearson's correlation coefficient (r) for the linear relation between each solute.

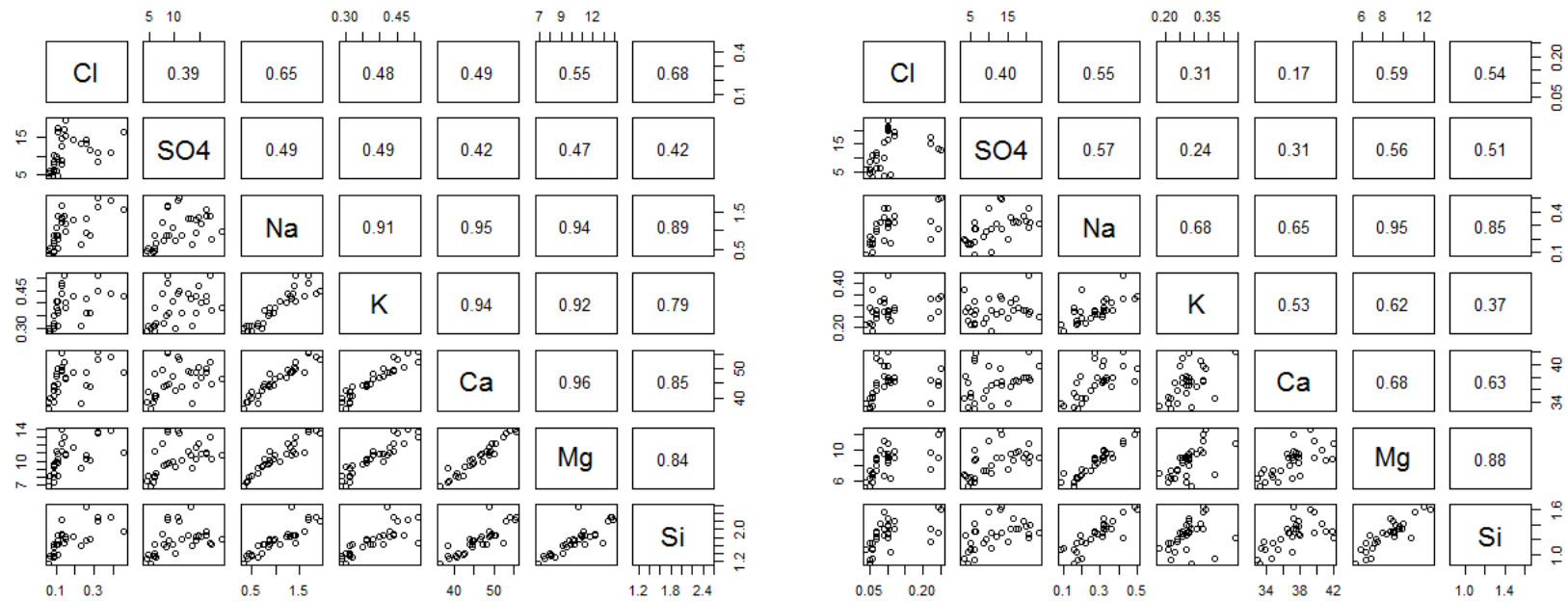


Figure 4.3: Bivariate plots of stream water chemistry at Star West Lower (left) and Star West Upper (right). Ions are measured in mg/l. Top half of plots represents the Pearson's correlation coefficient (r) for the linear relation between each solute.

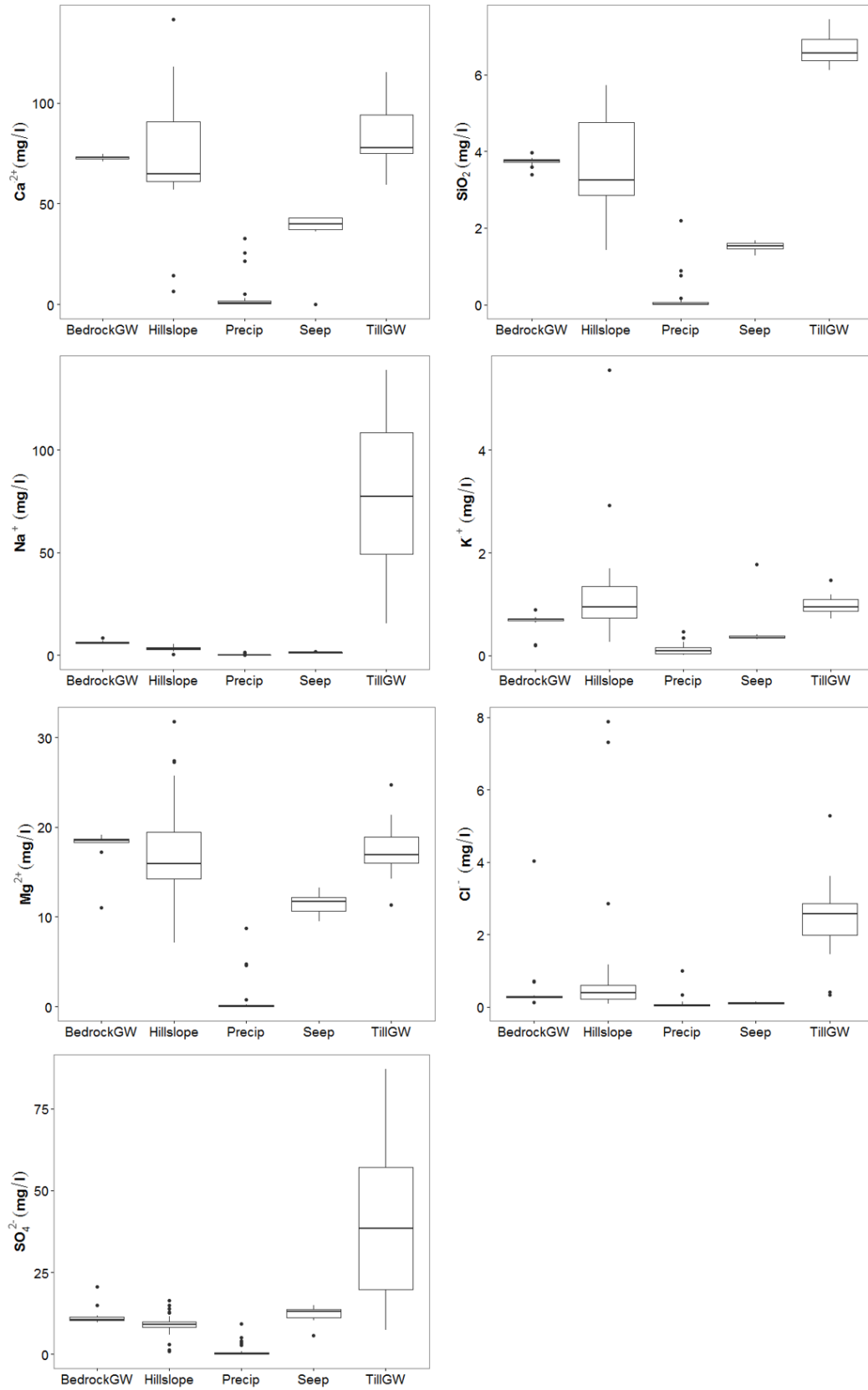


Figure 4.4: Box plots for Star East Lower showing the ranges in chemistry for potential sources.

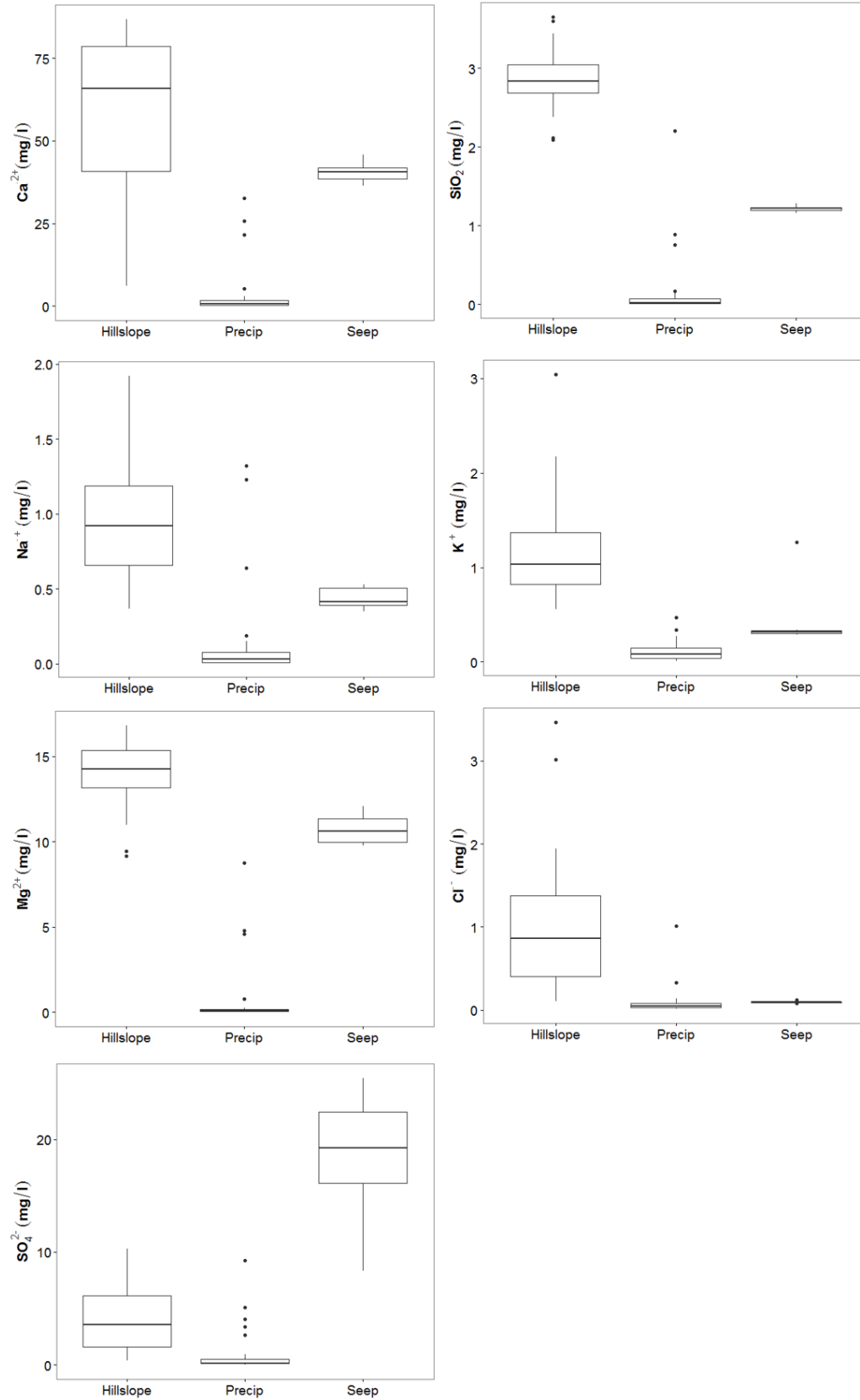


Figure 4.5: Box plots for Star East Upper showing the ranges in chemistry for potential sources.

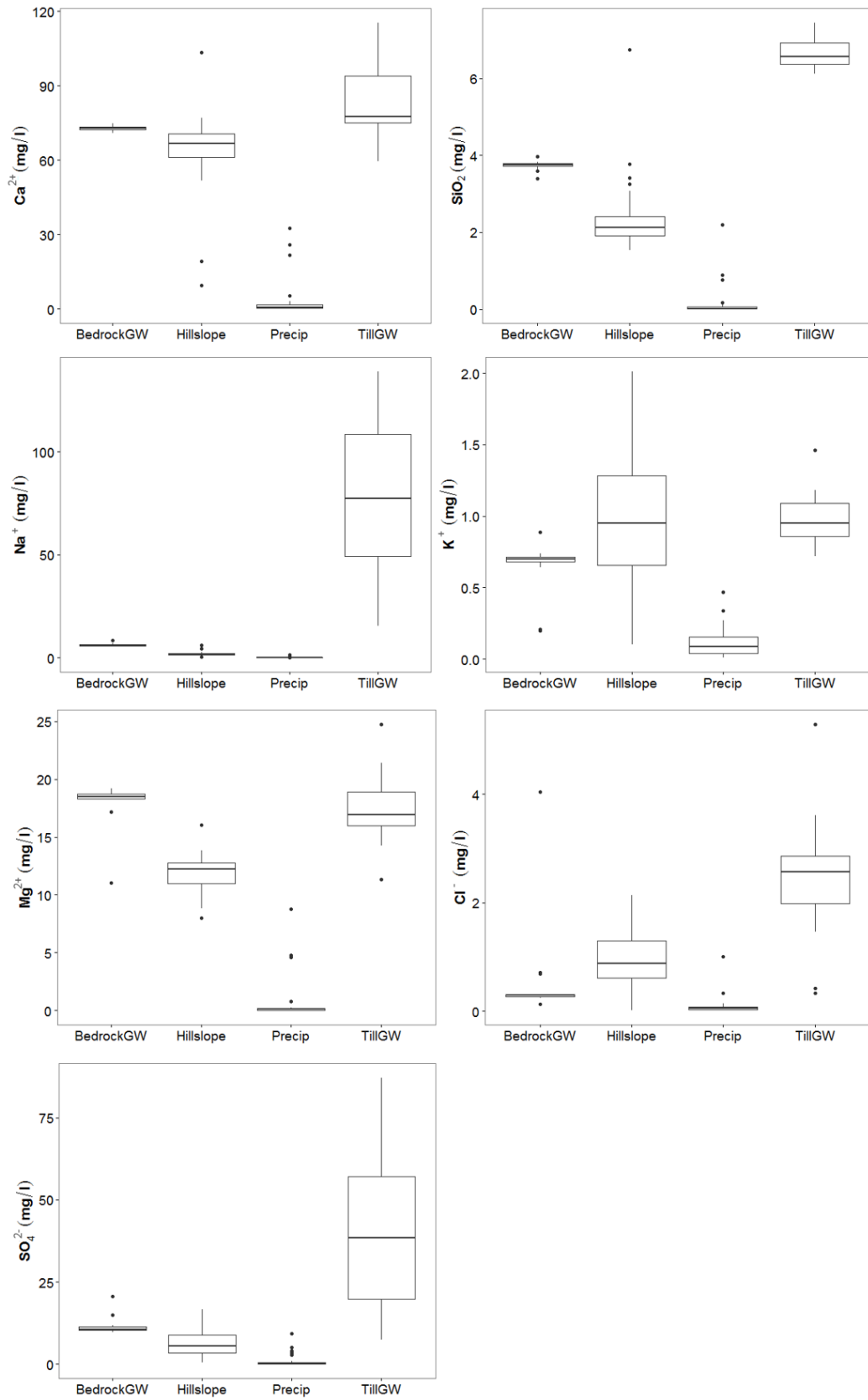


Figure 4.6: Box plots for Star West Lower showing the ranges in chemistry for potential sources.

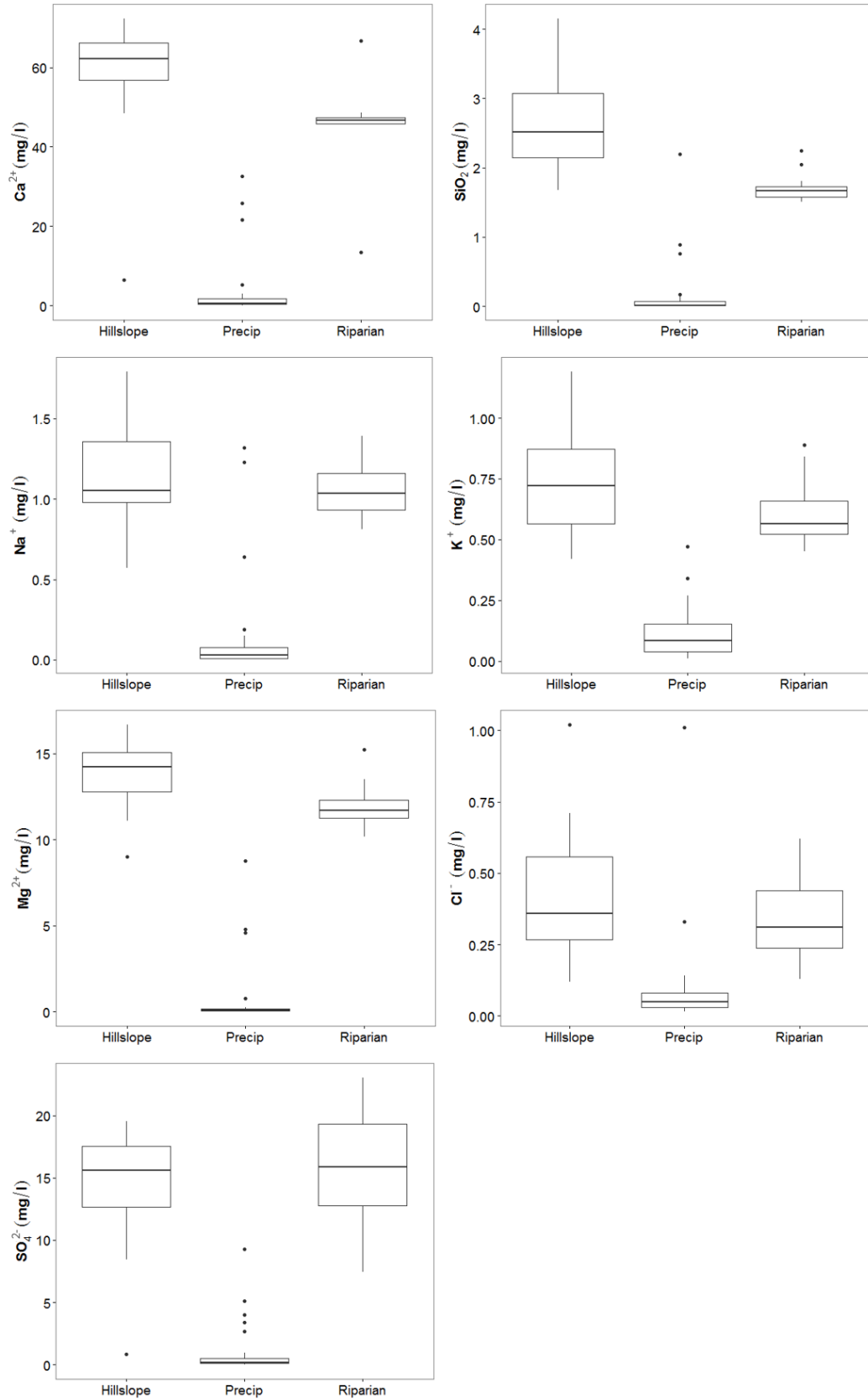


Figure 4.7: Box plots for Star West Upper showing the ranges in chemistry for potential sources.

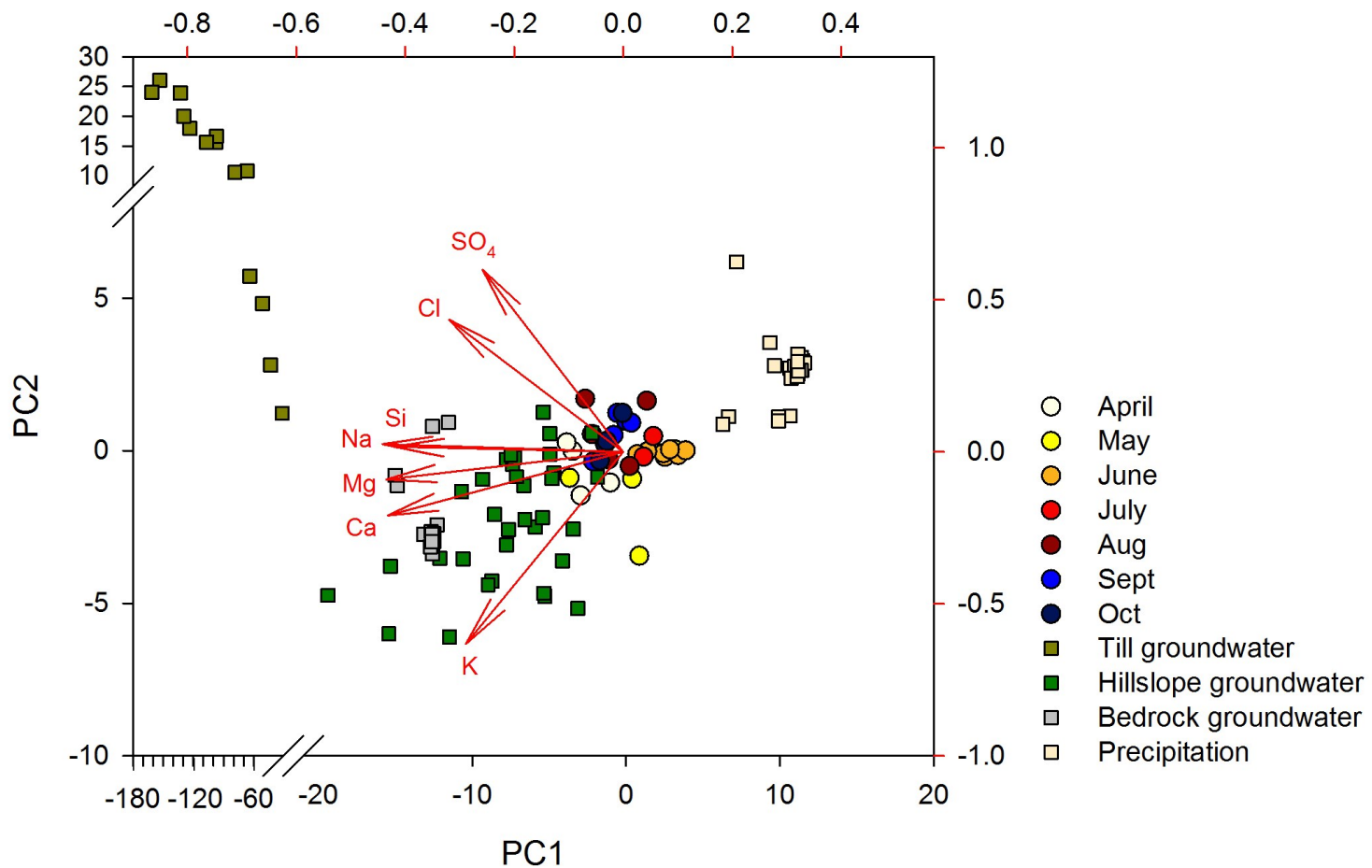


Figure 4.8: Star West Lower stream water chemistry from April to October in 2-D mixing space, which was derived from principal components analysis. Source water (precipitation, hillslope groundwater, till groundwater, and bedrock groundwater) was projected into the stream water mixing space. PC1 and PC2 represent the first and second principal components.

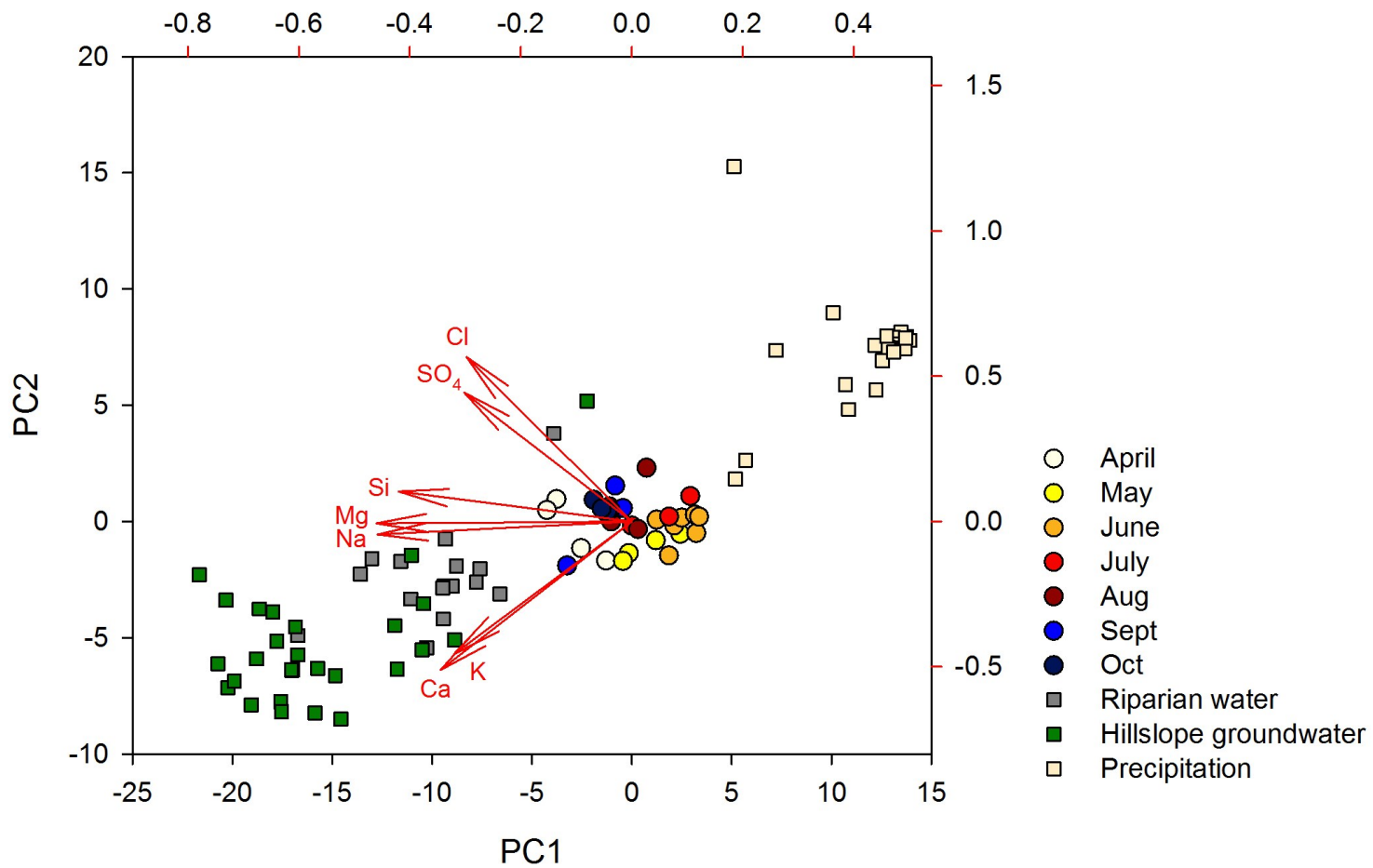


Figure 4.9: Star West Upper stream water chemistry from April to October in 2-D mixing space, which was derived from principal components analysis. Source water (precipitation, riparian water, and hillslope groundwater) was projected into the stream water mixing space. PC1 and PC2 represent the first and second principal components.

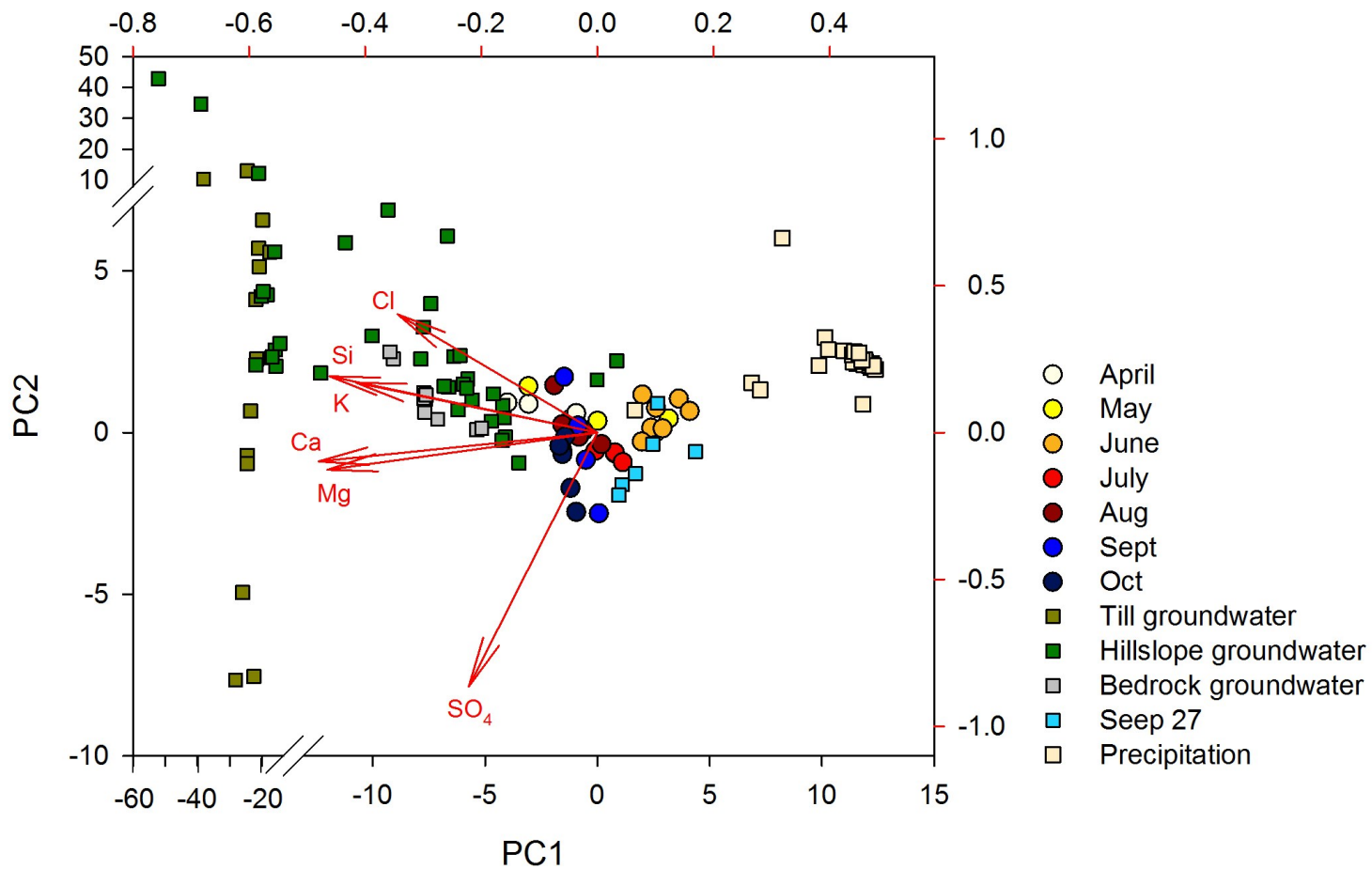


Figure 4.10: Star East Lower stream water chemistry from April to October in 2-D mixing space, which was derived from principal components analysis. Source water (precipitation, hillslope groundwater, till groundwater, bedrock groundwater, and seep 27) was projected into the stream water mixing space. PC1 and PC2 represent the first and second principal components.

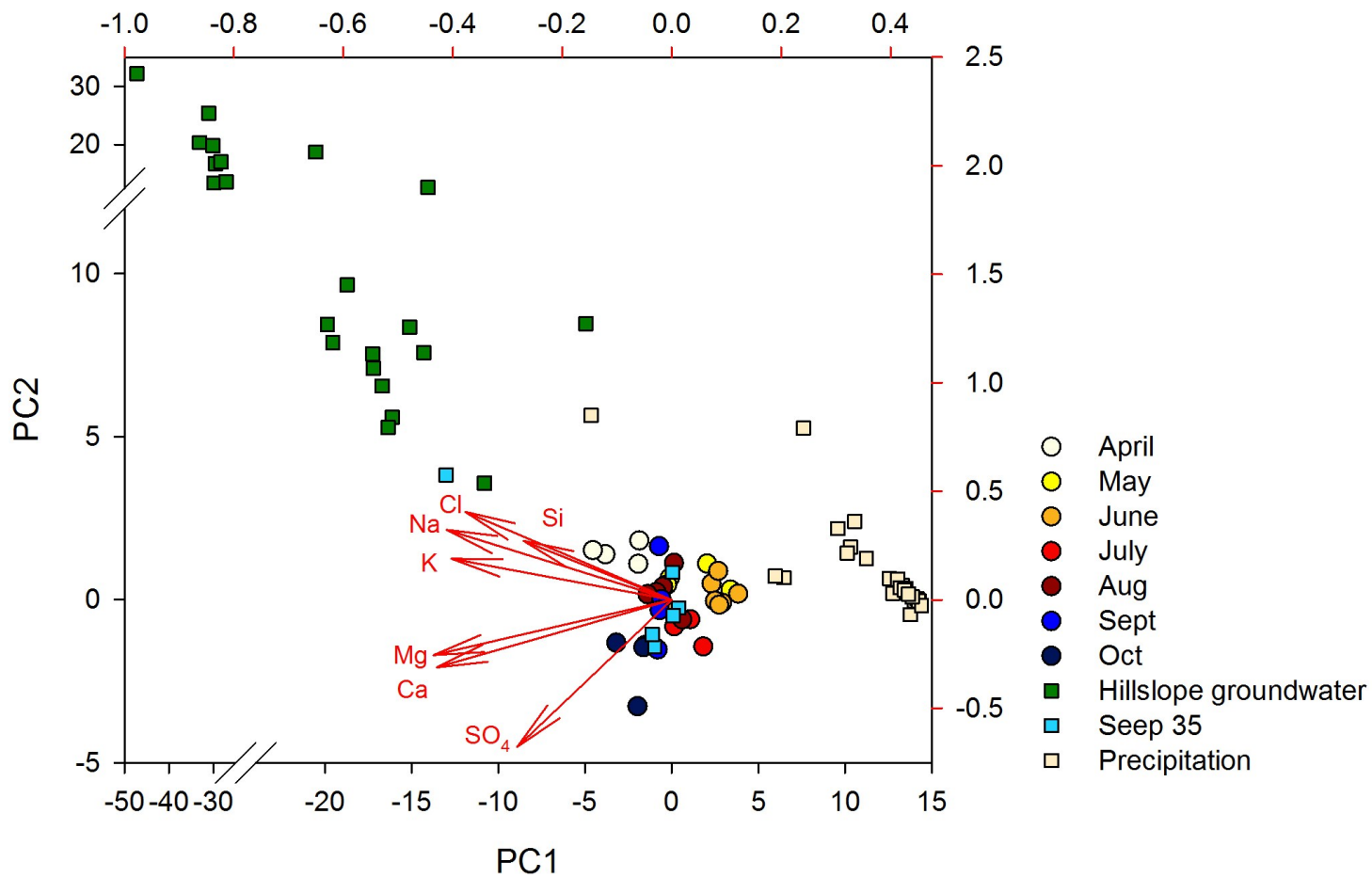


Figure 4.11: Star East Upper stream water chemistry from April to October in 2-D mixing space, which was derived from principal components analysis. Source water (precipitation, hillslope groundwater, and seep 35) was projected into the stream water mixing space. PC1 and PC2 represent the first and second principal components.

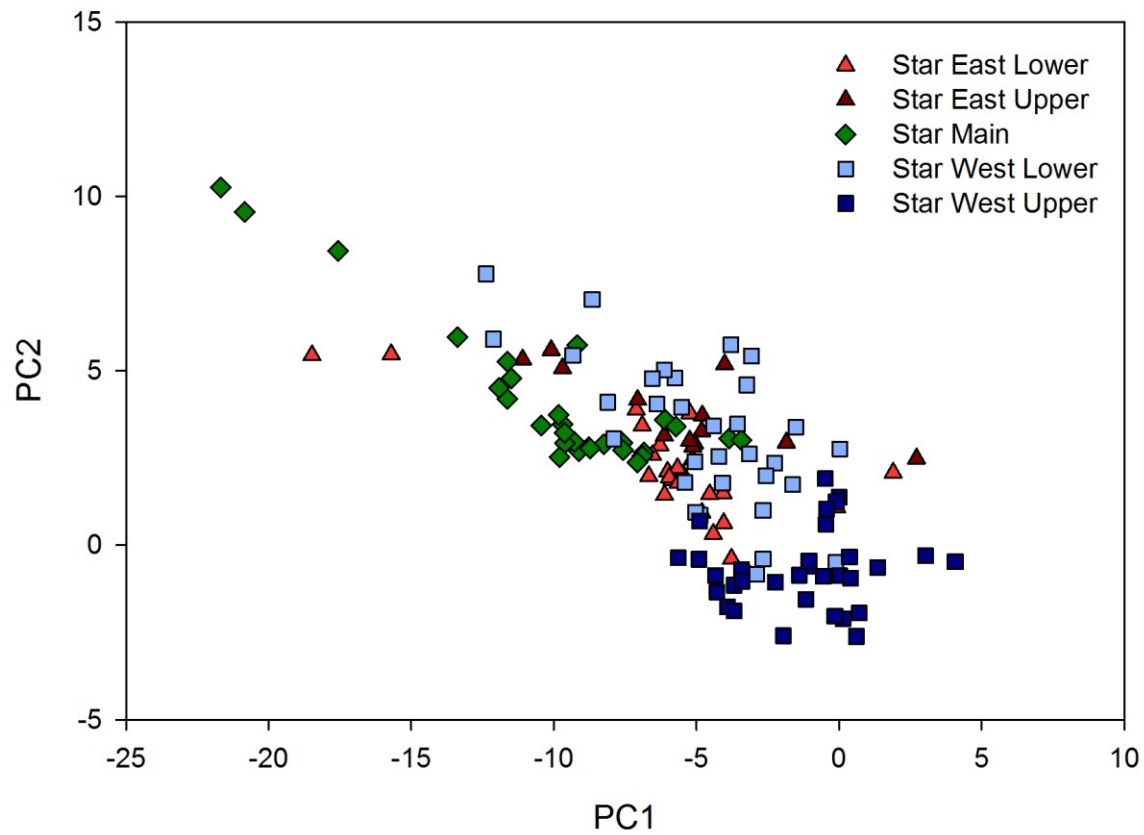


Figure 4.12: Hillslope groundwater from all sub-watershed sites in 2-D mixing space, which was derived from principal components analysis of Star Main stream water. PC1 and PC2 represent the first and second principal components.

Chapter 5. Synthesis

Star Creek is a steep mountain watershed with shallow soils, deep glacial till, and fractured sedimentary bedrock. The combination of multiple permeable surficial layers can complicate subsurface runoff dynamics compared to other watersheds that have shallow soils and relatively impermeable bedrock (e.g., Maimai research watersheds in New Zealand, Fudoji watershed in Japan, and Panola Mountain Research Watershed in Georgia, USA). Thus, the main objective of this research was to describe the first order controls on runoff generation in Star Creek watershed by 1) quantifying precipitation-runoff relationships and watershed storage; 2) characterizing how and when hydrologic connectivity between hillslopes and streams occur, and; 3) characterizing differential source water contributions to streamflow across the dominant hydrologic season.

The first data chapter (Chapter 2) characterized precipitation-runoff relationships and quantified watershed storage in two adjacent sub-watersheds (Star East and Star West) and developed a conceptual model of runoff generation for Star Creek. Multi-year dry and wet precipitation patterns were observed between the 2008-2010 water years and the 2013-2014 water years, respectively, and corresponded with more streamflow contributions in Star East and Star West Creeks. Star West Lower changed from a net losing to net gaining stream over the study period. Star East Lower showed weaker increases in streamflow and persisted as a gaining stream. Despite the increase in streamflow, there was no difference in event-based rainfall-runoff responses between the dry period and the wet period. Rather, snowmelt dominated the event-based responses, where there was a greater streamflow response closer to the snowmelt period than further from the snowmelt period. Variation in annual runoff ratios was partly explained by total rainfall during the previous fall (carry-over of storage). Differences between Star East and Star West were evident in estimates of dynamic storage (487 mm and 595 mm,

respectively). Baseflow recession characteristics suggested that Star West had a more consistent baseflow source that maintained streamflow in the late summer, while Star East baseflows were consistently less and even stopped flowing in the upper reaches late in the summer. Together, these results suggest that Star West has a larger storage capacity than Star East.

Results from this study provide important conceptual insights into higher-order controls on precipitation-runoff dynamics exerted by watershed storage in post-glacial mountain regions with permeable fractured bedrock. Shallow subsurface storage (soil and glacial till) influenced the carry-over of storage between seasons, streamflow response during snowmelt or large rainfall events later in the summer, and hillslope connectivity. In contrast, bedrock storage influenced annual streamflow response to multi-year precipitation patterns due to the dominance of vertical percolation and groundwater recharge. Other studies have shown that fractured or permeable bedrock was a key subsurface storage zone (Hale & McDonnell, 2016; Uchida et al., 2006). However, deep soils or glacial till can add additional complexity to subsurface flow pathways (Kuras et al., 2008; Creed and Band, 1998; Shanley et al., 2015). Although previous research has provided insights in subsurface flow systems in a region with both sedimentary bedrock and glacial till (Burns et al., 1998; Smith et al., 2014), none has quantified the storage capacity for a watershed with both permeable structures.

In the second data chapter (Chapter 3), instantaneous discharge measurements were made at sixteen locations along Star Creek to identify reaches that were gaining water from throughflow or groundwater or losing water to groundwater. Measurements were taken during high flow, recession flow, and baseflow to capture the changes in hillslope-stream connectivity and differences in runoff sources and pathways. Streamflow contributions were used to determine if a) upslope accumulated area (UAA) can be used to estimate the relative magnitude of throughflow contributions to the stream, b) geology or surficial geology control groundwater

upwelling and contributions to the stream, or c) snow accumulation and snowmelt control throughflow contributions and streamflow timing. Alpine zones contributed the most streamflow during high flows, while the lower reaches contributed minimal to no streamflow. Lower reaches contributed more flow during annual hydrograph recession and baseflow than during high flow, but the Star West alpine zone continued to contribute the greatest streamflow during all flow conditions. Streamflow contributions were more consistent between flow conditions and between years in Star East than in Star West. Although the largest UAAs often corresponded with visible seeps or large draws that appeared to flow historically, streamflow contributions did not correlate with UAA. Conversely, downslope index, a proxy for potential groundwater inflows, corresponded with lower reaches of the watershed that contributed more flow during the hydrograph recession and baseflow. Hillslope groundwater well responses suggested that hydrologic connectivity occurred primarily during snowmelt or large storm events (>50 mm) later in the summer. Results suggest that topography was not a primary driver of hydrologic connectivity or streamflow contributions. Instead, snow accumulation and snowmelt, groundwater flow pathways, and surficial geology were key drivers of temporal trends in streamflow contributions and hydrologic connectivity.

In the third data chapter (Chapter 4), stream water and source water (snow, rain, hillslope groundwater, till groundwater, and bedrock groundwater) were sampled to determine the relative dominance and timing of these sources in their contribution to streamflow over the hydrologic season. Principal component analysis was conducted on stream and source water chemistry and showed that hillslope groundwater contributed to the stream at the onset of spring melt. This was followed by a dilution effect as the snowmelt saturated the landscape, recharged groundwater, and connected the hillslope to the stream. Stream water was most chemically similar to precipitation in May and June at Star East Lower and Star East Upper, in June and July in Star West Lower, and May to July in Star West Upper. The delayed response

in Star West Lower and the extended response in Star West Upper were consistent with the results in Chapters 2 and 3 that suggested Star West had a greater storage capacity than Star East. Fall baseflows were dominated by either hillslope groundwater or bedrock groundwater in Star West Lower and Star West Upper; additional tracers would be needed to differentiate between these two sources. Conversely, in Star East Lower and Star East Upper, stream water was similar to hillslope groundwater in August but was unlike the measured sources in September and October. Seeps that followed a similar temporal pattern into the fall as stream water had low variability in temperature, like bedrock groundwater, but were cooler suggesting a deeper groundwater source. However, the water chemistry of both seeps was very different from the bedrock groundwater well lower in the watershed. Contamination of the glacial till groundwater well limited the inferences that could be made from the water chemistry in the well. However, slow recharge rates suggest that the release of till groundwater would be delayed and may contribute to consistent baseflow contributions. Other studies have suggested that glacial till groundwater contributes to late season baseflows (Shanley et al., 2015; Blumstock et al., 2015), which may be the case for Star Creek. It may also mute peak flow responses following disturbance.

5.1. Conceptualization of runoff generation in Star Creek

Results from the studies outlined above have been combined to develop a conceptualization of runoff generation in Star Creek and other steep, snow-dominated watersheds in Alberta's southern Rocky Mountains (Figure 5.1) to outline source water contributions and timing of hydrograph response. The onset of snowmelt in lower elevations triggered the delivery of old water, stored in soil storage over winter, to the stream (Figure 5.1 - 1). The first minor hydrograph response was associated with snowmelt from lower elevations (Figure 5.1 - 2). This was followed by the main snowmelt freshet and hydrograph peak triggered by snowmelt in the upper elevations or alpine zone (Figure 5.1 - 3), which diluted stream water chemistry. The

snowmelt period was also the only time that overland flow was observed in the watershed. However, more research is required to determine if overland flow is due to saturation in the soil, a perched water table due to percolation excess processes, or infiltration excess overland flow due to frozen soils. Snowmelt from the alpine also recharged bedrock groundwater (Figure 5.1 - 4) due to little storage capacity in soil or till in the alpine. MacDonald et al. (2014) also showed evidence that snowmelt was the main source of groundwater recharge in Star Creek. Contamination of till groundwater chemistry by bentonite clay hindered the interpretation of PCA biplots and the potential fate of till groundwater but water table responses in the till suggest that snowmelt and rain percolated into the glacial till and was likely slowly released through recession and baseflow periods (Figure 5.1 - 5). Late summer streamflow may have also been influenced by bedrock groundwater (Figure 5.1 - 6). New till groundwater wells or isotopic analysis would be required to determine which source dominated streamflow during baseflow. In Star East, late fall baseflows were unlike any measured source, but seep temperatures suggested that it was likely from a deeper groundwater source.

The delivery of old water to the stream at the onset of snowmelt is similar to the flushing mechanism observed in the Turkey Lakes Watershed in central Ontario (Creed and Band, 1998) where high nitrogen concentrations were observed prior to peak streamflow. McGlynn et al. (1999) also observed the displacement of old water to the stream at the onset of snowmelt and suggested this was due to a small volume of snowmelt being added to a large storage of water already in the subsurface. This was followed by a dilution effect from the snowmelt dominating streamflow. Other studies have reported that snowmelt creates a dilution response in the stream (Rademacher et al., 2005; Cowie et al., 2017). However, the opposite has also been observed as a previously disconnected source was connected to the stream and caused an increase in solute concentrations (McNamara et al., 2005). Although this was the main period of hydrologic

connectivity in Star Creek, we did not observe the change in stream water chemistry associated with new connected sources.

The multiple flow systems that contributed to streamflow or represent separate locations of storage are important for the conceptualization of runoff generation and should be accounted for in runoff generation models. Burns et al. (1998) stressed the differences in deep (bedrock) and shallow (soils and till) flow systems in the Catskill Mountains, a region with sedimentary bedrock overlain by glacial till, because they drove nitrate dynamics. Groundwater in deep flow systems (bedrock) was recharged by snowmelt, moderated streamflow through the summer, and was a source of high nitrate concentration in the summer, whereas, nitrate became depleted in the shallow flow system (soil and till). The conceptual model developed for Star Creek suggests three flow-systems as the water table in till groundwater and soil water have different response times and receding limbs. This conceptualization can be applied to or modified for any steep, snow-dominated watershed in Alberta's Rocky Mountains or other watersheds with three storage layers.

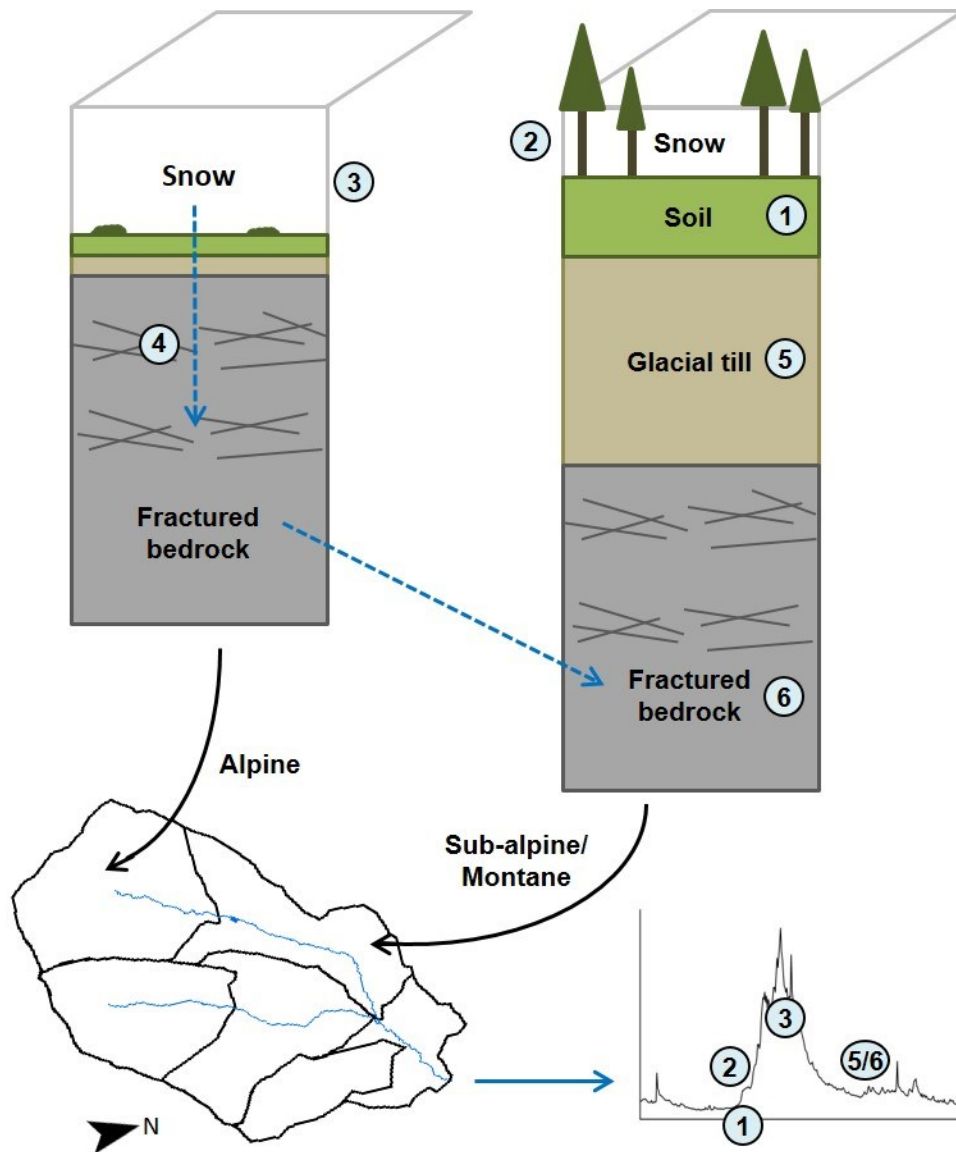


Figure 5.1: Conceptualization of runoff generation in Star Creek. Numbers on hydrograph correspond to numbers in subsurface block diagram and are described in Section 5.1.

5.2. Watershed resistance

Watershed resistance is the lack of change in streamflow following forest disturbance and has been linked to the dis-synchronicity between precipitation and runoff due to a large subsurface storage capacity (Carey et al., 2010). Results presented here suggest that the lack of change in streamflow following disturbance in the eastern slopes of the Rocky Mountains (Harder et al., 2015; Williams et al., 2015; Goodbrand and Anderson, 2016) is likely due to the presence of a

large storage capacity, the dominance of streamflow contributions from the alpine, and deep glacial till. First, estimates of dynamic storage by the water balance method showed that Star Creek has a large storage capacity (400 or 520 mm in SE or SW, respectively), similar to other watersheds with permeable, fractured bedrock (Hale et al., 2016; Sayama et al., 2011). When compared to the average annual precipitation (720-990 mm), it is possible that storage can mitigate the effects of the extra precipitation reaching the forest floor after forest disturbance. Second, changes to the landscape in areas of major streamflow contribution will have the largest impacts on streamflow. In Star Creek, snowmelt from the alpine region (above the forested hillslopes) dominated streamflow contributions at the watershed outlet. Thus, the overall streamflow regime would likely be resistant to changes in forest cover at lower elevations due to relatively minimal contributions to streamflow during snowmelt. Finally, glacial till appears to create a large storage opportunity that can retain excess water and buffer the stream from the additional precipitation that reaches the ground following forest disturbance. The additional precipitation would likely contribute to till groundwater recharge, muting potential increases in peak flow, and be slowly released to the stream during recession flow and baseflow.

When these characteristics are taken together, we would expect to see minimal changes to stream discharge in Star Creek and its sub-watersheds following the SRWP Phase-II forest harvesting that occurred in 2015. However, climate change may still pose the greatest risk to the streamflow regime because snowmelt not only dominates high flows, but it can also be the primary source of groundwater recharge and late summer flows. Increases in air temperature may result in more rainfall than snowfall in alpine and forested regions and increase the timing of melt (Pomeroy et al., 2015). Reductions in the alpine snowpack or conversion to a rainfall-dominated precipitation regime could cause significant changes to the hydrological regime. Most notably, the lack of a spring freshet could change the timing and magnitude of high flows, limit groundwater recharge, change the timing of hydrologic connectivity, and reduce the flushing

mechanism in the spring. In turn, this could cause significant water quality and quantity issues for downstream users (e.g., drinking water and irrigation) and change instream water chemistry, algal productivity, and invertebrate and fish communities.

5.3. Future Research

The results presented herein and the conceptualization of runoff in Star Creek are the initial interpretation of how water moves through and is stored in this watershed. Further research is needed to explore the following:

- Estimates of dynamic storage were some of the first calculated for snowmelt dominated watersheds and were the first calculated in the eastern slopes of Alberta's Rocky Mountains. Storage estimates from other watersheds in the eastern slopes would help corroborate these results. Marmot Creek Experimental Watershed would be an ideal location to quantify dynamic storage and data are available online.
- Major ions were used to identify which stream water sources (e.g., precipitation and bedrock groundwater) were contributing to streamflow during high flows, recession flows, and baseflows. The use of isotopes would better discriminate between sources and allow for the calculation of mean transit times or estimates of water age (Hale and McDonnell, 2016; Pfister et al., 2017). Building troughs into a hillslope and collecting water from various depths and subsurface layers would also allow for the quantification of subsurface runoff.
- Further questions of the flow pathways water takes as it infiltrates through the soil, to the till, and to the bedrock remain. Instrumenting a hillslope with numerous piezometers to assess the hillslope response to snowmelt and rainfall would help verify where saturation occurs and the direction of water movement vertically and horizontally (e.g., Smith et al., 2014).
- It is also clear from this research that a single groundwater well in the till and bedrock is not enough to capture the variability in responses across the heterogeneous landscape. Glacial

till is heterogeneous, with clay lenses or buried ice that can complicate subsurface flow pathways due to differences in hydraulic conductivity (Langston et al., 2011; Devito et al., 2005). Thus, more groundwater wells in the till and bedrock are needed to gain a better understanding of the water table responses and the variability in water chemistry across the watershed.

References

- AGS – Alberta Geological Survey. 2004. Bedrock geology of Alberta (GIS data). Accessed from: www.ags.gov.ab.ca
- Alberta Energy and Natural Resources. 1984. A policy for resource management of the eastern slopes, revised 1984. Government of Alberta. Edmonton, AB.
- Ali, G., Birkel, C., Tetzlaff, D., Soulsby, C., McDonnell, J.J., & Tarolli, P. 2014. A comparison of wetness indices for the prediction of observed connected saturated areas under contrasting conditions. *Earth Surface Processes and Landforms*, 39, 399-413. <https://doi.org/10.1002/esp.3506>
- Ali, G. A., Roy, A. G., Turmel, A-C, & Courchesne, F. 2010. Source-to-stream connectivity through end-member mixing analysis. *Journal of Hydrology*, 392, 119-135. <https://doi.org/10.1016/j.jhydrol.2010.07.049>
- Ali, G., Tetzlaff, D., McDonnell, J. J., Soulsby, C., Carey, S., Laudon, H., McGuire, K., Buttle, J., Seibert, J., & Shanley, J. 2015. Comparison of threshold hydrologic response across northern catchments. *Hydrological Processes*, 29, 3575-3591. <https://doi.org/10.1002/hyp.10527>
- Ajami, H., Troch, P. A., Maddock, T., Meixner, T., & Eastoe, C. 2011. Quantifying mountain block recharge by means of catchment-scale storage-discharge relationships. *Water Resources Research*, 47 (4), W04504. <http://doi.org/10.1029/2010ER009598>
- Amvrosiadi, N., Seibert, J., Grabs, T., & Bishop, K. 2017. Water storage dynamics in a till hillslope: the foundation for modeling flows and turnover times. *Hydrological Processes*, 31, 4-14. <https://doi.org/10.1002/hyp.11046>
- Anderson, M., & Burt, T. 1978. Role of topography in controlling throughflow generation. *Earth Surface Processes and Landforms*, 3, 331-44. <https://doi.org/10.1002/esp.3290030402>
- Andres, D., Van Der Vinne, G., & Sterenberg, G. 1987. Hydrologic, hydrogeologic, thermal, sediment and channel regimes of the Tri-Creeks experimental basin. Alberta Research Council. Rep. No. SWE-87/01. Vol. 1. 418 p.
- Barthold, F. K., Tyralla, C., Schneider, K., Vaché, K. B., Frede, H. G., & Breuer, L. 2011. How many tracers do we need for end member mixing analysis (EMMA)? A sensitivity analysis. *Water Resources Research*, 47 (8), 1-14. <https://doi.org/10.1029/2011WR010604>
- Bates, C. G. & Henry, A. J. 2005. Second phase of streamflow experiment at Wagon Wheel Gap, Colo. *Monthly Weather Review*, 56(3), 79-80. [https://doi.org/10.1175/1520-0493\(1928\)56<79:sposea>2.0.co;2](https://doi.org/10.1175/1520-0493(1928)56<79:sposea>2.0.co;2)
- Blume, T., & van Meerveld, H. J. From hillslope to stream: methods to investigate subsurface connectivity. *WIRES Water*, 2, 177-198. <https://doi.org/10.1002/wat2.1071>

- Blumstock, M., Tetzlaff, D., Malcolm, I. A., Neutzmann, G., & Soulsby, C. 2015. Baseflow dynamics: Multi-tracer surveys to assess variable groundwater contributions to montane streams under low flows. *Journal of Hydrology*, 527, 1021-1033.
<https://doi.org/10.1016/j.jhydrol.2015.05.019>
- Bracken, L. J., Waiwright, J., Ali, G. A., Tetzlaff, D., Smith, M. W. Reaney, S. M., & Roy, A. G. 2013. Concepts of hydrological connectivity: Research approaches, pathways and future agendas. *Earth-Science Reviews*, 119, 17-34.
<https://doi.org/10.1016/j.earscirev.2013.02.001>
- Burns, D. A., Murdoch, P. S., Lawrence, G. B., & Michel R. L. 1998. Effect of groundwater springs on NO₃⁻ concentrations during summer in Catskill Mountain streams. *Water Resources Research*, 34 (8), 1987-1996.
- Buttle, J. M. 2016. Dynamic storage: a potential metric of inter-basin differences in storage properties. *Hydrological Processes*, 30, 4644-4653. <https://doi.org/10.1002/hyp.10931>
- Buttle, J. M., Dillon, P. J., & Eerkes, G. R. 2004. Hydrologic coupling of slopes, riparian zones and streams: an example from the Canadian Shield. *Journal of Hydrology*, 287, 161-177.
<https://doi.org/10.1016/j.jhydrol.2003.09.022>
- Boon, S. 2012. Snow accumulation following forest disturbance. *Ecohydrology*, 5 (3), 279-285.
<https://doi.org/10.1002/eco.212>
- Brown, A. E., Zhang, L., McMahon, T. A., Western, A. W., & Vertessy, R. A. 2005. A review of paired catchment studies for determining changes in water yield resulting from alterations in vegetation. *Journal of Hydrology*, 310 (1-4), 28-61.
<https://doi.org/10.1016/j.jhydrol.2004.12.010>
- Burles, K., & Boon, S. 2011. Snowmelt energy balance in a burned forest plot, Crowsnest Pass, Alberta, Canada. *Hydrological Processes*, 25 (19), 3012-3029.
<https://doi.org/10.1002/hyp.8067>
- Carey, S. K., Tetzlaff, D., Seibert, J., Soulsby, C., Buttle, J., Laudon, H., McDonnell, J., McGuire, K., Caissie, D., Shanley, J., Kennedy, M., Devito, K., & Pomeroy, J. W. 2010. Inter-comparison of hydro-climatic regimes across northern catchments: Synchronicity, resistance and resilience. *Hydrological Processes*, 24, 3591-3602.
<https://doi.org/10.1002/hyp.7880>
- Castro, N., & Hornberger, G. 1991. Surface-subsurface water interactions in an alluviated mountain stream channel. *Water Resources Research*, 27, 1613-21.
<https://doi.org/10.1029/91WR00764>
- Cey, E. E., Rudolph, D. L., Parkin, G. W., & Aravena, R. 1998. Quantifying groundwater discharge to a small perennial stream in southern Ontario, Canada. *Journal of Hydrology*, 210, 21-37.

- Chen, Z., Hartmann, A., Wagener, T., & Goldscheider, N. 2018. Dynamics of water fluxes and storages in an Alpine karst catchment under current and potential future climate conditions. *Hydrology and Earth System Sciences*, 22(7), 3807-3823. <http://doi.org/10.5194/hess-22-3807-2018>
- Cherlet, E., Williams, C. H. S., Herlein, K., Hawthorn, K., & Silins, U. 2018. Evaluating accuracy of simple winter precipitation overspill systems with tipping bucket gauges for winter precipitation monitoring in remote mountain weather station networks. American Geophysical Union, Fall Meeting 2018, Abstract ID: H13P-1980, Washington, D.C., USA.
- Christophersen, N., & Hooper, R. P. 1992. Multivariate analysis of stream water chemical data: The use of principal components analysis for the end-member mixing problem. *Water Resources Research*, 28 (1), 99-107. <https://doi.org/10.1029/91WR02518>
- Clow, D. W., Schrott, L., Webb, R., Campbell, D. H., Torizzo, A., & Dornblaser, M. 2003. Ground water occurrence and contributions to streamflow in an alpine Colorado front range. *Ground Water*, 41(7), 937-950.
- Comer, G., & Zimmermann, R. 1969. Low-flow and basin characteristics of two streams in northern Vermont. *Journal of Hydrology*, 7, 98-108.
- Conrad, O., Bechtel, B., Bock, M., Dietrich, H., Fischer, E., Gerlitz, L., Wehberg, J., Wichmann, V., & Böhner, J. 2015. System for automated geoscientific analyses (SAGA) v. 2.1.4, *Geosci. Model Dev.*, 8, 1991-2007. <https://doi.org/10.5194/gmd-8-1991-2015>
- Covino, T. P., & McGlynn, B. L. 2007. Stream gains and losses across a mountain-to-valley transition: Impacts on watershed hydrology and stream water chemistry. *Water Resources Research*, 43, W10431. <https://doi.org/10.1029/2006WR005544>
- Cowie, R. M., Knowles, J. F., Dailey, K. R., Williams, M. W., Mills, T. J., & Molotch, N. P. 2017. Sources of streamflow along a headwater catchment elevational gradient. *Journal of Hydrology*, 549, 163-178. <https://doi.org/10.1016/j.jhydrol.2017.03.044>
- Creed, I. F. & Band L. E. 1998. Export of nitrogen from catchments with a temperate forest: Evidence for a unifying mechanism regulated by variable source area dynamics. *Water Resources Research*. 34 (11), 3105-3120.
- Dahlke, H.E., Easton, Z.M., Lyon, S.W., Walter, M.T., Destouni, G., & Steenhuis, T.S. 2012. Dissecting the variable source area concept-subsurface flow pathways and water mixing processes in a hillslope. *Journal of hydrology*, 420, 125-141. <http://doi.org/10.1016/j.jhydrol.2011.11.052>
- Day, T. J. 1976. On the precision of salt dilution gauging. *Journal of Hydrology*, 31, 293-306.
- DeBeer, C. M. & Pomeroy, J. W. 2010. Simulation of the snowmelt runoff contributing area in a small alpine basin. *Hydrology and Earth System Sciences*, 14, 1205-1219. <https://doi.org/10.5194/hess-14-1205-2010>

- Deng, Y., Flerchinger, G. N., & Cooley, K. R. 1994. Impacts of spatially and temporally varying snowmelt on subsurface flow in a mountainous watershed: 2. Subsurface processes. *Hydrological Sciences Journal*, 39 (5), 521-533. <https://doi.org/10.1080/02626669409492772>
- Detty, J. M., & McGuire, K. L. 2010a. Threshold changes in storm runoff generation at a till-mantled headwater catchment. *Water Resources Research*, 46, W07525. <https://doi.org/10.1029/2009WR008102>
- Detty, J. M., & McGuire, K. J. 2010b. Topographic controls on shallow groundwater dynamics: implications of hydrologic connectivity between hillslopes and riparian zones in a till mantled catchment. *Hydrological Processes*, 24, 2222-36. <https://doi.org/10.1002/hyp.7656>
- Devito, K. J., Creed, I. F., & Fraser, C. J. D. 2005. Controls on runoff from a partially harvested aspen-forested headwater catchment, Boreal Plain, Canada. *Hydrological Processes*, 19, 3-25. <https://doi.org/10.1002/hyp.5776>
- Devito, K., Mendoza, C., & Qualizza, C. 2012. Conceptualizing water movement in the Boreal Plains. Implications for watershed reconstruction. Synthesis report prepared for the Canadian Oil Sands Network for Research and Development, Environmental and Reclamation Research Group. 164 pp.
- Dingman, S.L. 2002. *Physical hydrology*. Prentice Hall: New Jersey, USA.
- Dixon, D., Boon, S., & Silins, U. 2014. Watershed-scale controls on snow accumulation in a small montane watershed, southwestern Alberta, Canada. *Hydrological Processes*, 28, 1294-1306. <https://doi.org/10.1002/hyp.9667>
- Dunne, T., & Leopold, L. B. 1978. *Water in environmental planning*. W.H. Freeman and Company: USA.
- Emelko, M. B., Silins, U., Bladon, K. D., & Stone, M. 2011. Implications of land disturbance on drinking water treatability in a changing climate: Demonstrating the need for “source water supply and protection” strategies. *Water Research*, 45, 461-72. <https://doi.org/10.1016/j.watres.2010.08.051>
- Evans, J. E., Prepas, E. E., Devito, K. J., & Kotak B. G. 2000. Phosphorus dynamics in shallow subsurface waters in an uncut and cut subcatchment of a lake on the Boreal Plain. *Canadian Journal of Fisheries and Aquatic Science*, 57 (Suppl. 2), 60-72.
- Fang, X., Pomeroy, J. W., Ellis, C. R., MacDonald, M. K., DeBeer, C. M., & Brown, T. 2013. Multi-variable evaluation of the hydrological model predictions for a headwater basin in the Canadian Rocky Mountains. *Hydrology and Earth System Sciences*, 17, 1635-1659. <https://doi.org/10.5194/hess-17-1635-2013>
- Fisheries and Oceans Canada. 2014. Recovery strategy for the Alberta populations of Westslope Cutthroat Trout (*Oncorhynchus clarkii lewisi*) in Canada [Final]. Species at Risk Act Recovery Strategy Series. Fisheries and Oceans Canada, Ottawa. iv + 28 pp + Appendices.

- Floriantic, M. G., van Meerveld, I., Smoorenburg, M., Margreth, M., Naef, F., Kirchner, J. W., & Molnar, P. 2018. Spatio-temporal variability in contributions to low flows in the high Alpine Poschiavino catchment. *Hydrological Processes*, 32 (26), 3938-3953. <https://doi.org/10.1002/hyp.13302>
- Freeze, R. A., & Cherry J. A. 1979. *Groundwater*. Prentice-Hall, New Jersey.
- Freeze, R. A., & Witherspoon P. A. 1967. Theoretical analysis of regional groundwater flow. 2. Effect of water-table configuration and subsurface permeability variation. *Water Resources Research*, 3 (2), 623-634.
- Gabrielli, C. P., McDonnell, J. J., & Jarvis, W. T. 2012. The role of bedrock groundwater in rainfall-runoff response at hillslope and catchment scales. *Journal of Hydrology*, 450, 117-33. <https://doi.org/10.1016/j.jhydrol.2012.05.023>
- Gannon, J. P., Bailey, S. W., & McGuire K. J. 2014. Organizing groundwater regimes and response thresholds by soils: A framework for understanding runoff generation in a headwater catchment. *Water Resources Research*. 50, 8403-8419. <https://doi.org/10.1002/2014WR015498>
- Goodbrand, A. & Anderson, A. 2016. Hydrologic resilience of a Canadian Foothills watershed to forest harvest. *Geophysical Research Abstracts*, 18, EGU2016-10932. EGU General Assembly 2016, Vienna, Austria.
- Gov. AB. 1996. State of the Environment Report. Chapter 2: Origin and distribution of surface water in Alberta. pp.7-16. Alberta Environmental Protection. Edmonton, AB.
- Grabs, T. J., Jencso, K. G., McGlynn, B. L., & Seibert, J. 2010. Calculating terrain indices along streams: A new method for separating stream sides. *Water Resources Research*, 46, W12536. <https://doi.org/10.1029/2010WR009296>
- Green K. C. & Alila, Y. 2012. A paradigm shift in understanding and quantifying the effects of forest harvesting on floods in snow environments. *Water Resources Research*, 48, W10503. <https://doi.org/10.1029/2012WR012449>
- Hale, V. C., & McDonnell, J. J. 2016. Effect of bedrock permeability on stream base flow mean transit time scaling relations: 1. A multiscale catchment intercomparison. *Water Resources Research*, 52, 1358-1374. <https://doi.org/10.1002/2014WR016124>
- Hale, V. C., McDonnell, J. J., Stewart, M. K., Solomon, D. K., Doolittle, J., Ice, G. G., & Pack, R. T. 2016. Effect of bedrock permeability on stream base flow mean transit time scaling relationships: 2. Process study of storage and release. *Water Resources Research*, 52, 1375-1397. <https://doi.org/10.1002/2015WR017660>
- Harder, P., Pomeroy, J. W., & Westbrook, C. J. 2015. Hydrological resilience of a Canadian Rockies headwaters basin subject to changing climate, extreme weather, and forest management. *Hydrological Processes*, 29, 3905-3924. <https://doi.org/10.1002/hyp.10596>

- Hayashi, M., Hood, J., Langston, G., Muir, D., McClymont, A. F., & Bently, L. R. 2010. Storage and transmission of groundwater in alpine moraine and talus deposits. American Geophysical Union, Fall Meeting 2010, Abstract ID: C13C-02, San Francisco, USA.
- Hewlett, J. D., & Hibbert, A. R. 1967. Factors affecting the response of small watersheds to precipitation in humid areas. *Forest hydrology*, 1, 275-290.
- Hjerdt, K. N., McDonnell, J. J., Seibert, J., & Rodhe, A. 2004. A new topographic index to quantify downslope controls on local drainage. *Water Resources Research*, 40, W05602. <https://doi.org/10.1029/2004WR003130>
- Hood, J. L., & Hayashi, M. 2015. Characterization of snowmelt flux and groundwater storage in an alpine headwater basin. *Journal of Hydrology*, 521, 482-497. <https://doi.org/10.1016/j.hydrol.2014.12.041>
- Hooper, R. P. 2003. Diagnostic tools for mixing models of stream water chemistry. *Water Resources Research*, 39 (3), 1055. <https://doi.org/10.1029/2002WR001528>
- Hopp, L., & McDonnell, J. J. 2009. Connectivity at the hillslope scale: Identifying interactions between storm size, bedrock permeability, slope angle and soil depth. *Journal of Hydrology*, 376 (3-4), 378-391. <https://doi.org/10.1016/j.jhydrol.2009.07.047>
- Inamdar, S. 2011. The use of geochemical mixing models to derive runoff sources and hydrologic flow paths. In Levia, D.F., Carlyle-Moses, D., Tanaka, T. (Eds.). *Forest hydrology and biogeochemistry: Synthesis of past research and future directions*, 216, 163-183. <https://doi.org/10.1007/978-94-007-1363-5>
- Inamdar, S., Dhillon, G., Singh, S., Dutta, S., Levia, D., Scott, D., Mitchell, M., Van Stan, J., & McHale, P. 2013. Temporal variation in end-member chemistry and its influence on runoff mixing patterns in a forested, Piedmont catchment. *Water Resources Research*, 49 (4), 1828-1844. <https://doi.org/10.1002/wrcr.20158>
- Istanbulluoglu, E., Wang, T., Wright, O. M., & Lenters, J. D. 2012. Interpretation of hydrologic trends from a water balance perspective: The role of groundwater storage in the Budyko hypothesis. *Water Resources Research*, 48 (3), W00H16. <https://doi.org/10.1029/2010WR010100>
- James, A. L., & Roulet, N. T. 2006. Investigating the applicability of end-member mixing analysis (EMMA) across scale: A study of eight small, nested catchments in a temperate forested watershed. *Water Resources Research*, 42 (8), 1-17. <https://doi.org/10.1029/2005WR004419>
- Jencso, K. G., & McGlynn, B. L. 2011. Hierarchical controls on runoff generation: Topographically driven hydrologic connectivity, geology, and vegetation. *Water Resources Research*, 47, W11527. <https://doi.org/10.1029/2011WR010666>
- Jencso, K. G., McGlynn, B. L., Gooseff, M. N., Bencala, K. E., & Wondzell, S. M. 2010. Hillslope hydrologic connectivity controls riparian groundwater turnover: Implications of catchment structure for riparian buffering and stream water sources. *Water Resources Research*, 46, W10524. <https://doi.org/10.1029/2009WR008818>

- Jencso, K. G., McGlynn, B. L., Gooseff, M. N., Wondzell, S. M., Bencala, K. E., & Marshall, L.A. 2009. Hydrologic connectivity between landscapes and streams: Transferring reach-and plot-scale understanding to the catchment scale. *Water Resources Research*, 45, W04428. <https://doi.org/10.1029/2008WR007225>
- Jenicek, M., Seibert, J., Zappa, M., Staudinger, M., & Jonas, T. 2016. Importance of maximum snow accumulation for summer low flows in humid catchments. *Hydrology and Earth Systems Science*, 20, 859-879. <https://doi.org/10.5194/hess-20-859-2016>
- Jiménez Cisneros, B. E., Oki, T., Arnell, N. W., Benito, G., Cogley, J. G., Döll, P., Jiang, T., & Mwakalila, S. S. 2014. Freshwater resources. In: *Climate change 2014: Impacts, adaptation, and vulnerability. Part A: Global and sectoral aspects. Contribution of working group II to the fifth assessment report of the Intergovernmental Panel on Climate Change* [Field, C. B., Barros, V. R., Dokken, D. J., Mach, K. J., Mastrandrea, M. D., Bilir, T. E., Chatterjee, M., Ebi, K. L., Estrada, Y. O., Genova, R. C., Girma, B., Kissel, E. S., Levy, A. N., MacCracken, S., Mastrandrea, P. R., & White, L. L. (eds.)]. Cambridge University Press, Cambridge, United Kingdom and New York, NY, USA, pp. 229-269.
- Johannessen, M. & Henriksen, A. 1978. Chemistry of snow meltwater: Changes in concentration during melting. *Water Resources Research*, 14 (4), 615-619.
- Jost, G., Weiler, M., Gluns, D. R., & Alila, Y. 2007. The influence of forest and topography on snow accumulation and melt at the watershed-scale. *Journal of Hydrology*, 347, 101-115. <https://doi.org/10.1016/j.jhydrol.2007.09.006>
- Kienzle, S.W. 2008. A new temperature based method to separate rain and snow. *Hydrological Processes*, 22, 5067-5085. <http://doi.org/10.1002/hyp.7131>
- Kirchner, J. W. 2009. Catchments as simple dynamical systems: Catchment characterization, rainfall-runoff modeling, and doing hydrology backward. *Water Resources Research*, 45, W02429. <https://doi.org/10.1029/2008WR006912>
- Kosugi, K.I., Fujimoto, M., Katsura, S.Y., Kato, H., Sando, Y., & Mizuyama, T. 2011. Localized bedrock aquifer distribution explains discharge from a headwater catchment. *Water Resources Research*, 47(7), W07530. <http://doi.org/10.1029/2010WR009884>
- Kuras, P. K., Weiler, M., & Alila, Y. 2008. The spatiotemporal variability of runoff generation and groundwater dynamics in a snow-dominated catchment. *Journal of Hydrology*, 352, 50-66. <https://doi.org/10.1016/j.jhydrol.2007.12.021>
- Langston, G., Bentley, L. R., Hayashi, M., McClymont, A., & Pidlisecky, A. 2011. Internal structure and hydrological functions of an alpine proglacial moraine. *Hydrological Processes*, 25, 2967-2982. <https://doi.org/10.1002/hyp.8144>
- Lanni, C., McDonnell, J. J., & Rigon, R. 2011. On the relative role of upslope and downslope topography for describing water flow path and storage dynamics: a theoretical analysis. *Hydrological Processes*, 25, 3909-3923. <https://doi.org/10.1002/hyp.8263>
- Leach, J. A., & Moore, R. D. 2011. Stream temperature dynamics in two hydrogeomorphically distinct reaches. *Hydrological Processes*, 25, 679-690. <https://doi.org/10.1002/hyp.7854>

- Lindsay, J. 2017. Whitebox Geospatial Analysis Tools (Version 3.4) (Computer Software). Retrieved Oct. 6, 2017.
- Liu, F., Williams, M. W., & Caine, N. 2004. Source waters and flow paths in an alpine catchment, Colorado Front Range, United States. *Water Resources Research*, 40, W09401. <https://doi.org/10.1029/2004WR003076>
- MacDonald, R. J., Boon, S., Byrne, J. M., & Silins, U. 2014. A comparison of surface and subsurface controls on summer temperature in a headwater stream. *Hydrological Processes*, 28, 2338-2347. <http://doi.org/10.1002/hyp.9756>
- McCallum, J. L., Cook, P. G., Berhane, D., Rumpf, C., & McMahon G. A. 2012. Quantifying groundwater flows to streams using differential flow gauging and water chemistry. *Journal of Hydrology*, 416, 118-32. <https://doi.org/10.1016/j.jhydrol.2011.11.040>
- McClymont, A. F., Hayashi, M., Bentley, L. R., Muir, D., & Ernst, E. 2010. Groundwater flow and storage within an alpine meadow-talus complex. *Hydrology and Earth System Sciences*, 14 (6), 859-872.
- McDonnell, J. J. 1990. A rationale for old water discharge through macropores in a steep, humid catchment. *Water Resources Research*, 26 (11), 2821-2832.
- McGlynn, B. L., McDonnell, J. J., & Brammer, D. D. 2002. A review of the evolving perceptual model of hillslope flowpaths at the Maimai catchments, New Zealand. *Journal of Hydrology*, 257 (1-4), 1-26. [https://doi.org/10.1016/S0022-1694\(01\)00559-5](https://doi.org/10.1016/S0022-1694(01)00559-5)
- McGlynn, B. L., McDonnell, J. J., Shanley, J. B., & Kendall, C. 1999. Riparian zone flowpath dynamics during snowmelt in a small headwater catchment. *Journal of Hydrology*, 222 (1-4), 75-92. [https://doi.org/10.1016/S0022-1694\(99\)00102-X](https://doi.org/10.1016/S0022-1694(99)00102-X)
- McGuire, K. J., McDonnell, J. J., Weiler, M., Kendall, C., McGlynn, B. L., Welker, J. M., & Seibert, J. 2005. The role of topography on catchment-scale water residence time. *Water Resources Research*, 41 (5), 1-14. <https://doi.org/10.1029/2004WR003657>
- McNamara, J. P., Chandler, D., Seyfried, M., & Achet, S. 2005. Soil moisture states, lateral flow, and streamflow generation in a semi-arid, snowmelt-driven catchment. *Hydrological Processes*, 19 (20), 4023-4038. <https://doi.org/10.1002/hyp.5869>
- McNamara, J. P., Tetzlaff, D., Bishop, K., Soulsby, C., Seyfried, M., Peters, N. E., Aulenbach, B. T. & Hooper, R. 2011. Storage as a metric of catchment comparison. *Hydrological Processes*, 25, 3364-3371. <https://doi.org/10.1002/hyp.8113>
- Moore, R. D. 2005. Introduction to salt dilution gauging for streamflow measurement Part III: Slug injection using salt in solution. *Streamline Watershed Management Bulletin*, 8 (2), 1-6.
- Mosley, M. P. 1979. Streamflow generation in a forested watershed, New Zealand. *Water Resources Research*, 15, 795-806. <https://doi.org/10.1029/WR015i004p00795>

- Nippgen, F., McGlynn, B., & Emanuel, R. E. 2015. The spatial and temporal evolution of contributing areas. *Water Resources Research*, 51, 1-24.
<https://doi.org/10.1002/2014WR016719>
- Nippgen, F., McGlynn, B. L., Emanuel, R. E., & Vose, J. M. 2016. Watershed memory at the Coweeta Hydrologic Laboratory: The effect of past precipitation and storage on hydrologic response. *Water Resources Research*, 52, 1673-1695.
<https://doi.org/10.1002/2015WR018196>
- Ocampo, C. J., Sivapalan, M., & Oldham, C. E. 2006. Field exploration of coupled hydrological and biogeochemical catchment responses and a unifying perceptual model. *Water Resources*, 29, 161-180. <https://doi.org/10.1016/j.advwatres.2005.02.014>
- Oda, T., Masakazu, S., Egusa, T., & Uchiyama, Y. 2013. Effect of bedrock flow on catchment rainfall-runoff characteristics and the water balance in forested catchments in Tanzawa Mountains, Japan. *Hydrological Processes*, 27, 3864-3872.
<https://doi.org/10.1002/hyp.9497>
- Payn, R. A., Gooseff, M. N., McGlynn, B. L., Bencala, K. E., & Wondzell, S. M. 2009. Channel water balance and exchange with subsurface flow along a mountain headwater stream in Montana, United States. *Water Resources Research*, 45, W11427.
<https://doi.org/10.1029/2008WR007644>
- Payn, R. A., Gooseff, M. N., McGlynn, B. L., Bencala, K. E., & Wondzell, S. M. 2012. Exploring changes in the spatial distribution of stream baseflow generation during a seasonal recession. *Water Resources Research*, 48, W04519.
<https://doi.org/10.1029/2011WR011552>
- Paznekas, A., & Hayashi, M. 2016. Groundwater contribution to winter streamflow in the Canadian Rockies. *Canadian Water Resources Journal*, 41 (4), 484-499.
<https://doi.org/10.1080/07011784.2015.1060870>
- Penna, D., Mantese, N., Hopp, L., Dalla Fontana, G., & Borga, M. 2015. Spatio-temporal variability of piezometric response on two steep alpine hillslopes. *Hydrological Processes*, 29, 198-211. <http://doi.org/10.1002/hyp.10140>
- Pfister, L., Martínez-Carreras, N., Hissler, C., Klaus, J., Carrer, G. E., Stewart, M. K., & McDonnell, J. J. 2017. Bedrock geology controls on catchment storage, mixing, and release: A comparative analysis of 16 nested catchments. *Hydrological Processes*, 31, 1828-1845. <https://doi.org/10.1002/hyp.11134>
- Pike, J.G. 1964. The estimation of annual run-off from meteorological data in a tropical climate. *Journal of Hydrology*, 2, 116-123.
- Pomeroy, J. W., Fang, X., & Rasouli, K. 2015. Sensitivity of snow processes to warming in the Canadian Rockies. *Proceedings. Paper presented at 72nd Eastern Snow Conference. Sherbrooke, Quebec, Canada. pp. 22-33.*

- Pulley, S., & Collins, A. L. 2018. Tracing catchment fine sediment sources using the new SIFT (Sediment Fingerprinting Tool) open source software. *Science of the Total Environment*, 635, 838-858. <https://doi.org/10.1016/j.scitotenv.2018.04.126>
- Pulley, S., Foster, I., & Antunes, P. 2015. The uncertainties associated with sediment fingerprinting suspended and recently deposited fluvial sediment in the Nene river basin. *Geomorphology*, 228, 303-319. <https://doi.org/10.1016/j.geomorph.2014.09.016>
- Rademacher, L. K., Clark, J. F., Clow, D. W., & Hudson, G. B. 2005. Old groundwater influence on stream hydrochemistry and catchment response times in a small Sierra Nevada catchment: Sagehen Creek, California. *Water Resources Research*, 41 (2), 1-10. <https://doi.org/10.1029/2003WR002805>
- R Core Team. 2014. R: A language and environment for statistical computing. R Foundation for Statistical Computing, Vienna, Austria. URL: <http://www.R-project.org/>
- Redding, T., & Devito, K. 2008. Lateral flow thresholds for aspen forested hillslopes on the Western Boreal Plain, Alberta, Canada. *Hydrological Processes*, 22, 4287-300. <https://doi.org/10.1002/hyp.7038>
- Redding, T., & Devito, K. 2010. Mechanisms and pathways of lateral flow on aspen-forested, Luvisolic soils, Western Boreal Plains, Alberta, Canada. *Hydrological Processes*, 24, 2995-3010. <https://doi.org/10.1002/hyp.7710>
- Remenda, V. H., & van der Kamp G. 1997. Contamination from sand-bentonite seal in monitoring wells installed in aquitards. *Ground Water*, 35(1), 39-46.
- Rinderer, M., van Meerveld, H. J., & Seibert, J. 2014. Topographic controls on shallow groundwater levels in a steep, prealpine catchment: When are the TWI assumptions valid? *Water Resources Research*, 50, 6067-6080. <http://doi.org/10.1002/2013WR015009>
- Rinderer, M., van Meerveld, I., Stähli, M., & Seibert, J. 2016. Is groundwater response timing in a pre-alpine catchment controlled more by topography or by rainfall? *Hydrological Processes*, 30 (7), 1036-1051. <https://doi.org/10.1002/hyp.10634>
- Ruehl, C., Fisher, A. T., Hatch, C., Los Huertos, M., Stemler, G., & Shennan, C. 2006. Differential gauging and tracer tests resolve seepage fluxes in a strongly-losing stream. *Journal of Hydrology*, 330, 235-248. <http://doi.org/10.1016/j.jhydrol.2006.03.025>
- Sayama, T., McDonnell, J. J., Dhakal, A., & Sullivan, K. 2011. How much water can a watershed store? *Hydrological Processes*, 25, 3899-3908. <https://doi.org/10.1002/hyp.8288>
- Scott, D. F. 1993. The hydrological effects of fire in South African mountain catchments. *Journal of Hydrology*, 150, 409-432. [https://doi.org/10.1016/0022-1694\(93\)90119-T](https://doi.org/10.1016/0022-1694(93)90119-T)
- Seibert, J., Bishop, K., Nyberg, L., & Rodhe, A. 2011. Water storage in a till catchment. I: Distributed modelling and relationship to runoff. *Hydrological Processes*, 25, 3937-3949. <https://doi.org/10.1002/hyp.8309>

- Shanley, J. B., Sebestyen, S. D., McDonnell, J. J., McGlynn, B. L., & Dunne, T. 2015. Water's Way at Sleepers River watershed—revisiting flow generation in a post-glacial landscape, Vermont USA. *Hydrological Processes*, 29 (16), 3447-3459. <https://doi.org/10.1002/hyp.10377>
- Shaw, S. B., McHardy, T. M., & Riha, S. J. 2013. Evaluating the influence of watershed moisture storage on variations in base flow recession rates during prolonged rain-free periods in medium-sized catchments in New York and Illinois, USA. *Water Resources Research*, 49(9), 6022-6028. <http://doi.org/10.1002/wrcr.20507>
- Silins, U., Anderson, A., Bladon, K. D., Emelko, M. B., Stone, M., Spencer, S. A., Williams, C. H. S., Wagner, M. J., Martens, A. M., Hawthorn, K. 2016. Southern Rockies Watershed Project. *Forestry Chronicle*, 92 (1), 39-42. <https://doi.org/10.5558/tfc2016-012>
- Silins, U., Stone, M., Emelko, M. B., & Bladon, K. D. 2009. Sediment production following severe wildfire and post-fire salvage logging in the Rocky Mountain headwaters of the Oldman River Basin, Alberta. *Catena*, 79, 189-197. <https://doi.org/10.1016/j.catena.2009.04.001>
- Smith, R. S. 2011. Space-time dynamics of runoff generation in a snowmelt-dominated montane catchment. PhD thesis. University of British Columbia, Vancouver, B.C. <https://circle.ubc.ca/handle/2429/38132>
- Smith, R., Moore, R., Weiler, M., & Jost, G. 2014. Spatial controls on groundwater response dynamics in a snowmelt-dominated montane catchment. *Hydrology and Earth System Sciences*, 18, 1835-1856. <https://doi.org/10.5194/hess-18-1835-2014>
- Smith, R., & Redding, T. 2012. Cumulative effects assessment: Runoff generation in snowmelt dominated montane and boreal plain catchments. *Streamline Watershed Management Bulletin*, 15, 24-34.
- Sörensen, R., Zinko, U., & Seibert, J. 2006. On the calculation of the topographic wetness index: evaluation of different methods based on field observations. *Hydrology and Earth System Sciences*, 10, 101-112. <https://www.copernicus.org/EGU/hess/hess/10/101>
- Spence, C., & Woo, M. 2003. Hydrology of subarctic Canadian shield: soil-filled valleys. *Journal of Hydrology*, 279 (1), 151-166. [https://doi.org/10.1016/S0022-1694\(03\)00175-6](https://doi.org/10.1016/S0022-1694(03)00175-6)
- Spencer, S. A., Anderson, A., & Bladon, K. D. 2016. Long-term watershed research in Alberta. *Forestry Chronicle*, 92 (1), 3-5. <https://doi.org/10.5558/tfc2016-001>
- Staudinger, M., Stoelzle, M., Seeger, S., Seibert, J., Weiler, M., & Stahl, K. 2017. Catchment water storage variation with elevation. *Hydrological Processes*, 31, 2000-2015. <https://doi.org/10.1002/hyp.11158>
- Staudinger, M., Weiler, M., & Seibert, J. 2015. Quantifying sensitivity to droughts – an experimental modeling approach. *Hydrology and Earth System Sciences*, 19, 1371-1384. <https://doi.org/10.5194/hess-19-1371-2015>

- Stednick, J. D. 1996. Monitoring the effects of timber harvest on annual water yield. *Journal of Hydrology*, 176 (1-4), 79-95. [https://doi.org/10.1016/0022-1694\(95\)02780-7](https://doi.org/10.1016/0022-1694(95)02780-7)
- Tague, C., & Grant, G. E. 2009. Groundwater dynamics mediate low-flow response to global warming in snow-dominated alpine regions. *Water Resources Research*, 45, W07421. <https://doi.org/10.1029/2008WR007179>
- Taniguchi, M. 1993. Evaluation of vertical groundwater fluxes and thermal properties of aquifers based on transient temperature-depth profiles. *Water Resources*, 29 (7), 2021-2026.
- Tetzlaff, D., Buttle, J., Carey, S. K., McGuire, K., Laudon, H., & Soulsby, C. 2015. Tracer-based assessment of flow paths, storage and runoff generation in northern catchments: a review. *Hydrological Processes*, 29, 3475-3490. <https://doi.org/10.1002/hyp.10412>
- Tomasella, J., Hodnett, M. G., Cuartas, L. A., Nobre, A. D., Waterloo, M. J., & Oliveira, S. M. 2008. The water balance of an Amazonian micro-catchment: the effect of interannual variability of rainfall on hydrological behaviour. *Hydrological Processes*, 22, 2133-2147. <https://doi.org/10.1002/hyp.6813>
- Tromp-van Meerveld, H. J., & McDonnell, J. J. 2006a. Threshold relations in subsurface stormflow: 1. A 147-storm analysis of the Panola hillslope. *Water Resources Research*, 42: W02410. <https://doi.org/10.1029/2004WR003778>
- Tromp-van Meerveld, H. J., & McDonnell, J. J. 2006b. Threshold relations in subsurface stormflow: 2. the fill and spill hypothesis. *Water Resources Research*, 42: W02411. <https://doi.org/10.1029/2004WR003800>
- Uchida, T., Asano, Y., Ohte, N., & Mizuyama, T. 2003. Analysis of flowpath dynamics in a steep unchannelled hollow in the Tanakami Mountains of Japan. *Hydrological Processes*, 17, 417-430. <https://doi.org/10.1002/hyp.1133>
- Uchida, T., McDonnell, J. J., & Asano, Y. 2006. Functional intercomparison of hillslopes and small catchments by examining water source, flowpath and mean residence time. *Journal of Hydrology*, 327, 627-642. <https://doi.org/10.1016/j.jhydrol.2006.02.037>
- Venables, W. N. & Ripley, B. D. 2002. *Modern applied statistics with S*. Fourth Edition. Springer, New York. ISBN 0-387-95457-0
- Weih, C., Ligges, U., Luebke, K., & Raabe, N. 2005. klaR analyzing German business cycles. In Baier, D., Decker, R., & Schmidt-Thieme, L. (eds.). *Data analysis and decision support*, 335-343, Springer-Verlag, Berlin.
- Weiler, M., McDonnell, J. J., Tromp-van Meerveld, I., & Uchida, T. 2005. Subsurface stormflow. In: Anderson, M. G. (Ed.). *Encyclopedia of Hydrological Sciences*. pp. 1719-1732. John Wiley & Sons, Inc. <https://doi.org/10.1002/0470848944.hsa119>
- Williams, C., Silins, U., Bladon, K. D., Martens, A. M., Wagner, M. J., & Anderson, A. 2015. Rainfall-runoff dynamics following wildfire in mountainous headwater catchments, Alberta, Canada. American Geophysical Union, Fall Meeting 2015, Abstract ID: H34B-06, San Francisco, USA.

- Williams, C. H. S., Silins, U., Spencer, S. A., Wagner, M. J., Stone, M., & Emelko, M. B. 2019. Net precipitation in burned and unburned subalpine forest stands after wildfire in the northern Rocky Mountains. *International Journal of Wildland Fire*.
<http://doi.org/10.1071/WF18181>
- Williams, C., Silins, U., Wagner, M. J., Bladon, K. D., Martens, A. M., Anderson, A., Stone, M., & Emelko, M. B. 2014. Impacts of wildfire on interception losses and net precipitation in a sub-alpine Rocky Mountain watershed in Alberta, Canada. American Geophysical Union, Fall Meeting 2014, Abstract ID: H51I-0721, San Francisco, USA.
- Winkler, R., Spittlehouse, D., & Boon, S. 2017. Streamflow response to clear-cut logging on British Columbia's Okanagan Plateau. *Ecohydrology*, 10 (2), 1-15.
<https://doi.org/10.1002/eco.1836>
- Varhola, A., Coops, N. C., Weiler, M., & Moore, R. D. 2010. Forest canopy effects on snow accumulation and ablation: An integrative review of empirical results. *Journal of Hydrology*, 392 (3-4), 219-233. <https://doi.org/10.1016/j.jhydrol.2010.08.009>

Appendix A: Supplementary figures

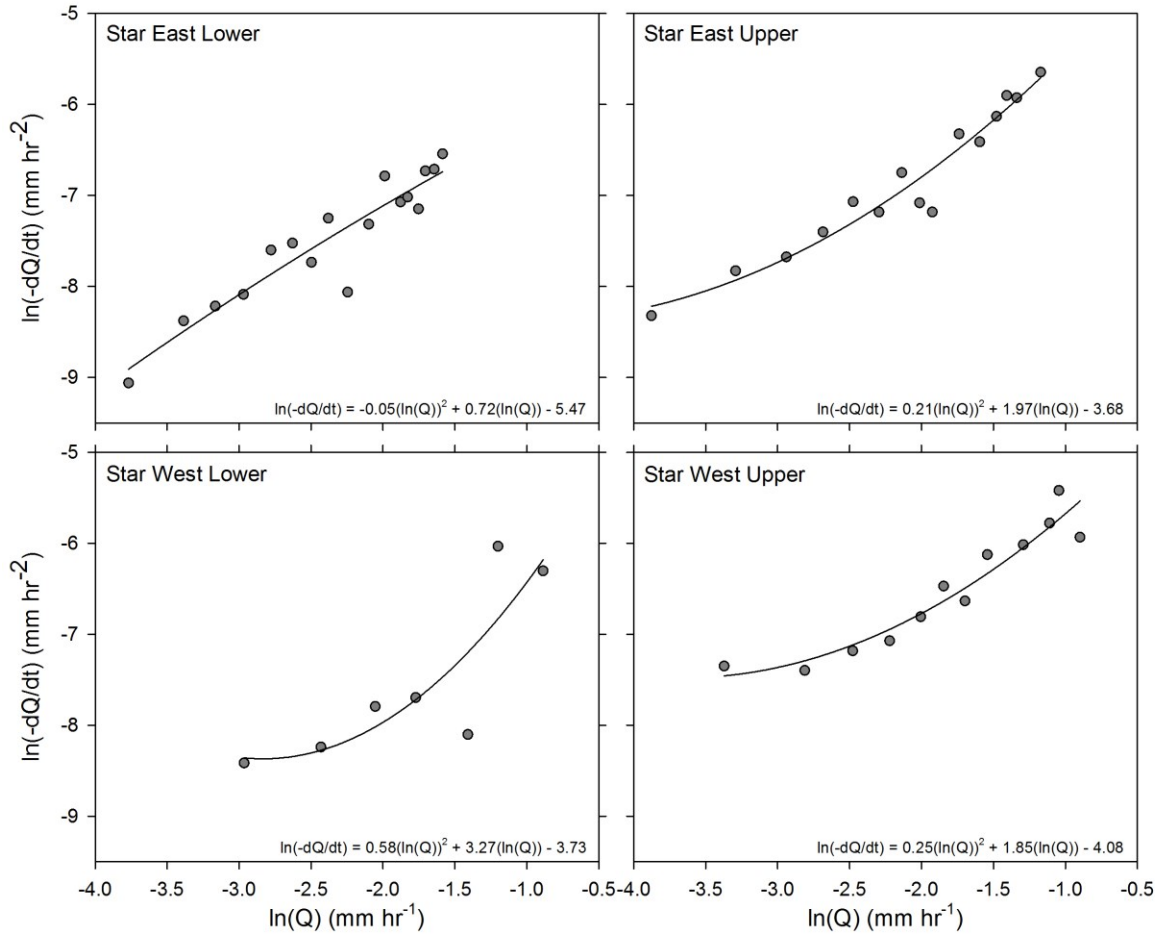


Figure A1: In the discharge sensitivity calculation, binned data were averaged (Q and dQ/dt) to generate a single value for each bin. The quadratic function displayed here was subsequently used to calculate $g(Q)$.

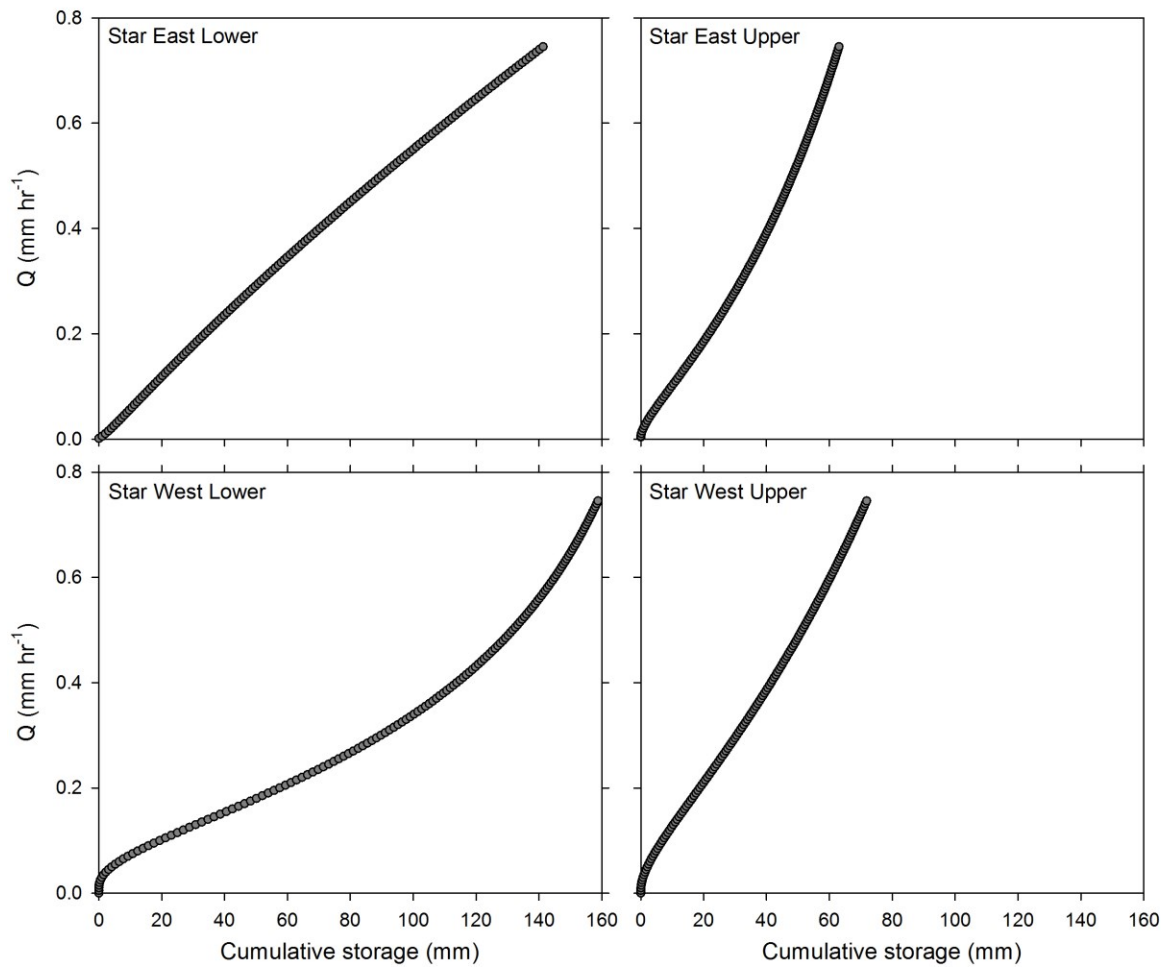


Figure A2: Relationship between cumulative storage (cumulative dS) from the discharge sensitivity calculation and stream discharge (Q). The maximum and minimum discharges between 2009 and 2014 and the corresponding dS were used to estimate dV_{Bf} .

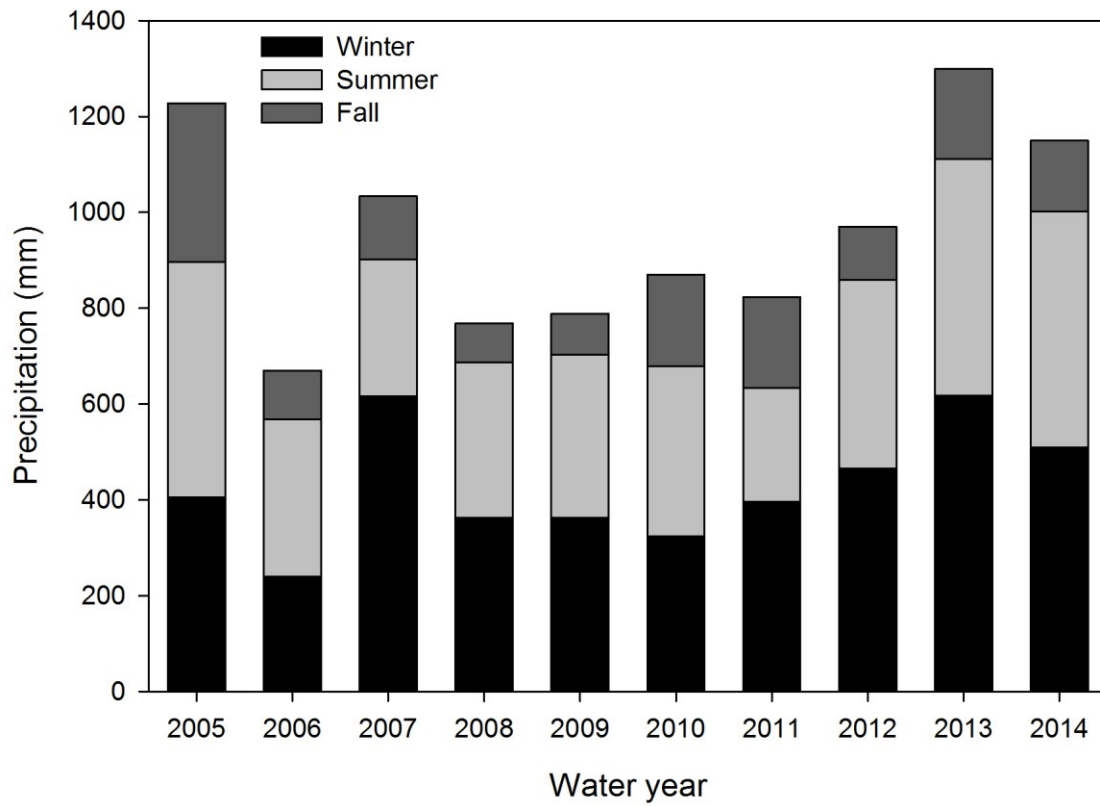


Figure A3: Seasonal, area-weighted precipitation for Star West sub-watershed. Total precipitation was separated into winter precipitation, summer rainfall, and fall rainfall. Dates for the start and end of each category varied based on when snow started to accumulate in the upper watershed and when rainfall began in the spring. September 1 was fixed as the start of fall rainfall.

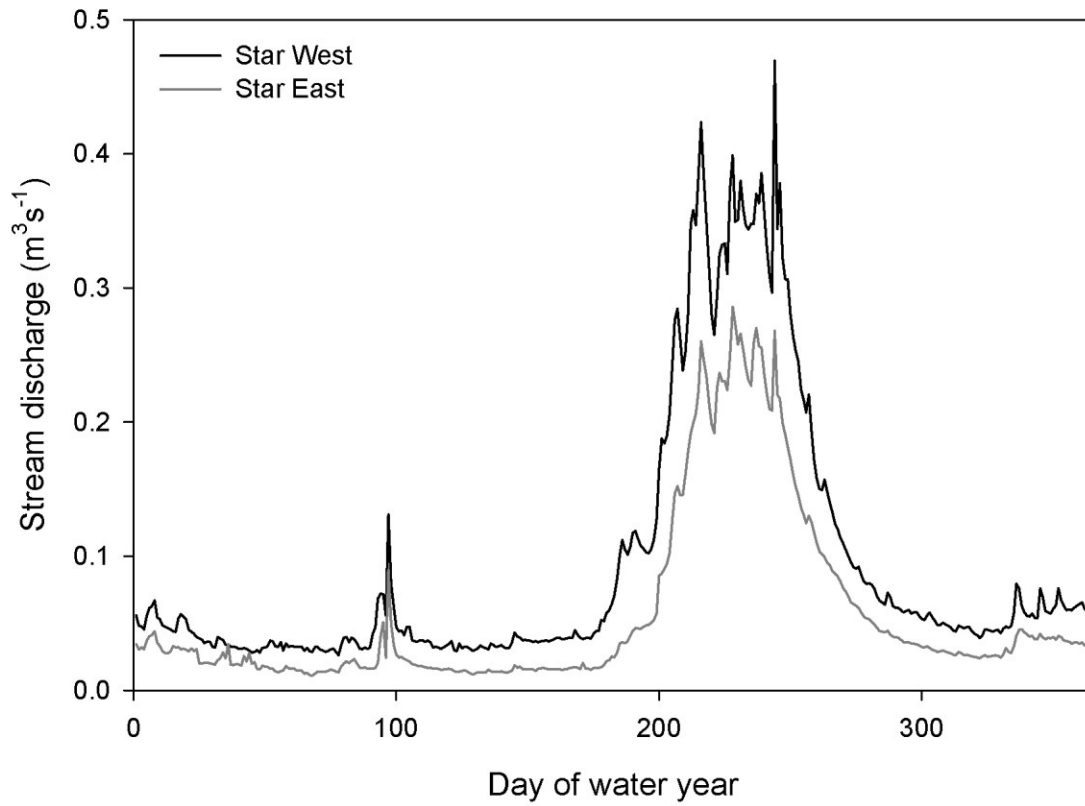


Figure A4: Mean annual streamflow hydrographs for Star East and Star West sub-watersheds (2005-2014). Beginning of the water year was variable based on the start of permanent snow accumulation in the upper area of the watershed.